The effects of PF4 on *Ascaris suum* somatic muscle cells: an electrophysiological study

Jenny Purcell

Ph.D. – The University of Edinburgh – 2001

Declaration

The experimental work described herein was performed under the supervision of Dr. R.J. Martin, Dr. D.P. Thompson and Dr C.A. Ingham during the tenure of a Faculty studentship. The work was carried out in the Department of Preclinical Veterinary Sciences, R.(D.)S.V.S., University of Edinburgh.

I hereby declare that the experimental work is my own and that I have composed this thesis. The work has not been submitted in part or as a whole to this or any other university.

Jenny Purcell B.Sc., B.V.Sc.

Acknowledgements

My thanks are due to my three supervisors, Dr. C.A. Ingham, Dr. R.J. Martin and Dr. D.P. Thompson for their guidance and advice throughout this project. I would also like to thank Dr. T. Harroun for his helpful comments on the mathematical description of diffusion (Chapter Three).

Fresh *Ascaris suum* were supplied by Dr. D. Burden of Ridgeway Science, Gloucester; Sandyford Abattoir, Paisley; and Stevenson and Co., Cullybackey, County Antrim. I am indebted to the members of the Parasitology Research Group at the Queen's University of Belfast, for collecting worms from the Cullybackey abattoir and sending them to Edinburgh when the other sources failed.

Thanks to Dr. T.G. Geary and Dr. D.P. Thompson, of Animal Health, Pharmacia and Upjohn, Inc., for supplying the PF1 and PF4 for the project free of charge.

I am pleased to acknowledge the technical expertise of Mr. G. Goodall in light microscopy and Mr. S. Mitchell in electron microscopy. Mr. C. Warwick's artistic touch can be seen in several of the figures.

I am especially grateful to Dr. A.P. Robertson for frequent discussions and valuable advice.

This project was funded by the Faculty of Veterinary Medicine, University of Edinburgh, UK and Animal Health, Pharmacia and Upjohn Inc., Kalamazoo, USA.

Table of Contents

Table of Figures

List of Tables

List of Abbreviations

5HT	Serotonin
Å	Angstroms
°C	degrees centigrade
µl	microlitre
µM	microMolar
µm	microns
A. suum	*Ascaris suum*, a parasitic nematode.
ANOVA	Analysis of Variance
ARS	*Ascaris* Ringers Solution
C. elegans	*Caenorhabditis elegans*, a free-living nematode.
ClC	chloride ion channels, members of a voltage-dependent "super family" of channels
cm	centimetre
EC50	effective concentration 50, or the molar concentration required to produce 50% of the maximum response.
EGTA	ethylene glycol-bis (β-aminoethyl ether)-N,N,N',N'-tetraacetic acid; a calcium chelating agent.
FaRP	FMRFamide-Related Peptide
FLI	FMRFamide-Like Immunoreactivity
FMRFamide	Phe-Arg-Met-PheNH_2 (cardioexcitatory peptide isolated from the mollusc *Macrocalista nimbosa*)
GABA	γ-amino butyric acid
GDP-β-S	guanosine 5'-O-(2-thiodiphosphate); a non-hydrolyzable GDP analogue used as a G-protein inhibitor.
Kg	Kilogram
KHz	KiloHertz
LyCEP	cardioexcitatory peptide derived from *Lymnea stagnalis*
mg	milligram
ml	millilitre
mM	milliMolar

n	number of observations
NPAF	neuropeptide AF, a FaRP derived from bovine brain
NPFF	neuropeptide FF, a FaRP derived from bovine brain
NPSF	neuropeptide SF, a FaRP encoded by the human genome
P	probability
PAS	periodic acid-Schiff, a histological stain that colours collagen pink.
PF1	ser-asp-pro-asn-phe-leu-arg-phe-NH_2, the first FaRP to be isolated from *Panagrellus redivivus*.
PF4	lys-pro-asn-phe-ile-arg-phe-NH_2, the fourth FaRP to be isolated from *Panagrellus redivivus*.
P. redivivus	*Panagrellus redivivus*, a free-living nematode.
PTAH	phosphotungstic acid-haematoxylin, a histological stain that colours collagen red.
pM	picoMolar
rmp	resting membrane potential
SCB	sodium cacodylate buffer, pH 7.4.
™	trade mark
UK	United Kingdom
USA	United States of America
UTR	untranslated region (of messenger RNA)

Electrophysiological terms and units

μS	microSiemens
GΩ	GigaOhms
MΩ	MegaOhms
mV	milliVolts
pA	picoAmperes
P_{open}	Probability of channel opening
pS	picoSiemens

Abstract

Nematode parasites are found in humans and other species world-wide. Infected host animals show morbidity and sometimes death, which has prompted the search for safe and effective anti-parasitic drugs (anthelmintics). The essential feature of safe anthelmintics is that they are specific for the parasite and do not damage the host. To this end, differences between the physiology of nematodes and that of their vertebrate hosts can be exploited to design safe anti-parasitic drugs. One such difference is the neuroactive peptides that have been discovered in invertebrates, including nematodes. Known as FaRPs, from *F*MRF*a*mide *R*elated *P*eptide*s*, these neuropeptides are widespread amongst nematodes and much less common in vertebrates. This has caused interest in FaRP receptors as potential drug targets. PF4 is a FaRP which was isolated from the free-living nematode *Panagrellus redivivus* and which has been shown to have activity in other nematodes, including *Ascaris suum*. *A. suum*, the large parasitic nematode found in domestic pigs, is often used as an experimental model in studying nematodes due to its large size and easy availability. The *A.suum* used in this study were obtained from three different sources.

The action of PF4 on the somatic muscle cells of *A. suum* was investigated using the two electrode current clamp technique. PF4 caused these cells to hyperpolarise by 2 to 12 mV. The FaRP also caused an increase in membrane conductance of up to 3 μS. The response to PF4 was shown to be due to the opening of chloride ion channels in the somatic muscle cell membrane. In experiments to examine the delay between application of PF4 and the response, PF4 was found to act as rapidly as the directly gating ligand γ-amino butyric acid. This observation is consistent with the argument that PF4 directly gates ion channels.

PF4 was investigated further with patch clamp experiments that were carried out on membrane vesicles produced by treating the muscle cells with collagenase. Using vesicle-attached and isolated inside-out patches, PF4 was shown to open small amplitude channels (channel conductance of 1.5 to 6.2 pS) with a relatively high probability of opening (P_{open}) of 0.05 to 0.65 at [PF4] 0.003 μM. The channel

conductance and the P_{open} recorded in each experiment varied with the origin of the worms, suggesting genetic diversity within *A. suum*.

The mean open time of the channel was found to be voltage sensitive; it varied from 522 ± 333 ms at -80 mV to 25 ± 7 ms at +120 mV. The behaviour of the channels did not alter after patch isolation, which is further evidence for them being directly gated by PF4. When the cytoplasmic side of the patches was exposed to a G-protein inhibitor (guanosine 5'-O-(2-thiodiphosphate)), the conductance of the channels reduced and the P_{open} increased. This finding suggests that these ion channels can be modulated by one or more G-proteins.

The results of this project suggest that the FaRP, PF4, directly activates low conductance chloride channels by combining with a receptor on the outside of the muscle membrane. The channels are different from those described previously in nematodes or vertebrates and therefore present a potential target for anthelmintic drugs.

Chapter 1. Literature review

1.01 Introduction

Nematode parasites successfully infect humans and other animals world wide. Recent estimates of the prevalence of human helminthiasis (see Crompton, 1999 for a review) show that there are 138 species of nematode that can parasitise people. The nematode *Ascaris lumbricoides* is an example of a successful and wide spread parasite of man. In the 1998 world population of about 5,750 million people, it was estimated that 1, 472 million were infected by *A. lumbricoides*. Of these, 23% (335 million people) suffered morbidity; showing signs of fatigue, poor general health and failure of children to grow. Some 60, 000 humans infected by *A. lumbricoides* die from their infection annually. It is assumed that a quarter of the world population is infected with *A. lumbricoides* (World Health Organisation, 1998).

The obvious financial and welfare implications of ascariasis and other parasitic infections have led to the development of a variety of drugs against parasitic worms: the "anthelmintics". The major classes of anthelmintic available at present are shown in the table below:

Table 1.01 Chronological table of anthelmintic introduction

Anthelmintic	Year introduced	First recorded resistance
benzimidazoles	1960	1964
levamisole morantel	early 1960's	early 1970's
avermectins	1981	1990

after Waller, 1994

The adaptability of the intestinal parasites in the face of anthelmintic selection pressure has led to resistant nematode strains developing to all the available drugs (see Table 1.01). The search for safe, effective and resistance-proof anthelmintics is a continuous process. There are different approaches to drug discovery, including mass screening of randomly generated compounds at one extreme and rational drug design

at the other (Geary *et al.*, 1995). The latter takes the form of searching for novel drug targets in the parasites' metabolism or physiology to circumvent the problem of resistance. In order to be safe, the ideal target is also absent in the host species. To design a broad-spectrum anthelmintic, this could mean selecting a target that was an invertebrate characteristic not found in vertebrates.

The most thoroughly investigated class of nematode neuropeptides (see Section 1.05) are the FMRFamide-Related Peptides, or FaRPs, which are found in several vertebrate species as well as being numerous in invertebrates (see Section 1.05). They fulfil some of the criteria for being potential targets for anthelmintics outlined by Geary *et al.*, 1992a. The structure of nematode FaRPs differs from that of the vertebrate FaRPs. This difference, together with their cross-species occurrence in nematodes and their potent effects on worm physiology means that FaRP receptors are possible drug targets (Geary *et al.*, 1995).

A variety of peptides, less well understood than the FaRPs, exist in nematodes. When their functions are established, they may also provide potential sites for anthelmintic action. One of the non-FaRP classes of nematode neuropeptides is represented by the peptide TKQELE, which was isolated from *Ascaris suum* (Smart *et al.*, 1992). Other nematode neuropeptides include those encoded by the *Caenorhabditis elegans* genes *nlp-1* and *nlp-2* (Li *et al.*, 1999). *nlp-1* codes for neuropeptides similar to buccalin, a peptide found in the mollusc *Aplysia californica,* while *nlp-2* encodes neuropeptides similar to myomodulin found in the mollusc *Lymnaea stagnalis*. Various other peptides have been identified in nematodes by immunocytochemistry (see Day & Maule, 1999 for a review). Due to cross-reactivity of antisera, the existence of those peptides indicated by immunological techniques must remain equivocal until they are identified in nematode genomes and/or isolated from nematode tissue. Until the purpose of these less familiar nematode neuropeptides is known, FaRPs and their receptors are more attractive as targets for anthelmintic drug design.

1.02 *Ascaris suum*

This large, common parasite has been used in electrophysiological experiments for several decades (Jarman, 1959; Dixon *et al.*, 1993). It is a parasitic roundworm of

pigs. After migrating through the liver and lungs of its host, *Ascaris* feeds in the small intestine on the porcine gut contents, a diet that includes digested food and cellular debris (Urquhart *et al.*, 1987). As a result, *Ascaris*' hosts show varying degrees of morbidity and mortality, and hence poor productivity. A similar picture is seen in humans parasitised by *A. lumbricoides* (Manson-Bahr & Bell, 1987), a parasite closely related to *A. suum*, and indeed any host affected by an intestinal nematode parasite.

There are several reasons for selecting *A. suum* as an experimental model: it is common in the domestic pig population so can be readily obtained *post mortem* at abattoirs; its relatively large size makes it easier to dissect than the smaller nematode species; it is closely related to other parasitic nematodes making it a representative model. There is recent evidence to suggest that *Ascaris* is also reasonably close, phylogenetically, to *C. elegans*, allowing genetic information obtained from *C. elegans* to be applied to *Ascaris*, see Section 1.06.1. For all of the above reasons, *A. suum* is a useful laboratory model for studies on parasitic roundworms.

1.03 The anatomy of *Ascaris suum*

Ascaris suum is a large nematode parasite of pigs. Adult worms are 20 to 30 cm long and ~5 mm in diameter, which facilitates dissection (see Figure 1.01). Like other intestinal parasites, *Ascaris* has a protective covering; the cuticle (Cox, 1992). The cuticle prevents absorption of hydrophillic compounds by the worm (Sheehy *et al.*, 2000) so to study the effect of such compounds on *A. suum* muscle cells, the cuticle must be circumvented. This is the case in electrophysiological study of the somatic muscle cells, since access is required to the internal aspect of the body wall. The muscle layer can be accessed by dissecting the worm and making a flap preparation to expose the muscle cells (Jarman, 1959; Holden-Dye *et al.*, 1989; and see Section 2.03, materials and methods), which exposes the muscle layer. A cross section of *A. suum* and a diagram of an individual muscle cell are shown in Figure 1.02.

***Figure 1.01 Photograph of* Ascaris suum**

This photograph shows Ascaris suum *within 24 hours of extraction from the host's gut. The pinkish colour and the vitality of the nematodes indicates that they are in good body conditon. The photo also illustrates the large size of* A. suum*; adults are 20 to 30 cm long and about 5 mm in diameter.*

1.03.1 The muscle cell

Ascaris somatic muscle cells differ in structure from their vertebrate counterparts. As can be seen in Figure 1.02, the muscle cells are composed of three distinct regions. There is the spindle or fibre; the muscle bag or belly; and the arm. This nomenclature was first used by Cappe de Baillon, 1911, cited by DeBell *et al.*, 1963. The structure of the muscle cells is dictated by function and has been investigated by a number of workers (Cappe de Baillon, 1911, cited by DeBell *et al.*, 1963; Rosenbluth, 1965a).

The somatic muscle cells are arranged longitudinally and can be divided into two groups on the grounds of their innervation. The dorsal mass of somatic muscle is innervated by the motor axons in the dorsal nerve cord; the ventral mass receives innervation from the motor component of the ventral nerve cord (Stretton *et al.*, 1985). Excitation of the muscle cells results in waves of contraction that are propagated along the nematode's body in the dorso-ventral plane. By this means, the worm can move forwards or backwards.

1.03.2 The spindle

The spindle contains actin and myosin and is the contractile part of the cell. Actin and myosin are arranged in over-lapping rows that produce striations, as in vertebrate skeletal muscle. However, in nematode body wall muscle, the striations are not aligned perpendicular to the long axis of the muscle. Instead, the muscle is obliquely striated (Rosenbluth, 1965b), which confers extensibility with high-speed contraction.

1.03.3 The muscle bag

The bag region of the cell contains the nucleus and is rich in glycogen and mitochondria (Rosenbluth, 1965a), see also Figure 3.13. It therefore acts as the energy store for the muscle cell. There is also an argument for a support function for the muscle bag. In life, the bag bulges inwards towards the gut; it has been proposed (Harris & Crofton, 1957) that the turgor of the muscle bags supports the nematode, acting as an endoskeleton. Due to the restricted number of cells in nematodes (Riddle *et al.*, 1997), after the maximum number of cell divisions have taken place, growth

continues by means of cellular expansion. As a result, all the nematode cells reach a relatively large size. The muscle bags are 100-200 μm in diameter in fully-grown worms. This is useful in electrophysiological experiments because the large size facilitates insertion of electrodes (see Section 2.04.3).

Figure 1.02 The anatomy of Ascaris suum

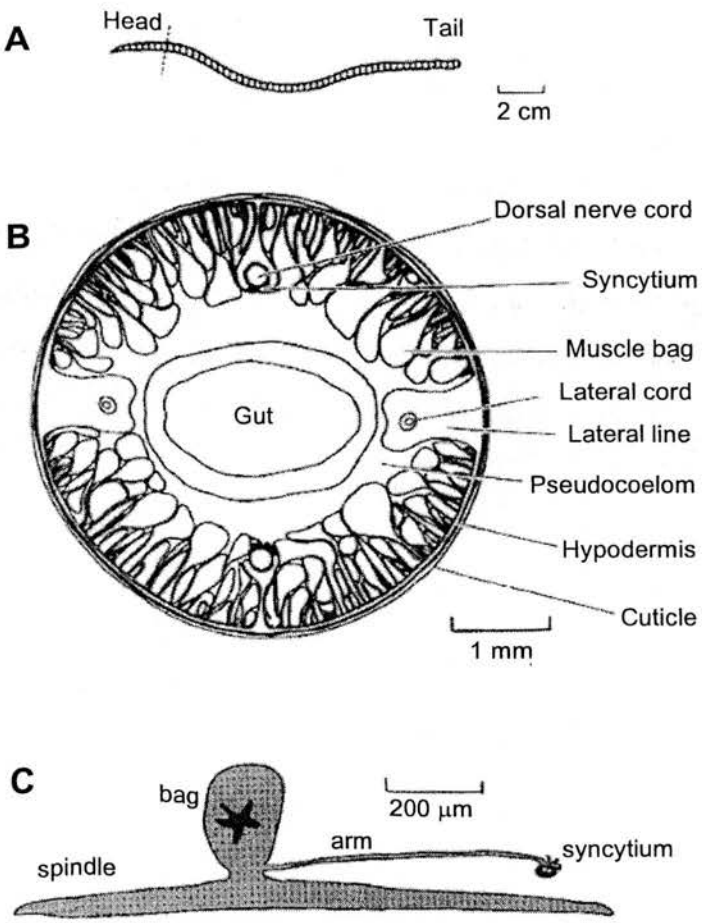

The diagram shows the body wall anatomy of Ascaris suum:
***A** shows an intact adult worm. **B** is a transverse section through the anterior half of the worm (the approximate position of the section is indicated by the dotted line in **A**). The gut extends the full length of the body, the reproductive organs are confined to the posterior part of the worm. At the level of the section, the body wall encircles the gut only. In adult females, the reproductive system can occupy the rear two thirds or three quarters of the body. The body wall is composed of somatic muscle cells. These are positioned with their contractile spindles arranged longitudinally against the hypodermis and the bag region, which contains the nucleus and glycogen granules (the energy source for the cell) orientated towards the gut. The body wall is surrounded by the hypodermis and the entire structure is protected by the collagenous cuticle. **C** shows a single somatic muscle cell. Details of the anatomy will be found in the text, Sections 1.03.1 to 1.03.4.*

1.03.4 The arm

The muscle arm is the connection from the cell to the nerve cord. The *Ascaris* neuromuscular system differs markedly from that found in vertebrates in that nematode muscle cells have projections to the neurones, rather than *vice versa* (DeBell *et al.*, 1963). Each muscle cell has one or more arms that extend from the muscle bag towards the nerve cord in the hypodermis. At their termination, each muscle arm branches into processes that join with those from other arms to form a syncytium, or functional network, around the nerve cord (Del Castillo *et al.*, 1989). The individual processes are separated from each other by tight junctions (Rosenbluth, 1965a), which ensures electrical coupling between muscle cells. Synapses are seen at the junction between the terminal divisions of the muscle arm and the nerve (Rosenbluth, 1965a).

1.03.5 Ascaris *nervous system*

The neural anatomy of *A. suum*, like that of the other nematodes that have been studied, is consistent and relatively non-complex. There are only approximately 300 neurones in *A. suum* (Stretton *et al.*, 1978). There is a concentration of sensory and motor neurones at the head and the tail of the nematode. The rest, about 90 motor neurones, are arranged in a repeated pattern along the length of the body; they supply the innervation to the somatic muscle cells. This layout is predictable in all individuals of the species. There is a simple pattern of *Ascaris* somatic muscle cell innervation, see Stretton *et al.*, 1985 for a review. Due to an elementary system of negative feedback circuits, excitatory impulses to the ventral muscle are combined with inhibitory impulses to the dorsal muscle, and *vice versa*. This combination of signals results in contraction of one block of muscle whilst the opposing muscle mass relaxes, allowing the nematode to progress forwards or backwards with a wave-like motion.

1.04 *Ascaris* physiology

1.04.1 Membrane potential

The resting membrane potential (rmp) of *Ascaris suum* somatic muscle cells has been reported as around -30 mV (Jarman, 1959; Holden-Dye *et al.*, 1997). These observations are echoed in studies on *Ascaris lumbricoides*, a nematode closely related to *A. suum*, where the rmp has also been recorded at about -30 mV (DeBell *et al.*, 1963; Brading & Caldwell, 1971). To date, the mechanism controlling the rmp in *Ascaris* has not been elucidated.

Interestingly, the rmp has been shown to be relatively insensitive to changes in the ionic composition of the surrounding medium (Brading & Caldwell, 1964; Del Castillo *et al.*, 1964a; Brading & Caldwell, 1971). A ten-fold increase in the extracellular potassium concentration caused a 1.5 mV decrease in the *Ascaris* rmp (Brading & Caldwell, 1964). This small effect is in marked contrast to the equivalent situation in excitable tissue (Hodgkin, 1951), in which the rmp has been shown to be dependent on potassium ions (Adrian, 1956). Del Castillo *et al.* (1964a) considered that organic anions contributed to the rmp in *Ascaris*, but ascribed the maintenance of the membrane potential to the intracellular chloride battery. Initial investigations led Brading and Caldwell (1964) to the conclusion that a sodium shunt was operating to control the rmp. However, on further examination of the contributions of the potassium, sodium and chloride ions to the *Ascaris* rmp, they observed that the ion concentrations were insufficient to account for the rmp (Brading & Caldwell, 1971). Instead, they hypothesised that an electrogenic pump, operating across the muscle cell membrane, was responsible for maintaining the rmp. The hypothesis stated that carboxylic acids (see Section 1.04.2) were pumped out of the cell to control the membrane potential. This hypothesis has not been superseded, although it may be questionable as Brading and Caldwell suggested that γ-amino butyric acid (GABA) acts directly on the proposed electrogenic pump. It has been shown that GABA acts on chloride ion channels in the *Ascaris* muscle cell membrane (Martin, 1980); no evidence to date has shown that GABA acts on an ion pump. Brading and Caldwell's suggestion that an electrogenic pump is a target for GABA may indicate that their experimental conditions were unsatisfactory and/or that their hypothesis is incorrect.

More recent work has showed that the movement of carboxylic acids across the *Ascaris* cuticle is closely linked to the rmp (Blair *et al.*, 1998). However, Blair *et al.* showed that the excretion of carboxylic acids from the worm is the result, rather than the cause, of the rmp.

1.04.2 Metabolism in Ascaris

Like numerous other nematodes, parasitic and free-living, *Ascaris* has an anaerobic metabolism. Its energy source is intracellular glycogen, stored in the muscle bags (Harpur, 1963), see also Figure 3.12. The end-products of the anaerobic breakdown of glycogen are carboxylic acids. The glycogen is broken down into malate in a series of steps (Tielens & van der Bergh, 1993). Malate is the principal substrate for mitochondrial fermentation (Saz, 1981), which produces volatile fatty acids. As a result of anaerobic metabolism, the perienteric fluid, which bathes the somatic muscle cells, is rich in carboxylic acids. The carboxylic acids are excreted through the non-specific anion channels that also conduct chloride ions (Valkanov *et al.*, 1994; Valkanov & Martin, 1995). The driving force for excretion is thought to be the electrical gradient set-up by the rmp. The gradient is 16 to 27 mV, depending on the individual volatile fatty acid, which tends to push carboxylic acid molecules out of the worm (Blair *et al.*, 1998).

1.04.3 Neuromuscular physiology and pharmacology

Despite the topographical simplicity of the nematode nervous system (see Section 1.03.5), there is evidence for a large number of *A. suum* neurotransmitters. These are listed below:

- acetylcholine (Baldwin & Moyle, 1949; Johnson & Stretton, 1985; Pennington & Martin, 1990)
- serotonin (5HT) (Brownlee *et al.*, 1994)
- γ-aminobutyric acid (GABA) (Martin, 1980)
- glutamate (although does not fulfil all the criteria for recognition as a neurotransmitter in nematodes) (Adelsberger *et al.*, 1997)

- FMRFamide-related peptides (FaRPs) (Cowden *et al.*, 1989; Sithigorngul *et al.*, 1990; Maule *et al.*, 1995a)

The range of neurotransmitters that have been identified in the *Ascaris* nervous system indicate more complexity than is suggested by the straight-forward neuroanatomy. Some of the *Ascaris* neurotransmitters appear to be co-localised in the nervous system; immunoreactivity to pancreatic polypeptide and FMRFamide has been demonstrated in the same neurones (Brownlee *et al.*, 1993; Brownlee *et al.*, 1994). Interaction between *Ascaris* neurotransmitters has yet to be demonstrated. It seems likely, in view of the evidence of neurotransmitter co-localisation, and because such interactions have been reported in *C. elegans*. Serotonin and acetylcholine have been shown to interact in the control of egg laying in *C. elegans* (Waggoner *et al.*, 1998). Electrophysiological studies have demonstrated the function of some of the neuroactive substances, but their integration within the nervous system is not fully understood.

Acetylcholine is an excitatory neurotransmitter that acts on cation channels (Pennington & Martin, 1990) causing muscle contraction (Baldwin & Moyle, 1949). Acetylcholine-gated channels are targets for the nicotinic anthelmintics, e.g. levamisole, pyrantel (Harrow & Gration, 1985). The nicotinic acetylcholine channel properties are different in anthelmintic-resistant nematodes (Robertson *et al.*, 1999; Robertson *et al.*, 2000).

Serotonin has modulatory effects on the *Ascaris* pharynx (Brownlee *et al.*, 1995) and the vagina vera (Fellowes *et al.*, 1998). It is also involved in glycogen metabolism (Donahue *et al.*, 1981). Immunocytochemistry has showed that serotonin is present throughout the nervous system (Johnson *et al.*, 1996). In *Ascaris*, the serotonin receptor is linked to an intracellular cyclic AMP system different from that found in vertebrates (Donahue *et al.*, 1981). The *Ascaris* serotonin receptors have been characterised and are pharmacologically distinct from vertebrate serotonin receptors (Williams *et al.*, 1992).

GABA is an inhibitory neurotransmitter in *A. suum*, producing hyperpolarisation of somatic muscle cells and muscular relaxation (Del Castillo *et al.*, 1964b; Martin,

1980). GABA acts on chloride ion channels that are the target for the anthelmintic piperazine, a GABA agonist (Martin, 1985).

Glutamate acts as an inhibitory neurotransmitter in *Ascaris* motor neurones supplying the somatic muscle and pharynx (Martin, 1996). It acts directly on a chloride ion channel that is the target for the avermectin group of anthelmintics (Cully *et al.*, 1996).

FaRPs See section 1.05 (below).

1.05 FMRFamide-Related Peptides

The tetra peptide FMRFamide was isolated from the mollusc *Macrocallista nimbosa* (Price & Greenberg, 1977). FMRFamide, short for Phe-Met-Arg-Phe-NH_2, is cardioexcitatory in *M. nimbosa* and is neuroactive in other invertebrates (Painter, 1982; Green *et al.*, 1994; Graham *et al.*, 1997). *F*MRF*a*mide-*R*elated *P*eptide*s*, or FaRPs, have been identified in species other than molluscs. Immunoreactivity to FMRFamide has been shown in rats, chickens, cattle, frogs and teleost fish, in addition to numerous invertebrate species, for reviews, see Raffa, 1988 and Maule *et al.*, 1996. Further study demonstrated that the immunoreactivity is due to various endogenous FaRPs, for example, AF1 and AF2 (Cowden *et al.*, 1989; Cowden & Stretton, 1993). Since the discovery of the original FaRP, FMRFamide, FaRPs have become recognised as an important group of neuroactive peptides, particularly amongst invertebrates. The widespread occurrence of FaRPs in the nematodes studied to date (Maule *et al.*, 1996; Nelson *et al.*, 1998) underlines their important role in nematode biology. Fewer FaRPs have been isolated from vertebrates (Yang & Majane, 1990). In the vertebrate FaRPs that have been found to date, the molecular structures are different from those of nematode FaRPs. Nematode FaRP receptors, therefore, present potential targets for anthelmintic design (Thompson *et al.*, 1996).

All of the FaRPs identified in nematodes act on the neuromuscular system. The majority has been tested on somatic muscle preparations but some have been shown to act on ovarian smooth muscle (Fellowes *et al.*, 1998). Their inhibitory and

excitatory effects have been demonstrated at nanomolar concentrations, which indicates the high potency of these compounds (Maule *et al.*, 1995a). Some act on the nervous system only, e.g. AF8 (PF3) (Maule *et al.*, 1994a; Brownlee *et al.*, 1995); others are independent of the nerve cord, e.g. PF1 and PF4 (Franks *et al.*, 1994; Maule *et al.*, 1995b). A range of responses is seen including relaxation, contraction and in some cases a biphasic relaxation-contraction response.

For brevity, the amino acids named in this account will be referred to by the single letter system, see Table 1.02.

Table 1.02 Amino acid abbreviations

Amino acid	3 letter abbreviation	Single letter system
Alanine	Ala	A
Arginine	Arg	R
Asparagine	Asn	N
Aspartic acid	Asp	D
Asparagine or aspartic acid	Asx	B
Cysteine	Cys	C
Glutamine	Gln	Q
Glutamic acid	Glu	E
Glutamine or glutamic acid	Glx	Z
Glycine	Gly	G
Histidine	His	H
Isoleucine	Ile	I
Leucine	Leu	L
Lysine	Lys	K
Methionine	Met	M
Phenylalanine	Phe	F

Proline	Pro	P
Serine	Ser	S
Threonine	Thr	T
Tryptophan	Trp	W
Tyrosine	Tyr	Y
Valine	Val	V

After Stryer, 1995

1.05.1 FaRP nomenclature

There are no exact criteria for designating a peptide as a FaRP (Maule *et al.*, 1996); initially only short peptides with a C terminal motif of Phe-X-Arg-Phe-NH_2 qualified. X was most often methionine, as in the original FaRP FMRFamide. The group expanded to include peptides where the Phe at position four from the C terminal was replaced with Tyr, another aromatic amino acid. Longer peptides were accepted as FaRPs, and eventually any peptide with the RFamide motif at the C terminal, or YFamide plus either F or Y at position four from the C terminal have been classified as FaRPs. Thus FLFQPQRFamide (known as NPFF) and AGEGLSSPFWSLAAPQRFamide (known as NPAF) from bovine brain (Yang *et al.*, 1985) and LPLRFamide from chickens have all been designated FaRPs (Maule *et al.*, 1996).

The shortened FaRP names, such as PF4 or AF2 indicate when and from where each FaRP was isolated. For example, PF4 was the fourth FaRP to be found in *Panagrellus redivivus*: P for *P. redivivus*; F for FaRP and 4 because it was the fourth. The 'A' in AF2 stands for *Ascaris suum*; AF2 was the second FaRP to be isolated from *A. suum*.

1.05.2 Nematode FaRPs

Following the discovery of FMRFamide in a mollusc in 1977 (Price & Greenberg), FMRFamide immunoreactivity was seen in nematodes in 1988 (Atkinson *et al.*) and the first nematode FaRP (AF1) was isolated from *A. suum* in 1989 (Cowden *et al.*). Since then, numerous FaRPs have been identified in the *C. elegans* genome and isolated from the free living nematodes *P. redivivus* and *C. elegans* as well as *A. suum* (see Day & Maule, 1999 for a review). FaRPs play an important signalling role in the nematode nervous system; FMRFamide-like immunoreactivity (FLI) has been found in sensory and motor neurones throughout the nervous system (Cowden *et al.*, 1993; Fellowes *et al.*, 1999).

The distribution of a neurotransmitter gives some indication of its contribution to neural signalling. According to this argument, nematode FaRPs make a sizeable contribution to nematode neurophysiology. The distribution of FLI in the *A. suum* nervous system has been variously estimated from "more than half" (Sithigorngul *et al.*, 1990), to 75% of the neurones (Brownlee *et al.*, 1993). Similarly, more than 50% of neurones in *C. elegans* have FLI (Li *et al.*, 1999). FLI may not give an accurate picture of FaRP occurrence in nematodes. The antibodies raised to FMRFamide may not be specific for FaRPs (Cowden *et al.*, 1993), although careful use of experimental controls maximises specificity (Fellowes *et al.*, 1999). The unequivocal test of nematode FaRP content is the isolation of FaRPs from worms.

FaRPs have been isolated from nematode tissue using acetone (Geary *et al.*, 1992b) or acid methanol (Cowden *et al.*, 1993) as extraction solvents. The choice of solvent dictates which FaRPs will be obtained from the tissue, basic peptides (e.g. AF1 and AF2) being more soluble in an acidic solution (Maule *et al.*, 1994a). Initially, it was thought that parasitic and free-living nematodes had mutually exclusive complements of FaRPs. This hypothesis was disproved when AF2, originally isolated from *A. suum*, was extracted from the free-living *P. redivivus* (Maule *et al.*, 1994b). AF2 has also been derived from the parasitic nematode, *Haemonchus contortus* (Keating *et al.*, 1995) and from the free-living nematode, *Caenorhabditis elegans* (Marks *et al.*, 1995). A *P. redivivus* FaRP, PF3, has been found in *A. suum* and *H. contortus* (Marks *et al.*, 1999), and in *C. elegans* (Marks *et al.*, 1998).

Given the strong evidence for conservation of FaRP structure among nematodes, it is not surprising that FaRPs isolated from one species are active in another. *A. suum* is commonly used as an experimental model for testing the effects of neuroactive peptides, see Section 1.01. Experiments investigating the action of nematode FaRPs have shown that these peptides have potent effects on *A. suum* somatic muscle and nerve tissue, see Day & Maule, 1999 for a review. Muscle relaxation was seen on application of PF1, PF2 and PF4 to muscle strip preparations. PF3, AF3 and AF4 caused muscle contraction. The FaRPs AF1 and AF2 elicited a biphasic response entailing relaxation followed by contraction. It is clear that *Ascaris* tissue responds to experimentally applied FaRPs derived from both *P. redivivus* and *A. suum*. The wide distribution of some FaRPs, e.g. AF2 and PF3, and the cross-species efficacy of others, e.g. PF4, suggests conservation of FaRP receptors among closely related species. This observation is consistent with the recent phylogenetic work that shows that *A. suum* is equally closely related to the free-living nematodes *P. redivivus* and *C. elegans*, see Section 1.06.1

1.05.3 Nematode FaRP structure

There are some marked similarities between the structure of the nematode FaRPs, see (Day & Maule, 1999) for a review:

- All the FaRPs that have been isolated from nematodes to date are between 7 and 14 amino acids long.
- All C terminals end with the RF-NH_2 motif.
- The amino acid at position 3 from the C terminal is methionine, leucine, isoleucine or valine.
- The position 4 amino acid is frequently aromatic.

Despite their broadly similar structure, the nematode FaRPs show variation in function that must reflect their constituent amino acids, provoking investigation of the structure-activity relationships. The structure-activity relationships so far elucidated (see below) illustrate that rules relating peptide function to structure vary between FaRPs (Geary *et al.*, 1999). The between-FaRP variation underlines the complexity of neuropeptide function within the nematode nervous system and suggests that *in vivo* FaRP-receptor reactions are highly specific.

Substitution of amino acids in AF1 and AF2 revealed that both the N and the C terminals are essential for biological activity; substituted peptides had no or reduced biological activity. Some of the analogue peptides produced a weak, but otherwise identical, AF1/AF2 response. The response to one analogue (AF2 with the leucine residue replaced by isoleucine) was indistinguishable from AF1. Hence, in some cases, amino acid substitution affected potency of the analogue peptides, providing evidence for the existence of different receptors for AF1 and AF2 (Bowman *et al.*, 1996).

The structure-function relationships in PF1 and PF2 were examined (Geary *et al.*, 1995) and the N terminal serine and aspartic acid residues were found to be unnecessary for biological activity. On the other hand, the phenylalanine and arginine residues (at positions 1, 2 and 4 from the C terminal) were essential for PF1 and PF2 activity.

Substitution of amino acids in PF4 showed that leucine in place of isoleucine (position 3 from the C terminal) did not affect the biological activity of the protein. The proline residue (position 6 from the C terminal) rendered PF4 resistant to enzymatic degradation. Proline also appeared to contribute to the biological activity of the molecule, probably due to its influence on tertiary structure (Kubiak *et al.*, 1996).

Some information about the relationship of structure to function of non-nematode FaRPs is known. The structure-function relationship of the mammalian FaRP, NPFF (see Section 1.05.1) was investigated (Gicquel *et al.*, 1994). They showed that the two N terminal amino acids were not essential for biological activity or receptor affinity. The remaining N terminal amino acids were found to control molecular conformation and hence receptor affinity, while the C terminal amino acids were necessary for biological activity. Hence, affinity for the receptor did not correlate with potency. This was also shown by an experiment to determine the structure-function relationship of FMRFamide (Malin *et al.*, 1996). Substituted analogues bound with lower affinity than FMRFamide, but had greater biological activity. It was hypothesised that this observation was due to the enzyme-resistance of the FMRFamide analogue, which conferred greater biological availability on the peptides.

Edison *et al.* carried out an investigation into the effect of FaRP structure on receptor binding (Edison *et al.*, 1999). They studied the molecular structure of related FaRPs from molluscs and observed that the number of turns in the molecule was inversely correlated with the receptor binding. Molecules that tended towards "extended" (linear) conformations bound to receptors with higher affinity than the FaRP molecules that tended towards a "turn" (twisted) conformation. The turn conformation was most likely to be seen when an aspartic acid residue formed hydrogen bonds with the protonated amide groups of pheylalanine and leucine residues. Hence, the presence of aspartic acid conspicuously reduced the ability of the FaRP to bind to a receptor. Like the studies mentioned above, this work demonstrates the important contribution of single amino acids to the FaRP structure and, therefore, function. The interaction between the amino acids of any of the FaRPs is complex; general rules relating peptide structure to function are difficult to determine (Geary *et al.*, 1999). However, there is little doubt that the subtle differences in FaRP structure confer a high level of binding specificity *in vivo*.

1.05.4 FaRP mechanisms of action

Nematode FaRPs. Electrophysiological work carried out on *Ascaris* shows that FaRPs can cause hyperpolarisation or depolarisation of muscle cells, and in some cases change the input conductance as well (Maule *et al.*, 1995a). Some of the nematode FaRPs have been investigated further to elucidate the ways in which signals from the stimulated receptors are relayed to the effector mechanisms of the cell. Observations on PF1 and PF2 suggested that they are mediated by nitric oxide, because their muscle relaxant effect was blocked by compounds preventing nitric oxide synthesis (Bowman *et al.*, 1995). AF1 and AF2 may act by increasing intracellular cyclic AMP while AF3 may act by decreasing it (Geary *et al.*, 1999). PF4 was shown to open non GABA-activated chloride ion channels in the somatic muscle cell membrane (Maule *et al.*, 1995a; Holden-Dye *et al.*, 1997).

Non-nematode FaRPs. Work has been carried out on other (non-nematode) FaRPs to determine their mode of action. Neuropeptide FF (NPFF), originally isolated from bovine brain (see Section 1.05.1) binds to G-protein linked receptors in rat neural

tissue (Payza & Yang, 1993). Binding is promoted by sodium and magnesium ions and the site is distinct from opioid receptors.

FMRFamide, the first FaRP to be identified, is thought to act via a G-protein in the sea slug *Aplysia californica*. The evidence for this is that the use of a non hydrolyzable GTP analogue mimicked the FMRFamide response, and pertussis toxin blocked it: responses characteristic of G-proteins (Brezina, 1988;Volterra & Siegelbaum, 1988).

LyCEP, a cardioexcitatory FaRP found in the mollusc *Lymnaea stagnalis*, also acts via a G-protein. A LyCEP receptor in *L. stagnalis* has the seven transmembrane domain structure that is characteristic of G-protein-linked receptors (Tensen *et al.*, 1998).

By contrast, the original FaRP, FMRFamide does not act via second messengers in the snail *Helix aspersa*, instead it directly gates two cation channels (Green *et al.*, 1994). Both are selective for sodium ions; one is sensitive to the sodium channel blocker amiloride, the other is not. The protein structure of the amiloride-sensitive sodium channel has been identified (Lingueglia *et al.*, 1995), making it the first directly peptide-gated ion channel to be discovered and characterised.

The evidence to date is that FaRP mechanisms of action are diverse, matching their broad species distribution and extensive range of functions.

1.05.5 Endogenous vertebrate FaRPs

Evidence of a FaRP in vertebrates was shown when immunohistochemistry and radioimmunoassays were used to identify FMRFamide-like material in rat, dog, chicken and frog tissue (Dockray *et al.*, 1983). The peptides were labelled in the central nervous system and gut, and were distinct from at least three of the endogenous neuroactive polypeptides; Met-enkephalin, neuropeptide Y and pancreatic polypeptide. The first mammalian FaRPs to be isolated and identified were found in cattle (Yang *et al.*, 1985). Both were isolated from bovine brain and were designated NPFF and NPAF, see Section 1.05.1.

1.05.6 Effects of FMRFamide on mammals

FMRFamide has diverse effects on mammalian physiology; for a review, see Raffa, 1988. There were effects on the cardiovascular system, principally an increase in blood pressure, when FMRFamide was administered to rats. The mechanism by which FMRFamide influenced the cardiovascular system was not elucidated. FMRFamide was also investigated for an effect on endogenous opioids and pain perception. Most experiments showed that FMRFamide blocked the effects of opioid compounds, despite having a relatively low affinity for the mu and kappa opioid receptors. FMRFamide, or an endogenous FaRP, may have a role in pain perception.

The bovine FaRPs (NPFF and NPAF, see Section 1.05.1) have been studied in mammals since their discovery, with particular emphasis on NPFF. It has a complex set of pro- and anti-opioid effects, and may be involved in the development of opioid tolerance (Panula *et al.*, 1996; Khan *et al.*, 1998; Demichel *et al.*, 1993). Numerous workers have studied the central effects of NPFF, and antibodies raised against it, in rats (see Panula *et al.*, 1996 for review). Both central and peripheral effects have been demonstrated, the peripheral effect has given rise to the suggestion that NPFF has hormonal action.

NPFF was shown to have peripheral effects in the guinea pig. Work carried out on the ileum suggests the presence of NPFF receptors which are coupled to opioid receptors and thus modulate the effects of endogenous and exogenous opiates on the gut (Demichel *et al.*, 1993).

In support of NPFF's role in the periphery, two distinct NPFF binding sites have been demonstrated on lymphocytes cultured from the Jurkat line (Minault *et al.*, 1995), giving rise to the suggestion that this FaRP could be involved with lymphocyte proliferation. This role for NPFF remains speculative as the binding sites were found in only two out of eleven cultured cell lines.

1.05.7 Human FaRPs

Work on the human genome has revealed a gene which codes for two FaRPs: the longer one differs from NPAF by the substitution of two amino acids, the shorter is three amino acids longer than NPFF. The latter, SQAFLFQPQRF.NH_2 , has been

named NPSF. It is thought that NPSF is subject to enzyme cleavage to remove the three N terminal amino acids, which would produce NPFF (Perry *et al.*, 1997). The presence of these FaRPs in humans indicates that there is some conservation of neuropeptide structures among vertebrates.

Sundblom *et al.* (1995), showed that NPFF was present in human plasma, providing further support for the suggestion that vertebrate FaRPs have a hormonal action in addition to a role in the nervous system.

1.06 Nematode genetics

1.06.1 Nematode phylogeny

The parasitic nematodes have always been considered to be closely related phylogenetically (Anderson, 1984); findings in one species were assumed to be relevant to others (Anderson, 1992). However, recent work has shown that parasites of the phylum Nematoda are not as closely related as was thought previously. New evidence suggests that parasitism of vertebrates evolved on four separate occasions among the nematodes, rather than evolving from a single common ancestor (Blaxter *et al.*, 1998; Dorris *et al.*, 1999). This recent taxonomic work was based on comparing the highly conserved regions of ribosomal DNA from >50 species of nematode. The dendrograms generated by the studies show that the parasitic order Ascaridia is removed from the strongylida, the strongyloididae, and trichocephalida; the three other nematode orders containing parasites of vertebrates, see Figure 1.03.

This new taxonomic description of nematodes disregards the traditional division into two classes and then into orders. Instead, the phylogenetic studies have shown that the nematodes are divided into five major "clades", or groups of organisms related by descent from a common ancestor (as defined by Dorris *et al.* (1999)). The order Ascaridida is placed in the same sub group of clades (clades III, IV and V) as the strongylida and the strongyloididae. Therefore, *Ascaris* shares a common ancestor with two out of three of the other parasitic orders and can be considered to be representative of the majority of nematode parasites.

The group of clades that include Ascaridida also contain the genera Panagrollaimidae and Rhabditina. These genera include the two free-living nematodes *P. redivivus* and *C. elegans*, respectively. Both are equally closely related to *Ascaris*, according to Dorris *et al.* (1999). The proposed phylogenetic proximity of *A. suum* and *P. redivivus* is consistent with the observations that a FaRP originally isolated from *P. redivivus* was active in *Ascaris* (Maule *et al.*, 1994a); and that a FaRP originally isolated from *A. suum* was also found in *P. redivivus* (Maule *et al.*, 1994b). The dendrogram that upholds the close relationship between *A. suum* and *P. redivivus* (Dorris *et al.*, 1999) shows that both are equally related to *C. elegans*. This finding vindicates the extrapolation of genetic information obtained from *C. elegans* to *A. suum, P. redivivus* and other nematodes in the subgroup of clades III, IV and V.

1.06.2 Variation amongst nematodes

There is high nucleotide diversity in nematodes. On average, there are 0.019 to 0.027 substitutions per nucleotide between individuals in the same population (Blouin *et al.*, 1995). The different nucleotides for a given position give rise to variation in alleles for each gene, and hence increases the range of proteins expressed in a population of nematodes. The nucleotide diversity may explain the adaptability of nematodes in the face of selection pressure. The widespread use of anthelmintics is one example of selection pressure faced by parasitic nematodes. The availability of alternative alleles provides scope for the proliferation of the anthelmintic resistant worms that are present in the wild population, see Section 1.01.

Figure 1.03 Nematoda dendrogram

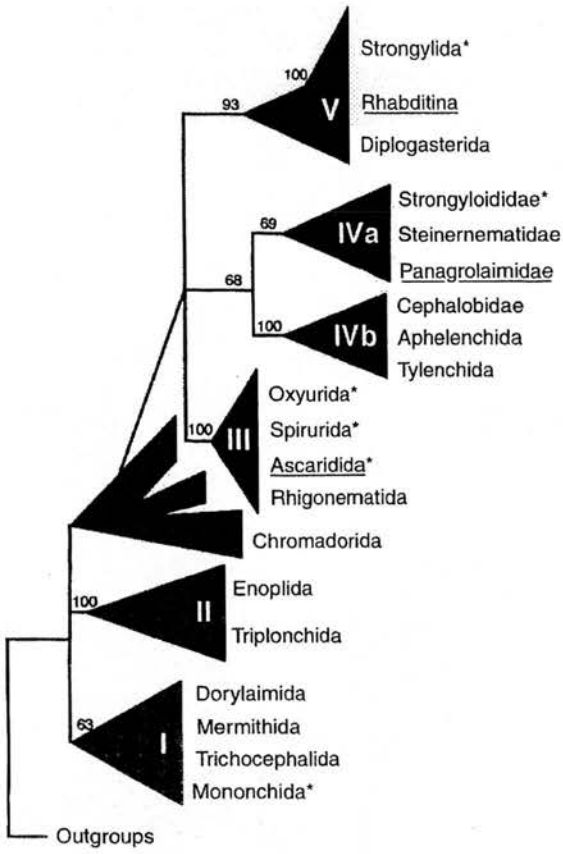

*The figure shows the new phylogenetic classification of nematodes based on ribosomal DNA analysis: from Dorris et al., 1999. The nematodes are divided into five clades, I to V. Those genera that contain vertebrate parasites are marked *. The underlined genera are those referred to in the text which contain the nematodes* C. elegans, P. redivivus *and* A. suum. *The numbers above the branches indicate the bootstrap support for each branching event.*

1.06.3 Alternative splicing

Another feature of nematode genetics that is particularly relevant to the production of nematode FaRPs is alternative splicing. This is the mechanism by which one gene can produce several different proteins, depending on which portions of the gene are transcribed. Splice factors, which are not yet fully understood, direct the transcription apparatus of the cell and determine which sections of the DNA are transcribed. By including different introns or excluding exons, different gene products (known as splice variants) are made. Thus, the same piece of DNA can give rise to several different transcripts, and ultimately several splice variants (Twyman, 1998).

Where there is conservation of amino acid sequence between several proteins, alternative splicing is an economical way of encoding several distinct proteins in a short length of DNA.

An example of alternative splicing in a FaRP-encoding gene has been documented in the nematode *C. elegans* (Rosoff *et al.*, 1992). The gene *flp-1* can be transcribed in two different ways. Each transcript gives rise to eight FaRPs. Seven are the same in both sets; the transcripts differ in the eighth FaRP. In one set, there is an extra copy of the FaRP SADPNFLRFamide (PF2), in the other there is a copy of AGSDPNFLRFamide. The reason for one transcript being produced instead of the other is not known, but it is postulated that the second FaRP may be age or sex specific. Therefore, AGSDPNFLRFamide could be produced at a specific stage of the nematode life cycle by alternative splicing (Nelson *et al.*, 1998).

1.06.4 Nematode FaRP genes

Molecular biologists have recognised twenty genes encoding FaRPs in *C. elegans*, which encode 56 FaRPs (for a review, see Li *et al.*, 1999). Of these, 13 FaRPs have been isolated. The *C. elegans* FaRP-encoding genes have been named *flp-1* to *flp-20*. To date, the FaRPs that have been extracted from *C. elegans* are encoded by *flp-1*, *-6*, *-8*, *-9*, *-13*, *-14*, and *-18*. Seven of the FaRP genes (in *C. elegans*) encode multiple copies of their peptides, which is in marked contrast to the situation in mammals. The FaRP-encoding genes that have been found in vertebrates carry only one copy of each peptide (Perry *et al.*, 1997). This may be important in differentiating nematode and vertebrate FaRPs (Panula *et al.*, 1996).

So far, one FaRP-encoding gene has been recognised in *A. suum*, and has been named *afp-1* (Edison *et al.*, 1997). It encodes six distinct FaRPs with the same C terminal sequence PGVLRFamide. This makes it similar to, perhaps homologous to, the *C elegans* gene *flp-18* (Nelson *et al.*, 1998). Of the FaRPs encoded on *afp-1*, three have been isolated from *A. suum* (Cowden & Stretton, 1995). The gene *afp-1* has single copies of each of the encoded peptides, like *flp-18*. Alternative splicing occurs in the transcription of *afp-1*, but unlike the process in *C. elegans*, the alternative transcripts

of *afp-1* differ only in their untranslated regions (UTRs). The reason for alternative transcripts that vary in the UTRs only is not known. It has been speculated that information contained in the UTRs may control gene expression by an unknown mechanism (Edison *et al.*, 1997).

1.07 Chloride ion channels

Chloride is an abundant anion in vertebrate and invertebrate biological systems. Since the larger anions can not move between cells, chloride ions are the predominant diffusable ions in most cells (Foskett, 1998). Various mechanisms allowing chloride ions through cell membranes are recognised, including Cl-HCO_3 exchange, $NaHCO_3$-HCl exchange, Na-K-Cl_2 cotransport, K-Cl cotransport and anion channels (Pusch & Jentsch, 1994). This overview will concentrate on anion channels in animal cell membranes.

In order to discuss the different channels that have been identified to date, individual channels are grouped together. Anion selective channels are diverse and poorly characterised in comparison with the widely studied cation channels selective for sodium, potassium and calcium (Hille, 1992). In many cases, anion channels are not tissue specific and their biological role is unknown, making them difficult to categorise (Franciolini & Petris, 1990). One approach to studying anion channels is to divide them into "gene families" but since not all known channels have been genotyped, this is not an inclusive classification. An alternative method of categorising the anion selective channels is by their channel properties, and a variation on this method is used here. Anion selective channels will be considered as three main classes according to their gating characteristics: voltage-dependent, calcium-dependent and ligand-gated.

Anion selective channels are, in fact, unselective in comparison with cation channels (Franciolini & Petris, 1990). They are often permeable to a variety of anions and cations, both mono and divalent. Hence "chloride channels" are usually slightly permeable to ions other than chloride. For simplicity, anion selective channels are referred to as chloride channels here. Chloride is generally distributed close to its electrochemical equilibrium, which is close to the resting membrane potential of most cells. When chloride channels open, the movement of chloride ions tends to oppose

any deviations from the resting membrane potential. For this reason, chloride channels stabilise membrane potentials in excitable cells (Pusch & Jentsch, 1994). Chloride channels have other roles depending on their location, including cell volume control, excretion and pH regulation.

1.07.1 Voltage-dependent chloride channels.

Many channels exhibit a degree of voltage-dependence, since in many cases, the probability of channel opening (P_{open}) changes with voltage. An example of strongly voltage-dependent anion channels are the channels encoded by the ClC gene family (Foskett, 1998). Nine ClC genes have been identified in mammals, producing 9 different channels. Expression of the ClC genes is tissue-specific; presumably function varies subtly between the isoforms.

The ClC-0 channel was isolated from the electric eel, *Torpedo marmorata* (Jentsch *et al.*, 1990), its function is to stabilise resting membrane potential. Each ClC-0 channel is composed of a large protein subunit that has 12 transmembrane domains. The subunits naturally occur as dimers, producing the so-called double-barrelled structure (Pusch & Jentsch, 1994). Pairs of identical subunits are gated individually but also as a pair, to produce characteristic single channel records with 3 equally-spaced conductance levels: closed, one channel open and both channels open (Middleton *et al.*, 1996; Ludewig *et al.*, 1996). Each ClC-0 has a low conductance of 10 pS. The individual channels open in response to membrane depolarisation, the dimer is gated by hyperpolarisation.

The other members of the ClC family that have been investigated have a similar amino acid sequence to the ClC-0 channel. Their channel architecture is less well understood, but some may have the same homodimeric structure as ClC-0 (Gadsby, 1996). The ClC-1 channel from mammalian skeletal muscle appears to have a tetrameric structure with a single pore (Steinmeyer *et al.*, 1994). The functions of the ClC family include stabilising the membrane potential and possibly cell volume regulation and chloride ion reabsorption. All are regulated by hyperpolarisation or depolarisation of the cell membrane (Pusch & Jentsch, 1994).

Other voltage-dependent chloride ion channels exist, which have yet to be investigated genetically. There are numerous "background" chloride channels, so called because their function appears to be to maintain the resting membrane potential at a value near to the chloride reversal potential (Franciolini & Petris, 1990). These channels are found in many different tissues, are modulated by voltage and have channel conductances from 10 to 100 pS.

There are also high conductance (>200 pS) chloride channels which are voltage-dependent. Again, these are found in various tissues, although at low density, and are generally active across a narrow range of potentials (Franciolini & Petris, 1990). One example of a large conductance, voltage-dependent anion selective channel was described by Gray *et al.*, (1984) as occurring in Schwann cell membranes. The conductance was ~500pS, and the channels opened between -10 and -40mV. In patch clamp experiments the channel became active only after a period of patch isolation, suggesting that an "internal factor" normally kept the channels in a closed state. Thus there was evidence of channel modulation.

1.07.2 Calcium-dependent chloride channels

Chloride channels that are gated by internal calcium ions have been found in several different tissues (Bader *et al.*, 1982; Barish, 1983; Thorn & Martin, 1987). There is considerable variation among these calcium-dependent channels, illustrated by the wide range of channel conductance values. Conductance varies from 1 to 2 pS (Marty *et al.*, 1984) to 380 pS (Young *et al.*, 1984). The function of the calcium-dependent channels is also variable; those channels found in the rat lacrimal glands are thought to have an excretory function (Marty *et al.*, 1984), while those in nematode muscle appear to stabilise the resting membrane potential (Thorn & Martin, 1987).

The calcium-dependent chloride channels found in nematodes have a conductance of 200 pS. Complex kinetics control the channel opening and closing; the probability of channels opening and the mean open time vary with cell membrane potential. At hyperpolarised potentials, the mean open time and the probability of opening of the channel are greater than when the membrane is depolarised (Thorn & Martin, 1987).

1.07.3 Ligand-gated chloride channels

Chloride channels can be gated by the ligands γ-amino butyric acid (GABA), glycine, and, in invertebrates, glutamate (Hille, 1992; Cully *et al.*, 1996). There is growing evidence that chloride channels gated by the FMRFamide-related peptide PF4 exist in nematodes (Maule *et al.*, 1995a; Holden-Dye *et al.*, 1997). There appears to be a "super-family" of ligand-gated channels, which includes cation selective channels as well as the ligand-gated chloride channels. The term "superfamily" has been coined because, on the basis of the receptor subunit amino acid sequences, $GABA_A$, glycine and acetylcholine receptors have very similar structures (Schofield *et al.*, 1987; Grenningloh *et al.*, 1987).

The cystic fibrosis transmembrane regulator (CFTR) can also be included in the group of ligand-gated chloride channels. The CFTR is gated by an intracellular substance, cyclic AMP, which could be included in a broad definition of "ligand" because it binds to specific receptors. The CFTR channel is not a member of the "super-family" that contains $GABA_A$, glycine and acetylcholine channels, because it has a different structure from the other ligand-gated receptors (Foskett, 1998). Since it is has not been shown in nematodes, the CFTR will not be treated further here.

GABA directly gates channels made up of α, β and γ subunits ($GABA_A$ channels). The channels are composed of the GABA binding site and an anion selective pore, to form a receptor/channel complex (Hille, 1992). The conformational change in the receptor/channel molecule that follows the binding of GABA to the receptor site causes the channel to open. $GABA_A$ channels conduct chloride currents in the range ~30 pS (Franciolini & Petris, 1990).

Although all GABA channels are inhibitory, there are differences between receptors found in specific locations. The $GABA_A$ receptor and the $GABA_B$ receptor, both located in vertebrate CNS, are distinctly different in terms of their pharmacology (Bowery *et al.*, 1983) and their mode of action (Bourne, 1998). The $GABA_A$ channels are fast acting because they are directly-gated. That is, the $GABA_A$ receptor has an integral chloride ion channel. Channel opening occurs very rapidly; the time scale is a few milliseconds (Hille, 1992). In contrast, the $GABA_B$ receptor causes channel

opening via signal transduction, a much slower mechanism that involves intracellular components. The intracellular G-proteins, calcium and other signal transducers involved in connecting ligand-receptor binding with cellular responses are known as second messengers . Second messenger-mediated responses are slower than responses to directly-gating ligands; they can range from milliseconds to hours (Bourne, 1998). The GABA receptor found in nematodes is different again, responding to a slightly different range of antagonists (Holden-Dye *et al.*, 1989; Martin *et al.*, 1991), but is most similar to the vertebrate $GABA_A$ receptor (Holden-Dye *et al.*, 1989).

The GABA channels found in nematodes are situated at neuromuscular synapses and on the muscle cell surface (Martin, 1980). GABA is inhibitory in the nematode nervous system and when applied to somatic muscle cells: application of GABA to nematode muscle results in marked relaxation (Del Castillo *et al.*, 1964b). As befits a directly-gating ligand, the response of nematode muscle to GABA is rapid (Maule *et al.*, 1995a), and the conductance of the channels is 22 pS (Martin, 1985). Nematode GABA receptors are the target for piperazine, an anthelmintic which mimics the effect of GABA and hence causes muscle relaxation and flaccid paralysis of the parasite.

Glycine is an amino acid that acts as an inhibitory neurotransmitter in vertebrates. It is a directly-gating ligand; on binding with its receptor, glycine causes chloride channel opening. The glycine receptor/ion channel complex is very similar in structure to the $GABA_A$ receptor (Foskett, 1998), and is part of the same receptor "super-family" (Schofield *et al.*, 1987). It has not been identified in nematodes so will not be dealt with further here.

Glutamate, another neuroactive amino acid; appears to act as a neurotransmitter in both vertebrates and invertebrates, although it has not yet been unequivocally established as a neurotransmitter. While glutamate is excitatory in vertebrate neurones, it is inhibitory in invertebrates, and the glutamate-gated chloride channels found in nematodes have not been identified in vertebrates. Like GABA and glycine, glutamate acts as a directly-gating ligand and the glutamate receptor/chloride channel complex is part of the same "super-family" (Cully *et al.*, 1996).

The glutamate-gated channels investigated in nematodes are found on the pharyngeal muscle. The main subconductance state of these chloride channels is 21 pS (Adelsberger *et al.*, 1997) and their function is essential to the pharyngeal pumping, and thus feeding, in nematodes. The nematode glutamate receptor has been recognised as a target for ivermectin activity, an anthelmintic in the avermectin group (Cully *et al.*, 1996).

1.08 FaRP-gated channels

1.08.1 Directly-gated FaRP channels

FMRFamide, a molluscan cardioexcitatory peptide and the original FaRP, has neurotransmitter effects on the snail, *Helix aspersa* (Cottrell *et al.*, 1984). FMRFamide causes these effects by directly-gating two sodium channels in the *Helix* C2 neurone (Green *et al.*, 1994). One of the FMRFamide-gated sodium channels (identified by its sensitivity to amiloride, a sodium channel blocker) has been cloned and expressed in *Xenopus laevis* oocytes (Lingueglia *et al.*, 1995). Its pharmacology and channel characteristics are similar to a super-family of sodium channels, although there is low sequence identity (Lingueglia *et al.*, 1995). The sodium channel super-family is comprised of epithelial sodium channels and degenerins; it is known as the ENaCh/Deg super-family (Mano & Driscoll, 1999). The subunits of the FMRFamide-gated sodium channel show only 16% homology with the epithelial sodium channels and 13% with the degenerins. However, the protein structure of all three types of subunit is similar, having a large hydrophobic, membrane-spanning domain at each end of an extracellular loop, and one or two cysteine-rich regions. The FMRFamide-gated sodium channel subunits are arranged in groups of four, or tetramers, to form the functional channel (Coscoy *et al.*, 1998). The other super-families of ligand-gated channels that have been characterised to date (see Section 1.07.3) do not share these structural features.

1.08.2 Second messenger-mediated FaRP channels

FMRFamide also acts on sensory neurones in the sea slug, *A. californica* to open potassium channels. The mechanism is thought to be mediated by a G-protein linked

to an intracellular second messenger system, the arachidonic acid cascade (Brezina, 1988; Volterra & Siegelbaum, 1988).

The receptors of another molluscan FaRP, LyCEP, have been characterised (Tensen *et al.*, 1998). LyCEP was isolated from the snail, *L. stagnalis*, in which it acts as a cardioexcitatory peptide and has effects on the brain. The LyCEP receptor has a structure typical of G-protein coupled receptors, with seven transmembrane domains containing conserved sequences of amino acids. The receptor responded to both pure LyCEP and a crude extract (made from *L. stagnalis* brain) by mobilising intracellular calcium and opening chloride ion channels, a response typical of G-protein coupled receptors (Lehninger *et al.*, 1993).

1.08.3 Diversity of FaRP channels

It is clear that FaRPs are extensively involved in nematode muscle control (for a review, see Maule *et al.*, 1996). In view of the wide spectrum of functions mediated by FaRPs in nematodes, corresponding variation in nematode FaRP receptors would be predicted. The mechanisms of action of nematode FaRPs substantiate this prediction, see Section 1.05.4. Studies in other invertebrates demonstrate a variety of FaRP receptors linked to ion channels (see 1.08.1 and .2 above). It is likely that a similar range of FaRP receptors exist in nematodes, which would explain the range of mechanisms of action that are already known.

1.09 Electrophysiological techniques for studying electrical activity in cell membranes

Electrophysiology is defined as the study of electrical phenomena associated with living organisms, particularly nervous conduction, according to the Larousse dictionary of science and technology (edited by Walker, 1995). All cell membranes contain specialised pores (ion channels) which allow ions into and out of the cell. Ion movement is fundamental to the function of healthy cells therefore the investigation of ion channel function is essential to the understanding of cellular physiology. Investigation of cellular electrophysiology demands accurate measurement of cell membrane potential, and at the ultrastructural level, of the current flow through

individual ion channels. This is achieved by using fine electrodes in conjunction with a powerful electrical amplifier to record the potential difference across the cell membrane. The techniques involved in electrophysiological recording have been explained in detail (Standen *et al.*, 1987). Ion channel physiology is explored by Hille (1992) and Aidley & Stanfield (1996). A concise synopsis of the methods used in this project will be given here. Three approaches were taken; the first was the use of the two electrode current clamp to study the membrane potential of whole cells. The second method was the two electrode voltage clamp, which was used to measure whole cell current flow. The third technique was patch clamping, a method that isolates a small region of the cell membrane and thus enables measurement of individual ion channel activity.

The whole cell electrophysiological methods used in this project are modern versions of the pioneering intracellular work of the 1930s, when squid giant axons were impaled with simple glass microelectrodes in order to measure the electrical activity of the cell (Hodgkin & Huxley, 1939; Curtis & Cole, 1942). The microelectrode was refined (Ling & Gerald, 1949), allowing the electrical responses of smaller cells to be studied. The patch clamp work in this project closely follows the original patch clamp techniques carried out by Hamill *et al.* (1981).

1.09.1 The two electrode current clamp technique

This technique is used to measure two important electrical properties of the cell membrane: the potential difference across the membrane and the membrane resistance. This is achieved by inserting two sharp electrodes into the selected cell, see Figure 2.02. One electrode is used to record the potential difference across the membrane, that is, the membrane potential. The other electrode is used to inject pulses of current into the cell, which mimic the signals relayed from the neuronal input. The injected current pulses are hyperpolarising, since the current-voltage relationship seen in *A. suum* muscle bags is linear when the membrane is hyperpolarised (Martin, 1980). At depolarised membrane potentials, the current rectifies, resulting in a non-linear current-voltage relationship, which can not be used to calculate membrane conductance (see Equations 1.01 and 1.02). The electrodes are constructed from borosilicate glass and are filled with an electrolyte solution, (see Halliwell &

Whitaker, 1987). The fine tip of the glass microelectrodes pierces the cell membrane, which then seals around the glass, preserving the integrity of the cell (Aidley & Stanfield, 1996). Electrical changes in the cell membrane are detected by the microelectrode and measured with reference to the bath solution.

The cell membrane potential responds to changes in the current according to Ohm's law, which is described by Equation 1.01.

Equation 1.01 Ohm's law

$$V = I.R$$

where: *V is the potential difference across the cell membrane*
I is the injected current
R is the electrical resistance of the membrane

The resistance of the cell membrane can be calculated with Equation 1.01, using the membrane potential measured in experiments in which current pulses were injected into the cell. Since resistance is the inverse of electrical conductance, the conductance of the membrane is calculated using Equation 1.02.

Equation 1.02 Ohm's law expressed in terms of conductance

$$g = \frac{1}{R} = \frac{I}{V}$$

where: *g is the electrical conductance of the cell membrane*
V is the potential difference across the membrane
I is the injected current
R is the resistance of the membrane

The electrical conductance of a cell membrane is due to the ion channels in the membrane. Therefore, the information gained about the change in membrane potential with applied electrical current is the ionic conductance of the ion channels in the membrane.

The membrane potential is recorded and amplified to allow it to be measured. To this end, the recording microelectrode is connected in series with a high resistance (more than 10^{12} Ω) amplifier. High resistance is essential to ensure that the voltage drop across the amplifier is as small as possible. The recorded potential difference across the circuit is then attributable to the membrane potential. Underestimation of the membrane potential is avoided.

Substances can be applied to the cell during current clamping to observe their effects on the ion channels in the membrane. Application can be to the cell surface (as in Chapter Three) or by injection into the cell. Changes in membrane conductance indicate ion movement, and therefore ion channel opening, in response to the exogenous substances.

By altering the extracellular solution, selected populations of ion channels can be "switched off". This can be achieved in several ways: chemical substances that block specific channels can be used; ions that block specific channels can be added; endogenous substances that activate ion channels can be washed away or rendered inactive. In this way, attention can be focused on a specific channel or range of channels in the membrane (Standen, 1987). For example, tetrodotoxin, a natural substance derived from puffer fish and other poisonous animals, selectively blocks voltage-gated sodium channels. Caesium ions can be added to block potassium channels. Calcium, which opens some ion channels (see Section 1.07.2), can be chelated, making it inactive.

The two electrode current clamp method can be used to determine the responses of ion channels in an entire cell to electrical stimulation and to applied ligands. The population of ion channels to be studied can be selected by careful composition of the extracellular solution. Current clamping provides two pieces of information: the total ionic conductance of the cell membrane ion channels, and the change in membrane potential as a result of ion channels opening.

1.09.2 The two electrode voltage clamp technique

This experimental technique uses a similar set up to the two electrode current clamping outlined in 1.09.1. The whole cell is clamped at a predetermined potential

by the injection of current through one electrode, while the second electrode records the current responses of the membrane. Voltage clamping does not mimic a natural cellular process but it enables current responses to be measured directly. There are two main applications for voltage clamping. The first is the study of voltage-dependent channels; the second, which was used in this project (see Chapter Three), is the identification of the ions moving through open ion channels.

By clamping the cell membrane at a predetermined voltage, the electric field around the membrane is altered and thus the electrochemical gradient of the intra- and extracellular ions changes. Ion channels in the membrane open in response to application of suitable ligands and the appropriate ions will move through the membrane. Instead of moving in their accustomed direction, the ions will travel in the direction dictated by the imposed electrochemical gradient. For example, under normal physiological conditions, chloride ions move down their electrochemical gradient in to and out of *Ascaris suum* muscle cells. If the cell is clamped at a voltage more negative than the resting membrane potential (i.e. hyperpolarised), the chloride ion current is directed out of the cell. When it is clamped at a positive potential compared with the resting membrane potential, the chloride ions move into the cell. The potential at which the current changes direction (the "reversal potential") indicates which ion species is involved. Thus two electrode voltage clamping can be used to establish the specificity of the ion channels.

1.09.3 The patch clamp technique

This electrophysiological technique can be described as small-scale voltage clamping. It involves selecting a microscopic area of cell membrane and insulating it electrically from the rest of the cell. In this way, patch clamping allows close examination of individual ion channels. The patch clamp pipette is closely applied to the cell membrane so that a high-resistance seal (>1 GΩ, known as a gigaseal) forms (see Figure 1.04). The small area of membrane circumscribed by the pipette tip is electrically isolated from the rest of the cell. If there are ion channels present in the patch of membrane, their activity can be recorded.

Figure 1.04 The formation of a gigaseal during patch clamping

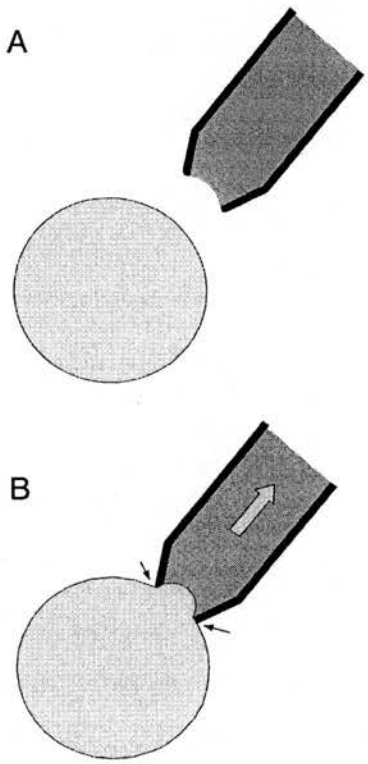

The diagram shows the two essential steps in the formation of a gigaseal between the patch pipette and the target cell. ***A*** *shows the patch pipette, filled with solution (dark grey), approaching the cell (pale grey).* ***B*** *shows the pipette positioned against the target cell with suction applied to the inside of the pipette (large arrow). An area of membrane is sucked into the tip of the pipette. The junction between the membrane and the tip become very narrow (small black arrows), which prevents ion leakage into or out of the pipette and hence reduces electrical noise. Factors which promote sealing are a clean, smooth edge to the pipette tip; an area of uniform, uncluttered cell membrane; the presence of magnesium ions in the surrounding solutions (Hamill et al., 1981).*

The patch clamp technique is a powerful tool for investigating single channel currents. Since the currents through ion channels are in the order of 10^{-12} Amps, considerable amplification is required to make measurement possible. Amplifiers used for this purpose have higher internal resistance than those required for whole cell current and voltage clamping. The electrical activity in the patch of membrane is recorded via the patch clamp pipette. Single channel records can be partially or even totally obscured by electrical interference (or "noise"), which is also amplified during the recording process. Various steps are taken to reduce the levels of electrical noise, more detail of this can be found in Section 2.05.

Ligands or channel blockers can be conveyed to the membrane patch in the pipette solution, and the resulting effects on ion channels can be monitored. The patch is

clamped at predetermined voltages to record channel currents, and therefore (using Equation 1.02) the channel conductance can be calculated. Other characteristics of the ion channels can be determined from the single channel records. Channel properties distinguish one ion channel species from another, hence the importance of single channel records. The channel properties that are resolved from single channel records include the probability of channel opening, the mean duration of opening (mean open time) and the mean closed time. Other useful criteria in describing or identifying a particular type of ion channel are the occurrence of channel run-down (loss of channel activity), receptor desensitisation (reduced/no response to high ligand concentration), and channel block (characteristic change in channel opening).

The patch configuration shown in Figure 1.04 is cell-attached. The intracellular surface is in contact with the intracellular solution, and the patch is continuous with the rest of the membrane. Further information can be obtained by isolating the patch from the parent cell, which is achieved by gently lifting the pipette. If the cell remains stationary, the upward motion of the pipette will tear the patch from the cell. The isolated patch is now in the inside-out configuration, since the intracellular surface is exposed to the extracellular solution. Isolating a membrane patch is useful in investigating the relationship of the ion channels to their intracellular environment. It can also be used to expose the intracellular face of the membrane to inhibitors or agonists, which gives more information on the ion channel physiology.

Patch clamping is an essential tool in determining ion channel characteristics and therefore in categorising ion channels.

1.10 Anthelmintics

Currently, three major groups of anthelmintics are available for therapeutic use against parasitic nematode infection. The three groups are the benzimidazoles, the nicotinic agonists and the avermectins. In addition, organophosphate compounds or piperazine are sometimes used to treat internal parasitic roundworms. Organophosphates are unpopular due to the dangers of host toxicity and piperazine has a relatively narrow spectrum, hence these two groups are seldom the anthelmintic of choice. The mechanisms of action are shown in Table 1.03.

Table 1.03 Anthelmintics and their modes of action

Chemical Group	Class	Mode of Action
1BZ	benzimidazoles, probenzimidazoles	Bind to the nematode structural protein, β-tubulin, adversely affecting nematode feeding and movement
2LM	levamisole, morantel, pyrantel	Nicotinic receptor agonists, which activate nematode acetylcholine receptors to open sodium channels, causing muscular paralysis.
3AV	avermectins, milbemycin	Agonists at the glutamate-gated chloride channel in nematode muscle, causing paralysis.
	organophosphates	Inhibit acetylcholinesterase, leading to increased stimulation of acetylcholine receptors and muscular paralysis.
	piperazine	Agonist at GABA-gated chloride channels, resulting in muscular paralysis.

(Adelsberger et al., 1997; edited by Bishop, 1998; Cully et al., 1996; Harrow & Gration, 1985; Martin, 1982)

In the three major groups, anthelmintic resistance is growing problem (see Section 1.01). The reason for identifying each of the commonly used anthelmintics with a chemical group (1BZ, 2LM or 3AV) is that mechanisms of nematode resistance are common within the group. It is important to design anthelmintic therapeutic programs to avoid the accumulation of resistant worms in the population. To assist in selecting a suitable anthelmintic, veterinary practitioners are advised to alternate between chemical groups. Despite this practice, there are examples of nematodes that are resistant to two different chemical groups (Waller, 1994), hence the increasing need for a new nematocidal drug for effective treatment of parasitic disease. Ideally, any new drug should act on an entirely different physiological system from the existing anthelmintics (see Table 1.02), to slow the development of resistant strains of nematode (Thompson *et al.*, 1996). The nematode FaRPergic system presents a suitable target for drug design (Day & Maule, 1999), see Section 5.07. In order to produce safe and effective drugs acting on nematode FaRP receptors, more knowledge is required concerning FaRP physiology in general and FaRP receptor

detail in particular (Geary *et al.*, 1999). This Ph.D. project was conceived with these aims in mind.

Project Aims

The initial working hypothesis for the project was "PF4 acts on receptors on *Ascaris suum* muscle cells to activate chloride ion channels". This gave rise to the following aims, which were addressed by carrying out sharp electrode current clamp experiments:

- To determine the location of PF4 receptors (or receptors responsive to PF4) on the muscle cell.

- To investigate the nature of the PF4 response in terms of measurable changes in the whole cell membrane (changes in input conductance and cell membrane potential).

- To determine which ions are involved in the response to PF4.

- To analyse the mode of action of PF4 by measuring the delay between application of PF4 to the cell and the appearance of a measurable response.

After the initial series of current-clamp experiments, the working hypothesis was refined to state "PF4 acts in a dose-dependent fashion to directly-gate chloride ion channels". As a result of the refined hypothesis, the objectives to be studied using the patch clamp technique were as follows:

- To characterise the PF4 channels in terms of amplitude, P_{open} and mean open time.

- To assess dose-dependence in the response to PF4.

- To investigate the involvement of intracellular second messengers in the response to PF4.

Chapter 2. Materials and Methods

2.01 Source of worms

Adult *Ascaris suum* worms were obtained from three sources. The initial supplier was Ridgeway Science, Gloucestershire, a company that set up *Ascaris* infections in pigs and delivered the worms after slaughter of the pigs. On occasion, the infections failed and worms were obtained from two alternative sources; Sandyford Abattoir, Paisley, and Stevenson and Company Abattoir, Cullybackey, County Antrim (near Belfast).

In all cases, the worms were sent to Edinburgh in transport medium (generally Locke's solution; composition in mM: NaCl 154; $CaCl_2$ 2.1; KCl 5.6; $NaHCO_3$ 1.8; glucose 5.6) inside vacuum flasks to maintain their body temperature between 25 and 35° C. They were sent by courier to ensure delivery within 24 hours of their removal from the host. Temperature maintenance and rapid delivery were measures taken to keep the worms in good condition.

2.02 Maintenance of worms

On arrival, the *A. suum* were removed from the vacuum flask. This procedure was carried out inside a fume hood to limit the exposure of laboratory personnel to potentially allergenic *Ascaris* body fluid. A two litre beaker was filled with Locke's solution and placed in a water bath set at 25° C (Unitemp, Laboratory Thermal Equipment, UK). 25° C was found to be successful because, although lower than the worms' environmental temperature *in vivo*, it was warm enough for nematode survival but limited muscular activity. Low activity conserved the *Ascaris* energy stores and allowed the worms to be kept alive for longer.

The worms were kept in the Locke's solution which was changed twice every 24 hours for 5-10 days. Regular solution changes increased the longevity of the worms in the laboratory, probably due to preventing accumulation of fatty acids (a by-product of *Ascaris* metabolism) in the solution (Blair *et al.*, 1998).

Figure 2.01 Electron micrographs of the Ascaris suum *flap preparation*

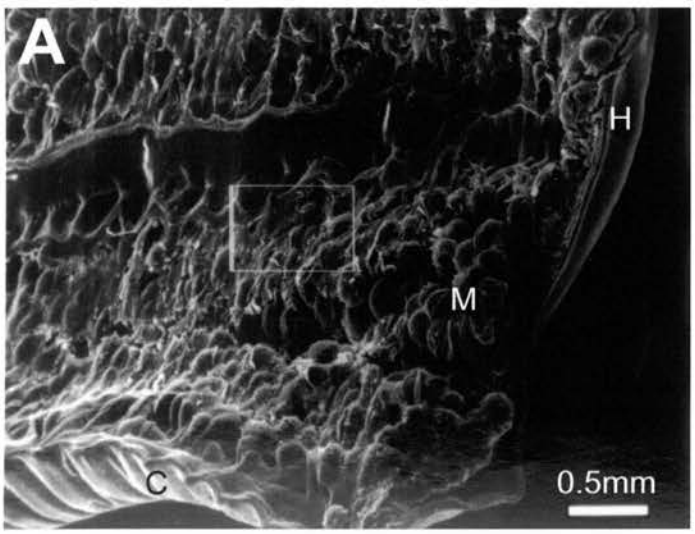

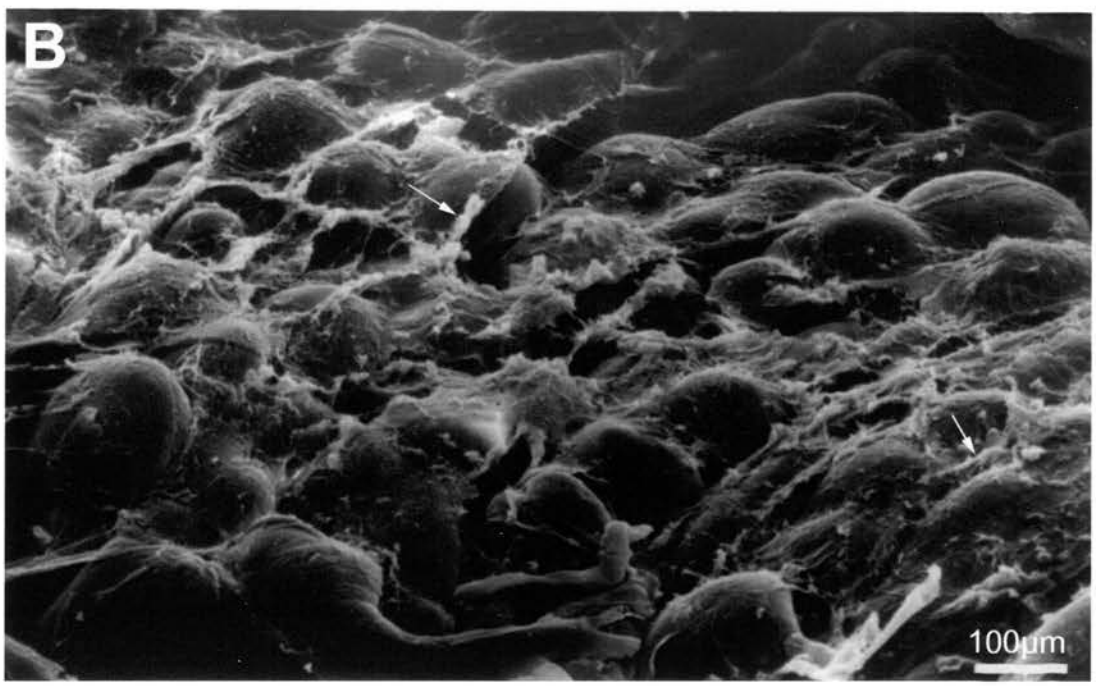

*The photograph **A** is a scanning electron micrograph (SEM) demonstrating the cuticle, **C**; the hypodermis, **H**; the bag regions of the somatic muscle cells, **M**.*
*Photograph **B** shows the inset in A at higher magnification SEM of the surface of the muscle bags, with the collagen matrix (arrows) covering the cell surfaces.*

2.03 Dissection

It was necessary to dissect the worms prior to conducting experiments in order to apply substances directly to the muscle cells. A short section (1-2 cm long) of the worm was cut from the anterior third of the body, avoiding the pharyngeal region (the rostral ~1 cm of the worm). The section was cut along one lateral line and the gut was removed. This resulted in a rectangular flap of *Ascaris* body wall: the flap preparation, see Figure 2.01. When it is positioned with the luminal side uppermost, the flap preparation allows access to the muscle bags of the somatic muscle cells (Jarman, 1959; Holden-Dye *et al.*, 1989).

2.04 The methods for sharp electrode experiments

2.04.1 Sharp electrode set up

Sharp electrode experiments are used to study the electrical activity of whole cells. Cell membrane potential and input conductance can be recorded using microelectrodes, and the reversal potential of ions can be calculated. To carry out sharp electrode experiments, the cell under investigation was impaled with two sharp glass microelectrodes and the electrical activity was recorded.

For the current clamp and voltage clamp experiments, the flap preparation was secured, cuticle side down, in a Perspex chamber of volume 2 cm^3. Entomological pins were used to secure the flap preparation and the floor of the chamber was lined with Sylgard™ to facilitate pinning out. The flap preparation was thus positioned with the muscle layer uppermost in the recording chamber. The chamber was placed on the microscope stage (Olympus, Japan) on an anti-vibration air table (Technical Manufacturing Corporation, USA). The equipment was contained within a custom-made Faraday cage to reduce electrical interference from cables and appliances in the laboratory. The recording chamber was constantly perfused with *Ascaris* Ringer Solution (ARS) at 5 ml per minute and was maintained at a temperature of 32-34° C by a water heater and pump (FH15, Grant Instruments, UK). This temperature is 5-7° C lower than that of the domestic pig (Mount, 1968), a host species for *A. suum* and the source of the worms used in these experiments. The slightly low temperature was selected to reduce the intrinsic myoactivity of the flap preparation without

impairing intracellular processes. The composition of ARS in mM was: NaCl 135; KCl 3.4; $CaCl_2$ 3; $MgCl_2$ 15.7; Glucose 3; TRIS 5; pH was adjusted to 7.6 with maleic acid. This is the same solution as the so-called "artificial sea water" used by previous workers (Jarman, 1959; Del Castillo *et al.*, 1964a), which enables results to be compared with the existing literature in the field.

2.04.2 PF4 preparation

PF4 was dissolved in distilled water and stored as a 1 mM solution at -20° C. 10 µl aliquots were defrosted and diluted with ARS to a final concentration of 10 µM as required. Prior to use, the PF4 solution was filtered through Nalgene syringe filters, pore size 0.2 µm (Nalge Company, USA). The filtered solution was loaded into the delivery tube, which was a 1 ml syringe that had been modified by drawing the tip to a fine tube of ~20 µm internal diameter, to produce the delivery tube illustrated in Figure 2.02. The delivery tube was connected to the pressure ejection system (see Section 2.04.5).

2.04.3 Microelectrode production and filling

Microelectrodes were pulled from borosilicate glass tubing (GC 120-15), Clark Electrical Instruments, UK) using a pipette puller (Scientific and Research Instruments, Ltd., UK). The pipette puller settings were adjusted to achieve a microelectrode resistance of 20-40 MΩ (measured after filling the electrodes). By gently heating the midpoint of the electrodes, they were bent to an angle of 45°. This modification enabled visualisation of the microelectrodes when they were in place above the recording chamber

The microelectrode solution was 2 M KAcetate, which was filtered (Nalge Company, USA) to avoid blocking the glass microelectrodes. Filling was achieved by dipping the tip of the electrode into filtered electrode solution to fill the shank region by capillary action. The glass tubes contained an inner filament to assist in the filling process. The body of the electrode was then half-filled with filtered solution with a syringe, which had been drawn to a fine tube. A couple of gentle taps to the body of the microelectrode dislodged any air bubbles blocking the tip. 2M KAcetate was

chosen as a suitable electrode solution instead of the more usual KCl because while both solutions fulfil the requirement for conducting electric current, the latter can leak chloride ions into the impaled cell (Martin, 1980). Since chloride ions were under investigation in this study, artificially increasing the intracellular chloride concentration was undesirable. Carboxylic acids are a by-product of *Ascaris* metabolism; leakage of acetate ions into the cytoplasm does not dramatically alter the intracellular environment.

The blunt end of each microelectrode was heated briskly after filling, in order to produce a smooth edge in contact with the electrode holder.

2.04.4 Microelectrode placement

With the aid of the binocular dissecting microscope, the flap preparation was visualised in the chamber (at magnification of 100 to140x). This arrangement allowed the accurate placement of two microelectrodes into a cell (the "target cell"), and the positioning of the delivery tube as close as possible to the target cell, see Figure 2.02. All instrumentation around the recording chamber was positioned with micromanipulators (Prior, UK).

Figure 2.02 Diagram of a sharp electrode experimental set up

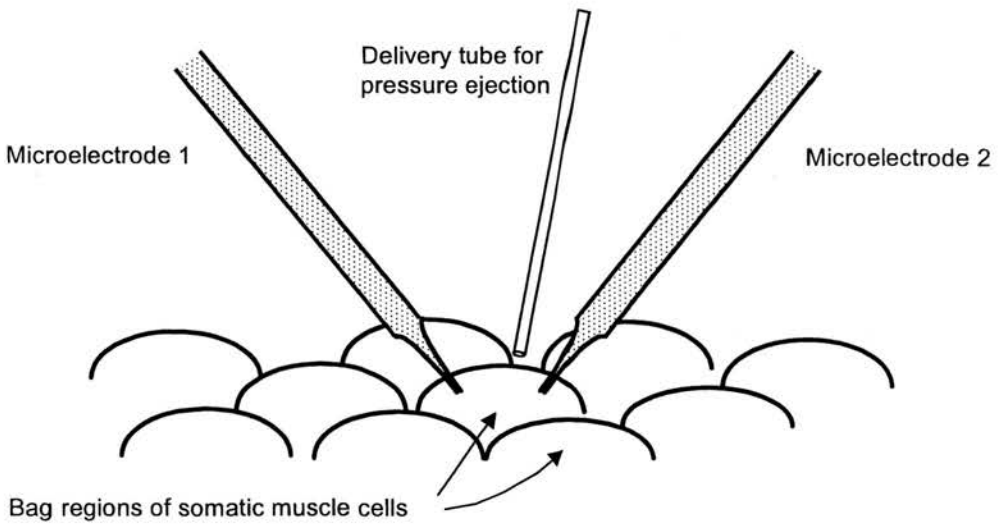

The diagram shows the flap preparation placed cuticle side down in the recording chamber. Two glass microelectrodes are inserted in the bag region of the target cell. The narrow plastic delivery tube is positioned above the target cell, as close as possible to the cell surface.

Both the microelectrodes were connected to an amplifier (Axopatch-2A Current and Voltage Clamp, Axon Instruments, USA). Microelectrode One injected pulses of current (-40nA) into the target cell. The signals recorded through Microelectrode Two were recorded on a chart recorder (Multitrace 2) or as digital signals on video tape (Betamax hifi, PAL stereo video cassette recorder SL-HF-100E, modified to record DC potentials from 0 to 10 KHz). Signals were simultaneously displayed on an oscilloscope (2210, Tektronix) to allow monitoring of the cell membrane potential during the experiment.

2.04.5 Compound delivery system

The compounds under investigation were delivered using a pressure ejection system (Neurophore BH-2 system, power supply model MS-2B, mainframe and balance BH-2 and pneumatic pump PPM-2), with the air pressure (2 kg/cm^2) provided by a modified hand pump (Hozelock 4036, UK). The pneumatic pump of the Neurophore BH-2 system was connected to a modified 1 ml syringe containing the compound to be tested. The syringe had been modified by drawing the end to a fine tube over a gentle flame. The pump was triggered for 2 to 20 second periods to expel a volume of solution from the delivery tube onto the flap preparation. The delivery system was calibrated by expelling distilled water into a petri dish of liquid paraffin for the same periods of time (based on McCaman *et al.*, 1977). The spherical drops of water were suspended in the liquid paraffin allowing the diameters to be measured under the light microscope using a graticule. The mean volume of solution expelled during each time period was calculated using the equation for the volume of a sphere; Equation 2.01.

Equation 2.01 Volume of a sphere

$$V = \frac{4}{3}\pi r^3$$

where: *V is the volume of the sphere*
r is the radius of the sphere.
π is the constant $22/7$

The quantity of PF4 ejected was calculated by multiplying the volume expelled by the concentration of the PF4 solution. There is a linear relationship between the pressure applied and the volume of liquid expelled by pressure ejection systems (McCaman *et*

al., 1977; Smith & Cunningham, 1983). Once calibrated, the equipment delivers a reproducible volume for a given pressure.

To rule-out any cell membrane effects arising from the effect of pressure alone, some test experiments were carried out. These involved the pressure ejection of ARS, the bathing solution (see Section 2.04.1), onto a target cell. Over five repetitions, there was no change in input conductance. However, two of the pressure ejections caused slight movement of the cell that resulted in small artefacts on the experimental traces. If the cause had not been recognised, these artefacts could be misinterpreted as small depolarisations (~1 mV). The occasional pressure artefacts were taken into account when analysing the experimental data, see Section 2.04.8.

2.04.6 Receptor location experiments

In the first set of experiments, the location of the receptors was investigated by applying the FMRFamide-Related Peptide PF4 at incremental distances from the centre of the muscle bag; gradually further from the target cell. The distance was measured accurately using the vernier scale on the Prior micromanipulators. The PF4 was applied at a concentration of 0.1 μM for 20 seconds. After each PF4 application, the PF4 was allowed to wash off for a period of at least 5 minutes. This ensured almost complete replacement of the contents of the recording chamber prior to the next application. The delivery tube was moved by increments of 50 μm after each application, to a total distance of 300 μm from the target cell. The target cell response, recorded by chart recorder, was a trace of the membrane potential and electrical resistance; see Figure 3.01 for an example. From this record, hyperpolarisation was measured and the conductance of the cell membrane was calculated.

2.04.7 Dose-response relationship of PF4

The second set of experiments was carried out to investigate a relationship between quantity of PF4 ejected and response. The PF4 was applied in pulses of 2, 5 and 10 seconds to the target cell and the resulting electrical activity was monitored as before.

The quantity of PF4 that was delivered in each pulse was calculated as described in Section 2.04.5.

2.04.8 Voltage clamp experiments

The third set of experiments explored the reversal potential of the PF4-activated responses. The technique employed was voltage clamping, which utilised the sharp electrode set up. Current was injected through Microelectrode One to clamp the cell at the required membrane potential while the resulting current flow was recorded through Microelectrode Two. The procedure was to hold (or clamp) the target cell at a series of potentials above and below the resting membrane potential. At each potential, PF4 was applied to the cell as described previously. γ-amino butyric acid (GABA) was applied to the same cells for comparative purposes. GABA is known to be a ligand of chloride ion channels (Martin, 1982). The response (the flow of electrical current through the cell membrane) was recorded on videotape (Betamax hifi PAL stereo video cassette recorder, modified to record DC potentials of 0 to 10 KHz).

The direction of current flow was dependent upon the membrane potential and the concentration of chloride ions on either side of the membrane. At the specific voltage at which the driving forces on the ions, due to concentration and potential, were in equilibrium, there was no net flow of chloride ions. The voltage at which there was no net chloride ion flow is the reversal potential. As the cell was clamped at the next potential in the series, the current changed direction. This change of direction was recorded for each voltage clamped cell.

2.04.9 Response time-course experiments

The fourth set of experiments was carried out to investigate the mode of action of PF4. This was done by measuring the delay between the application of PF4 to the target cell and the beginning of the cell's response; that is, "the delay of action". The period of PF4 application was marked on each recorded trace by using the "trigger" facility on the BH-2 Neuorophore. The beginning of the marked pulse therefore showed the point at which PF4 application started. The start of the response to PF4

was sometimes difficult to discern due to the occasional pressure ejection artefact obscuring the onset of hyperpolarisation, see Section 2.04.5. In order to delineate the response, it was necessary to fit a curve to the recorded trace. Since cell membrane hyperpolarisation is close to an exponential process, it was found that the experimental trace of the hyperpolarisation could be closely fitted with a first order exponential decay curve. The start of the response was the point at which the resting membrane potential intersected with the exponential decay curve describing the hyperpolarisation. By rearranging the equation of the exponential fit and substituting values obtained from the experimental trace, the start of the response was calculated using Equation 2.02. The exponential curve also provided the decay constant, which was a measure of the rate of development of the hyperpolarisation.

Equation 2.02 Exponential decay arranged in terms of the start of the hyperpolarisation response

$$x = x_0 - t_1 . \ln\left[\frac{y - y_0}{A_1}\right]$$

where:

x is the x intercept (start of the response),
x_0 is the x offset (close to the minimum value for x),
t_1 is the decay constant of the curve,
y is the y intercept (resting membrane potential),
y_0 is the y offset (the most negative value of y),
A_1 is the amplitude.

The delay of action was determined by simply subtracting the start of the PF4 application from the calculated start of the response.

The delay of action was made up of three components:

1. Mechanical delays due to the pressure ejection system,
2. Time for diffusion to the receptors on the target cell,
3. The physiological delay of signal transduction between the stimulated receptors and the ion channels.

The third parameter, the physiological delay, was of interest as it gave insight into the complexity of the intracellular signal transduction mechanism. A short physiological delay is associated with rapid relay of information from the receptor to the ion

channel, as with ligand-gated ion channels. A longer physiological delay is typical of the more complex signal transduction mechanisms that are seen with intracellular second messenger cascades.

However, it was not possible to separate the three components from an absolute measurement of the delay of action. In order to compensate for the mechanical and diffusional delays, the delay time for PF4 was compared with that of other compounds with known modes of action. The two criteria for choosing comparative ligands were that the ligands should act on receptors on the *Ascaris* muscle cell and that their modes of action should be known. A directly-gating ligand was required to provide a comparatively short delay of action and a second messenger mediated ligand was necessary to provide a comparatively long delay of action.
GABA was chosen for the first of the comparisons. The mode of action of GABA is that of a directly-gating ligand; that is, GABA binds with receptors to open intrinsic chloride ion channels without requiring any intracellular or membrane-delimited signal transduction (Hille, 1992). Directly-gating ligands act rapidly to elicit a response, see Section 1.07.3.

In contrast, the FaRP PF1 was selected as the comparatively slow-acting ligand. PF1 is thought to act via nitric oxide (Bowman *et al.*, 1995) as a second messenger system. Compounds that require second messenger activity to relay signals from the receptor to the ion channel (or other target) are slow to act.

PF4 was applied to each target cell before or after either GABA or PF1. Applying two different compounds to the same cell allowed direct comparison of the compounds by ruling out between-cell variation. Traces were recorded from the experiments on videotape and digitised using the Fetchan computer program (Axoclamp, USA). Curves were fitted to the hyperpolarisation phases of the responses using the computer program Origin 4.0.

2.05 Methods for the patch clamp experiments

Patch clamping (Hamill *et al.*, 1981) is an electrophysiological technique to examine individual ion channel activity in a small area of the cell membrane. It involves

isolating the small area, or "patch", by sealing a blunt micropipette onto a cell. The seal has to be tight to avoid leakage of ions through the gap between membrane and pipette tip. A low resistance seal (<1 GΩ) leads to current leakage through the gap, therefore results in a noisy recording. A clean, smooth membrane is required to ensure a high resistance seal between the membrane and the pipette tip.

2.05.1 Preparation of vesicles

To prepare suitable membranes, the flap preparation was treated with enzymes to produce clean membrane vesicles. A modified version of the method employed by previous workers was used (Standen *et al.*, 1984; Martin *et al.*, 1990). The enzyme treatment removes the collagen layer from the muscle cell surface and thus produces smooth membranes. Due to the hydrostatic pressure of the cells, an aspect of the enzyme treatment is the budding of vesicles from the muscle cell surfaces. These vesicles contain a small quantity of intracellular material. The membrane vesicles are suitable for using in patch clamp experiments as gigaseals are easier to form than with intact *Ascaris* muscle cells. The collagen treatment does not influence the ion channel population of the membrane (Standen *et al.*, 1984; Martin *et al.*, 1990).

To produce the membrane vesicles, the flap preparation was pinned-out in a small Petri dish lined with Sylgard™ and incubated in extracellular solution at 37° C for half an hour (Gallenkamp incubator, Fisons Electrical Equipment Division, UK). The composition of extracellular solution in mM was NaCl 35; NaAcetate 105; KCl 2; $MgCl_2$ 2; Glucose 3; HEPES 10; EGTA 1; Ascorbic acid 2; pH was adjusted to 7.2 with NaOH. The extracellular solution was poured off and replaced with freshly made enzyme solution containing 1 mg of crude collagenase per mililitre of solution. The composition of the enzyme solution in mM was as for extracellular solution without the EGTA. The flap preparation was incubated for a further 10 minutes at 37° C after which the enzyme solution was discarded. The preparation was washed with extracellular solution ten times to remove most of the collagenase and was incubated for 30 minutes. The preparation was examined under 40x magnification at the end of this period and vesicles that had formed were removed with a glass Pasteur pipette. Figure 2.03 shows a flap preparation that has produced vesicles.

The vesicles were expelled carefully into a recording chamber with approximately 1 ml of the extracellular solution from the petri dish. The base of the chamber was a clean glass coverslip. In an attempt to promote adhesion of vesicles, coverslips were coated with 10 % poly-L-lysine solution and allowed to dry prior to filling the recording chamber. This modification to the method did not make a noticeable improvement to vesicle adhesion so was abandoned. Instead, the glass coverslips were cleaned with water and detergent, rinsed thoroughly with hot water, then rinsed with 70% ethanol. This cleaning method resulted in acceptable vesicle adhesion: approximately 10% of vesicles would remain fixed to the base of the recording chamber after replacing the solution (see below).

After addition of the extracellular solution containing membrane vesicles, the recording chamber was left for 20-30 minutes at room temperature to allow the vesicles to adhere to the coverslip. After this period, as much of the extracellular solution as possible was removed by Pasteur pipette and was replaced with filtered bath solution (Nalgene syringe filters, Nalge Company, USA). The composition of bath solution, in mM, was CsCl 35; CsAcetate 105; $MgCl_2$ 2; HEPES 10; EGTA 1; the pH was adjusted to 7.2 with CsOH. The caesium ions were included to block potassium channels, the magnesium to promote giga seal formation (Hamill *et al.*, 1981); the HEPES to buffer hydrogen ions and the EGTA to chelate calcium ions (Marty & Neher, 1983). Of the anions present, chloride was at relatively low concentration, approaching intracellular chloride ion concentrations. Acetate made up the bulk of the anions in the bath solution.

The replacement procedure was repeated three times to replace as much of the extracellular solution as possible without destroying or washing away all the vesicles. The replacement procedure was essential for reducing the concentration of calcium in the recording chamber, both by dilution and by chelating free calcium ions. *Ascaris suum* membrane vesicles respond to calcium ions by opening chloride ion channels in the membrane (Thorn & Martin, 1987). While patch clamping, these large amplitude channel openings obscured any other channel activity in the membrane patch. At the beginning of the series of patch clamp experiments, calcium-dependent chloride channels were a common artefact. With more rigorous solution replacement (i.e. a greater volume removed from the chamber at each replacement step), the calcium

Figure 2.03 Electron micrograph of vesicle formation on a flap preparation

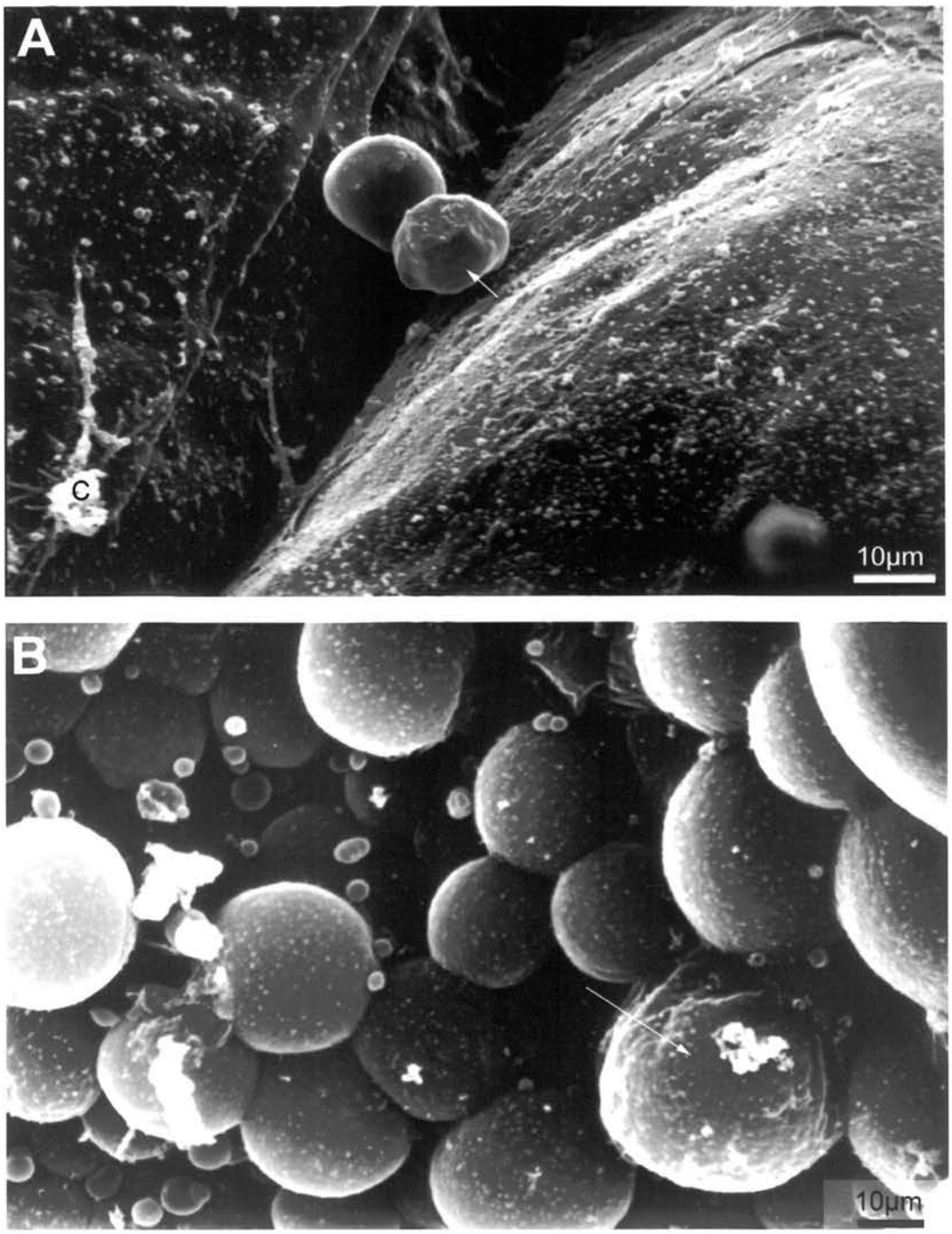

*The photographs show scanning electron micrographs (SEMs) of vesicle formation from the flap preparation following incubation with collagenase. SEM **A** shows adjacent muscle bags with two vesicles budding from the cell surface on the left. Traces of the collagen matrix, **C**, can be identified on the cell surface on the left. One vesicle has partially collapsed (indicated by arrow). The other vesicle is suitable for patch clamping, provided that it can be transferred to the recording chamber intact. SEM **B** shows a higher magnification view of vesicles forming on the cell surface. Collapsing vesicles can be recognised (arrow).*

concentration in the recording chamber fell and the large amplitude channel activity became rare.

The recording chamber was placed in position on the dissecting microscope stage (Nikon, Japan). In order to reduce the mechanical and electrical interference during experiments, the microscope was inside a custom-built Faraday cage, and rested on an anti-vibration air table (Technical Manufacturing Corporation, USA), as for the sharp electrode experiments (see Section 2.04).

2.05.2 PF4 preparation for inclusion in the pipette solution

PF4 was dissolved in distilled water and stored as a 1 mM solution at -20° C. 10 µl aliquots were defrosted and diluted with pipette solution to a final concentration of 0.3 to 0.003 µM as they were required. The pipette solution was filtered through Nalgene syringe filters, pore size 0.2 µm (Nalge Company, USA) to avoid blocking the pipettes.

2.05.3 Patch pipettes

Patch pipettes were made from borosilicate glass tubing (type 7052, Garner Glass, USA) using a PB-7 Micropipette puller (Narishge, Japan). The puller settings were adjusted to obtain a pipette tip diameter of ~1 µm. The pipette tips were coated in Sylgard™, carefully applied to cover the shank of the pipette and as much of the tip as possible without damaging or occluding the end. A spiral-shaped heating element was used to cure the Sylgard™. The pipette tips were then fire polished to melt the tip of the pipette and thus produce a clean, smooth rim to the glass, a feature that assisted seal formation. Fire polishing was carried out under a microscope (Vickers, UK) to allow visualisation of the pipette tip (magnification up to 400x). A platinum wire, heated to dull red, provided the heat source for fire polishing. The final stage of pipette preparation was to fill the micropipettes with filtered pipette solution. The composition of the pipette solution was CsCl 140; $MgCl_2$ 2; HEPES 10; EGTA 1. The pH was adjusted to 7.2 with CsOH and PF4 was added as required. The purpose of the pipette solution constituents was the same as for components of the bath

solution (see Section 2.05.1). However, all the anions in the pipette solution are chloride ions, to approximate extracellular solution.

Filling was achieved by dipping the tip of the pipette into filtered pipette solution to fill the narrow tip region by capillary action. The body of the pipette was then half-filled with filtered solution through a syringe, which had been drawn to a fine tube. A few sharp taps to the body of the pipette dislodged any air bubbles blocking the tip.

After filling each patch pipette, the blunt end was briskly heated to ensure that the edge in contact with the pipette holder was clean and smooth.

2.05.4 Recording channel activity

The filled patch pipette was firmly screwed into the amplifier head stage (Axon 200B Integrating Patch Clamp, Axon Instruments, USA). Static electrical discharge can damage the sensitive electronic components of the amplifier so care was taken to earth the operator prior to touching the head stage. The angle of the head stage was adjusted to about 45° to aim the patch pipette towards the recording chamber. The head stage was then moved down with micromanipulators (for coarse manipulation: Prior, UK; for fine movement: Narishige, Japan) until the pipette tip was adjacent to a vesicle. This delicate procedure was carefully monitored through the dissecting microscope (magnification 75-300x). On contact with the vesicle, gentle suction was applied to the patch pipette using a 1ml syringe, see Section 1.09.3 and Figure 1.04. Seal formation was recognised by a large increase in electrical resistance of the pipette. Seals of 10 GΩ or more were sufficiently high to be acceptable for experimental use. The oscilloscope trace was monitored to check the electrical noise levels of the resting membrane. Traces more than 0.5 pA wide at 0 mV were rejected as being excessively noisy. The electrical activity in those patches with suitable seals and low noise was recorded on digital audio tape (Digital Tape Recorder, DTR-1205, Biologic Science Instruments). Signals were filtered at 1 KHz (custom-built filter) and displayed on an oscilloscope (2210 Digital Storage Oscilloscope, Tektronix) simultaneously with the recording procedure, to allow monitoring during the experiments.

When a patch was successfully clamped at 0 mV, recording was started immediately and continued for 2 to 5 minutes. The patch was clamped at a series of negative and positive potentials; patch activity was recorded at each voltage. Where possible, sequential patches were clamped from the same vesicle with alternate pipettes containing PF4 and control solution. The population of receptors and ion channels over the muscle bag surface was assumed to be uniform as this was considered to be the simplest model of membrane structure. Since each vesicle was derived from a small area of muscle cell membrane, following the "simplest model" argument, the receptors and ion channels should be equally distributed across the surface of the membrane vesicle. Therefore, successive patches clamped from a single vesicle should all be representative of the parent muscle cell membrane. The strategy of exposing successive patches from a single vesicle to different solutions allowed the response to PF4 to be compared directly with the response to control solution in the same portion of membrane. Exposing the same vesicle to different stimuli was a stringent comparison since other variables, such as differences between individual vesicles, flap preparations or day-to-day experimental conditions did not affect the results. Pairing samples also allowed the use of the paired *t* test, a rigourous statistical test to determine the significance of any differences in results. It was not always feasible to make several consecutive patches from one vesicle due to bursting or movement of the vesicles.

A series of dose-response experiments was completed. The response to various PF4 concentrations (0.003 to 0.3 μM) was noted in vesicle-attached patches. Recordings were made in filtered bath solution (Nalgene syringe filters, 0.2 μm pore size, Nalge Company, USA).

2.05.5 Mode of action of PF4: patch isolation

To investigate the mode of action of the ion channels activated by PF4, several refinements were made to the basic dose-response protocol. The first of these refinements was the isolation of patches at the end of the dose-response experiment. By isolating the patch of membrane from the parent vesicle, any connections with intracellular signal transducers inside the vesicle were lost. A response to PF4 after isolation indicated that the channels' mode of action was independent of intracellular

mechanisms. Isolation was achieved by raising the pipette from the vesicle after recording patch activity across the range of potentials. In about 50 % of cases, elevating the pipette detached the patch from the parent vesicle; in the remainder, the patch failed to detach or ruptured during the procedure. 15 to 20 minutes were allowed to ensure dispersal of any remaining intracellular contents, then recordings were made from the isolated patch at positive and negative potentials.

2.05.6 Mode of action of PF4: effect of remote receptors

The second set of experiments to study the mode of channel action involved the addition of PF4 to the bath solution to determine whether receptors in the vesicle-attached patch responded to PF4 outside the pipette. The gigaseal (seal resistance greater than1 GΩ, (Neher, 1981; Hamill *et al.*, 1981)) formed at the junction of the patch pipette and the vesicle membrane leaves a narrow gap, ~1 Å wide, (Hamill *et al.*, 1981) between glass and membrane. The 1 Å gap is too narrow for molecules to pass through; PF4 applied to the vesicle outside the patch pipette will not gain access to the patch. Any increase in activity due to the PF4 in the bath indicated that receptors outside the pipette were relaying signals to channels in the patch. To carry out the investigation, a patch was clamped, exposed to a low concentration of PF4 in the pipette (0.003 μM PF4) and recorded as for the dose-response protocol. PF4 was then added to the bath to obtain a concentration of 0.1 μM. A period of 20 minutes was allowed for PF4 to diffuse through the bath, then recordings were made from the patch.

2.05.7 Mode of action of PF4: G-protein inhibition

The third set of experiments to look at channel mode of action involved the use of guanosine 5'-O-(2-thiodiphosphate) (abbreviated to GDP-β-S). This non-hydrolyzable GDP analogue inhibits G-protein activity by binding irreversibly to the α subunit of the G-protein. GDP-β-S is a large, charged molecule that is hydrophillic and so can not pass through membranes. The GDP-β-S was added to the bath solution to a concentration of 100 μM and recordings were made from vesicle-attached patches as for the dose-response study. The vesicle-attached configuration protected the intracellular surface of the membrane patches from the GDP-β-S, therefore these recordings were the experimental control. Each patch was then

isolated from the parent vesicle, exposing the intracellular surface of the patch to the GDP-β-S. A period of 15 to 20 minutes was allowed to elapse to ensure that any G-proteins on the inner surface of the patch had been inhibited by the GDP-β-S, and recordings were made as before. Any difference in the channel activity before and after exposure to GDP-β-S which could not be explained by isolation (tested in the first set of experiments to examine mode of action) was due to G-protein inhibition.

2.06 Materials

All chemicals were obtained from the Sigma-Aldrich Company Limited, Poole, UK; except for PF4 and PF1 which were gifts from the Pharmacia and Upjohn Corporation, Kalamazoo, USA.

2.07 Recipes for solutions

All quantities are grams per litre distilled water, unless stated otherwise.

Locke's solution

NaCl	9
KCl	0.42
$CaCl_2$	2.1 ml
$NaHCO_3$	0.15
Glucose	1

Ascaris Ringers solution

NaCl	7.9
KCl	0.21
$CaCl_2$	3 ml
$MgCl_2$	5.7 ml
Glucose	0.54
TRIS	0.605

pH to 7.6 with maleic acid.

Extracellular solution

NaCl	2.047
NaAcetate	8.613
KCl	0.142
$MgCl_2$	2 ml
Glucose	0.54
HEPES	2.38
EGTA	0.38
Ascorbic acid	0.352

pH to 7.2 with NaOH

Enzyme solution

As for extracellular solution (above) without the EGTA. Crude collagenase (Type I, activity: >125 collagen digestion units per mg solid, Sigma catalogue number C0130) was added to the enzyme solution just before use, at the rate of 1 mg collagenase per ml of solution.

Bath solution

CsCl	5.89
CsAcetate	20.15
$MgCl_2$	2 ml
HEPES	2.38
EGTA	0.38

pH to 7.2 with CsOH

Pipette solution

CsCl	23.57
$MgCl_2$	2 ml
HEPES	2.38
EGTA	0.38

pH to 7.2 with CsOH

2.08 Acceptance of experimental records and data analysis

2.08.1 Choice of records for analysis

Records were made of all experiments unless the electrical activity of the whole cell or the membrane patch was very obviously unstable or noisy at the outset. The first step in analysing data after the experiments were completed was to make an initial visual survey of the records. Ambiguous records were discarded at this stage and the remaining data was deemed clear enough to analyse objectively. Limits were set for acceptable records before carrying out the initial visual survey to reduce bias in data selection.

The limits were as follows for the current clamp experiments. Records had to show steady cell membrane behaviour in order to assess the effects of PF4, PF1 and GABA. To this end, at the start of the experiment, the input resistance of the cell had to be greater than 250 KΩ and the resting membrane potential had to be as steady as possible. A change of more than 5 mV per minute or 25 KΩ per minute led to rejection of the record. Equally, erratic changes in membrane potential due to mechanical vibration or muscular activity in the flap preparation made records unsuitable for analysis.

For patch clamp work, limits were set to minimise electrical noise so that any channel activity would be recognised. With this in mind, the gigaseal between the patch pipette and the vesicle membrane had to have a resistance of at least 10 GΩ and the electrical trace of patch activity had to be not wider than 0.5 pA. Records containing calcium-dependent chloride channel activity (see Section 1.07.2) were rejected on the grounds that these large amplitude channels obscured other ion channel activity.

2.08.2 Data analysis

All data, whether recorded on videotape or digital audio tape, had to be filtered and digitised prior to analysis. Filtration removed excess electrical noise from the recording to produce a clear trace; the recorded signals were filtered at 1 KHz (custom-built filter) before digitisation. Digitisation transformed the analogue data

from the channel records into a digital format suitable for computer analysis. Digitisation was carried out using a Digidata 1200 series interface (Axon Instruments, USA) in conjunction with a personal computer (IBM) and the computer software Clampex 7.0 (Axon Instruments, USA). The first 110 seconds of each record was digitised at a sampling interval of 100 μs.

To analyse the current clamp experiments, the computer program Origin 4.0 (Microcal Software Incorporated, USA) was used to fit exponential curves to the digitised data. The digitised patch clamp records were filtered at 100 Hz and converted into amplitude histograms and events lists with the computer program Fetchan 6.0.6.04 (Axon Instruments, USA). Analysis of the events lists was carried out in Pstat 6.0.5 (Axon Instruments, USA) and Excel 97(Microsoft Corporation, USA).

On occasion, it was necessary to use computer programs that utilised the NAG subroutine E044CC for mathematically fitting curves to data. This is a rigorous analysis tool because it treats each data point individually rather than taking the more rapid approach of using binned data. The Fortran computer programs used for fitting Gaussian curves to non-binomially distributed data and the Michaelis Menton equation to dose-response data applied the NAG subroutine E044CC to achieve an accurate fit.

2.09 Statistics

The statistical analysis was carried out in Excel 97 and Minitab 13.1 (Microsoft Corporation, USA). The Anderson Darling test for normality was carried out to assess the distribution of data. Groups of normally distributed data were compared with Student's *t* test or by Analysis of Variance (ANOVA). The two sample *t* test was used for comparing samples of small size ($n<30$). Where experiments produced sets of paired observations ($n<30$), the more stringent paired *t* test was utilised. For comparing three or more groups, ANOVA was chosen. In line with general convention, *P* values of less than 0.05 were considered to be significant and *P* values less than 0.01 were considered to be very significant.

2.10 Dose-response curves

When a physiological response to a drug is dependent on the drug concentration, the reaction can be described in terms of Michaelis Menton kinetics (Grahame-Smith & Aronson, 1992). For dose-response curves, the essence of the Michaelis Menton reaction is that the response increases with increasing drug concentration, until the physiological system is saturated. At this point, the response stays at maximum level regardless of further increase in drug concentration.

Michaelis Menton kinetics can be expressed mathematically because drug-receptor association and dissociation are governed by mathematical constants, and are therefore predictable; see Equation 2.03.

Equation 2.03 The Michaelis Menton equation for ligand-receptor interaction

$$R_O = \frac{[D]}{K_d + [D]}$$

where: R_O *is receptor occupancy, or the proportion of receptors occupied*
[D] is the drug concentration
K_d *is the equilibrium constant*

The simplest model of drug-receptor interactions assumes that there is a 1:1 ratio of drug molecules to receptors, and that each interaction between a single drug molecule and a single receptor contributes equally to the response. If this assumption is made in Equation 2.03: firstly, R_O (the proportion of receptors that are occupied by drug) is equivalent to response. Secondly, K_d, the equilibrium constant, is equal to the EC50, that is, the drug concentration that will produce 50 % of the maximum response. The EC50 is a measure of drug potency. A graphical representation of the interaction can be plotted on numerical axes to produce a hyperbolic curve, or as response against the log of drug concentration to give a sigmoid curve.

The Michaelis Menton equation is based on the assumption that one drug molecule interacts with each receptor molecule. However, not all drug-receptor interactions are so straightforward. In some cases, a response is seen only after several ligand molecules have bound to the receptor. A case in point is the nicotinic acetylcholine

receptor of frog muscle motor end-plates. Each receptor requires two agonist molecules to bind in order for the channel to open. The binding of the first molecule promotes the binding of the second; i.e. the binding process is cooperative (Dionne *et al.*, 1978). The Hill equation is a modification of the Michaelis Menton equation that takes the possibility of cooperative binding into account, see Equation 2.04.

Equation 2.04 The Hill Equation

$$R_O = \frac{[D]^n}{K_d{}^n + [D]^n}$$

where: R_O *is receptor occupancy, or the proportion of receptors occupied*
[D] is the drug concentration
K_d *is the equilibrium constant*
n is the Hill coefficient

Where there is one drug molecule per receptor, the Hill coefficient is 1, making the Hill equation identical to the Michaelis Menton equation. However, when cooperativity exists between drug molecules acting at a receptor site, the Hill coefficient will be >1, and will give an indication of the number of binding sites per receptor.

2.11 Distribution of Channel Events

When interpreting ion channel records, it is important to recognise the baseline of the record (zero current level; i.e. the periods during which all channels are closed) in order to count the number of channels that are active within the patch. Where a number of channels are active in the membrane patch, the recording of patch activity shows several levels of channel opening, making it difficult to identify the baseline. The difficulty in interpretation is compounded if the ion channels have a high P_{open} or a long mean open time, since both characteristics increase the duration of channel opening and hence the likelihood that several channels will be open simultaneously. A representative experimental record showing multiple channel openings is shown in Figure 2.04.

Figure 2.04 Experimental trace showing multiple channel activity in a membrane patch

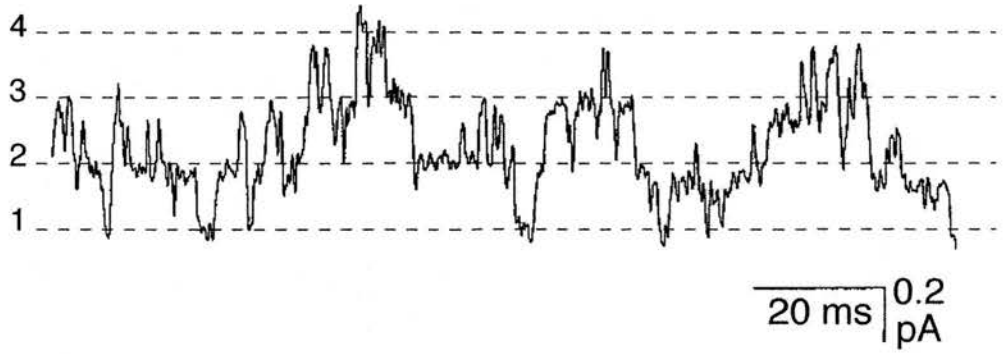

This trace is from an experiment in which several ion channels were active in the membrane patch. The trace shows the channel openings during a 150 ms period; the channel openings are represented as upward deflections. Four distinct levels of channel activity can be seen; each level is equivalent to the current passing through one channel. On visual examination, it is difficult to decide whether or not the lowest level (level 1) is the closed state, when no ion channels are open. This record illustrates the need for an objective judgement as to the position of the base line, or closed state, in a trace with multiple channel activity. It is important to know if the duration of a channel record is sufficient to show the base line clearly.

To ascertain whether the zero current level is likely to be visible in any given channel record, the distribution of channel openings must be considered. The durations of ion channel openings are binomially distributed (Colquhoun & Hawkes, 1983), since each opening is independent of the others occurring in the same or surrounding channels. Equation 2.05 describes the likelihood that channels in a patch will open (Colquhoun & Hawkes, 1983).

Equation 2.05 The probability of simultaneous channel opening

$$P_{(r)} = \frac{N!}{r!(N-r)!} \cdot {p_o}^r (1-p_o)^{N-r}$$

where: $P_{(r)}$ *is the probability that r channels are open*
N *is the total number of channels present*
r *is the number of channels open at the moment of observation*
p_o *is the* P_{open} *of the channel type.*

The distribution of channel openings according to this equation is shown in Figure 2.05.

Figure 2.05 Theoretical occurrence of channel openings in a membrane patch

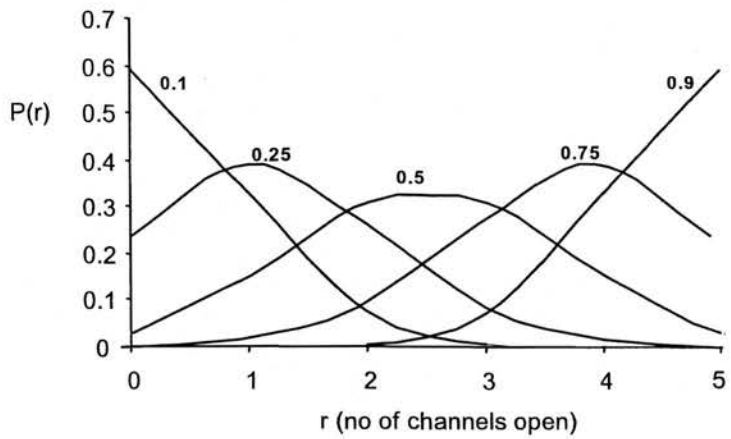

The number of channels observed in the theoretical patch (r in the equation) has been plotted against the probability that r channels are open ($P_{(r)}$ in the equation). There are five hypothetical membrane patches represented here, each with a different value of P_{open}, and the total number of channels per patch is five. Each set of data is a series of integers (it is impossible to observe a fraction of an ion channel) but for clarity, the histogram representing each membrane patch is delineated by a Gaussian curve. The number assigned to each curve is the relevant value of P_{open}. As the P_{open} of the channels increases, the distribution moves to the right because channels are open for longer, increasing the likelihood that all the channels in the patch open at once.

At high values of P_{open}, the baseline is unlikely to be seen in a short record. For example, consider the patch illustrated in Figure 2.05. This theoretical patch contains five ion channels; all, some or none of which are open at any given time. If the P_{open} of these hypothetical channels is 0.9, the probability of observing no channel openings ($P_{(r=0)}$) is $1x10^{-5}$. Therefore, the base line (no channels open) will be visible 0.001 % of the time, on average. In a one minute long record of the activity of this theoretical patch, the base line would be observed for an average of 0.6 ms. This short period of zero opening might be discounted during analysis, leading to underestimation of the total number of channels. However, 0.9 is an unusually high P_{open} value. The P_{open} values of the channel records obtained in the experiments fell into three groups: 0.05, 0.30 and 0.65. For a patch containing five ion channels with a P_{open} of 0.65, the $P_{(r=0)}$ is 0.005, giving an average of 300 ms of base line in a one minute long record. It can be assumed, therefore, that the base line can always be recognised where the P_{open} is less than 0.9 and there are five or fewer channels.

2.12 Light microscopy

Whole *Ascaris* were fixed for light microscopy by perfusing the body cavity with formal saline (10 % formaldehyde in 0.9 % saline), following the method of Rosenbluth (1965b). The rostral 2 cm of the worm was removed and a syringe needle was introduced into the body about half way along its length. 20 ml of formal saline was injected by syringe over a period of approximately 20 minutes, the formal saline and body fluid exiting rostrally. Sections 1 cm long were cut from the anterior half of the fixed worms and were embedded in wax prior to cutting serial sections (7 μm thick) with a microtome (American Optical 820). The sections were placed on microscope slides and some were stained with Mallory's phosphotungstic acid-haematoxylin to identify collagen. Others were stained with periodic acid-Schiff to stain carbohydrates.

The procedure for staining with Mallory's phosphotungstic acid-haematoxylin (PTAH) was as follows (Culling *et al.*, 1985): the cut sections were rehydrated and were placed in 0.25 % potassium permanganate solution for five minutes. After washing the sections in water, they were placed in 5 % oxalic acid for two minutes and then rinsed in distilled water. They were then left in PTAH overnight (16 to 18 hours). Excess stain was shaken off the slides and the sections were dehydrated with 95 % and absolute alcohol. The slides were then sealed with synthetic resin and viewed under the microscope.

The method for staining with periodic acid-Schiff (PAS) (Culling *et al.*, 1985) was as follows: the tissue sections were rehydrated, immersed in 1 % periodic acid solution for five minutes then washed in running water for five minutes. After rinsing in distilled water, the sections were placed in Schiff's reagent for 15 minutes. Sections were washed in running water for ten minutes then counterstained with Mayer's haematoxylin for two to three minutes. Finally, the sections were dehydrated with alcohol and cleared with xylene before mounting. The slides were then examined under the light microscope.

2.13 Electron microscopy

2.13.1 Scanning electron microscopy

The scanning electron micrograph of the flap preparation (Figure 2.01) was taken using routinely prepared tissue. The flap preparation was made as described above and was pinned-out in a petri dish lined with Sylgard™. The tissue was fixed for at least three hours by immersion in 3 % glutaraldehyde in 0.1 M sodium cacodylate buffer (pH 7.4), abbreviated to SCB. Fixation was followed by three 20 minute washes in 0.1 M SCB. A 1 % osmium tetroxide solution (in 0.1 M SCB) was used in a 1-2 hour post-fixation step (Sabatini *et al.*, 1962). The flap preparation was dehydrated in 30 minute steps using increasing concentrations of acetone (50-100 %) (based on Hayat, 1970). The tissue was dried using carbon dioxide and a critical point dryer (Poleron E3000 SIICPD) and sputter coated with a 20 nm layer of gold/palladium (60/40) in an Emscope SC500 sputter coater. The sample was viewed under an electron microscope (Philips 505).

Scanning electron micrographs of the formation of vesicles (Figure 2.03) were taken by incubating the flap preparation to produce vesicles (as described above) and arresting the vesicle formation by pouring off the extracellular solution and replacing it with 3 % glutaraldehyde in 0.1 M SCB. The preparation of the tissue proceeded as for the flap preparation outlined in the previous paragraph.

2.13.2 Transmission electron microscopy

Ascaris tissue was prepared for transmission electron microscopy by fixation with 3 % glutaraldehyde in 0.1 M SCB, injected into the worm as described for light microscopy, see Section 2.12. Transverse sections of *Ascaris*,1 cm long, cut from the anterior half of the body were left in 3 % glutaraldehyde in 0.1M SCB for 2 to 24 hours. After at least two hours, the fixed tissue was washed three times in the buffer solution for 20 minutes each time. The samples were then fixed in 1 % (w/v) osmium tetroxide in 0.1 M SCB for one hour at 4° C, after which they were washed three times in deionised distilled water for 20 minutes each time (Sabatini *et al.*, 1962).

The fixed tissue samples were dehydrated in a series of 10 minute incubations with increasing concentrations of acetone (50 %, 70 % and 90 %; based on Hayat, 1970). Dehydration was completed by three consecutive incubations with 100 % acetone. The dehydrated samples were infiltrated with 50/50 mixture of Araldite™ and 100 % ethanol overnight at 60° C and were then embedded in Araldite™ (Glauert & Glauert, 1958). A Diatome diamond knife was used to cut 80 nm sections of the tissue (Reichert OMU4 Ultracut Ultramicrotome), which were mounted on 200 mesh copper grids. An LKB Ultrostainer (Leica UK Ltd.) was used to stain the mounted sections with uranyl acetate and lead citrate (Reynolds, 1963). The sections were examined using a Philips CM 12 transmission electron microscope.

Chapter 3. Whole cell responses to PF4: results of sharp electrode work

In the sharp electrode experiments carried out on *Ascaris suum* muscle cells, the following results show that there are receptors that respond to PF4 on the cell surface. It was observed that activation of these receptors causes an increase in chloride conductance. The gross effect of PF4 application is muscle relaxation. Occasionally, the tissue movement during somatic muscle relaxation displaced the microelectrodes from the target cell, curtailing individual experiments.

The resting membrane potential of the *A. suum* somatic muscle cells was found to be -31.9 ± 0.9 mV (mean ± standard error of the mean, n=72). This observation is in line with the findings of previous workers, (Martin, 1980: -31 ± 1 mV; Holden-Dye *et al.*, 1997: -31.4 ± 0.4 mV). The input conductance was 2.27 ± 0.05 μS (n=102). Previous studies obtained similar values for the input conductance of *Ascaris* somatic muscle cells (Martin, 1980: 2.4 ± 0.2 μS; Holden-Dye et al., 1997: 1.79 ± 0.06 μS)

Figure 3.01 Application of PF4 to the bag region of* Ascaris suum *somatic muscle cell

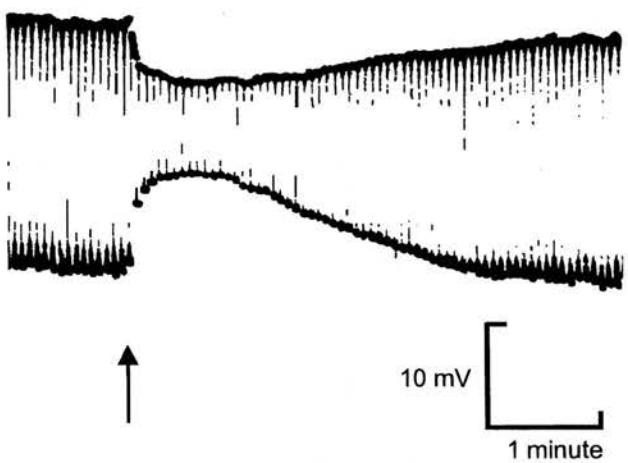

A recording of the membrane potential and input conductance of an Ascaris *muscle cell. The upper edge of the trace is the membrane potential of the cell, the downward deflections (initially 25 mV) are due to injections of current into the cell which cause corresponding hyperpolarisation. The width of the trace is inversely proportional to the electrical conductance of the membrane. Prior to the application of PF4 (marked by the arrow), the cell's resting potential was -27 mV and the conductance was 1.6 μS. The effect of PF4 was to hyperpolarise the cell to -33 mV and to increase its conductance to 4.7 μS.*

Figure 3.01 shows an example of the muscle cell response to PF4 application. PF4 acted rapidly (mean delay between application of PF4 and response was 1.5 seconds), with a similar time course to the neurotransmitter γ-amino butyric acid (GABA). In contrast, the peptide PF1, which also acts on the *Ascaris* muscle cells, has a slower time course (mean delay was 3.75 seconds) than PF4; see Figure 3.07.

3.01 Current clamp results: effects of focal PF4 application at different distances

The first set of current clamp experiments was carried out to determine where the PF4 receptors were located within the flap preparation. After the initial application of PF4 to the target cell, the delivery tube was moved laterally in increments of 50 μm. Thus, the PF4 was ejected further from the target cell and the peak response of the cell (measured as change in both conductance and membrane potential) declined. Figure 3.02 shows how the response became smaller as the PF4 was applied at increasing

Figure 3.02 The effect of distance from the target cell on the response to PF4

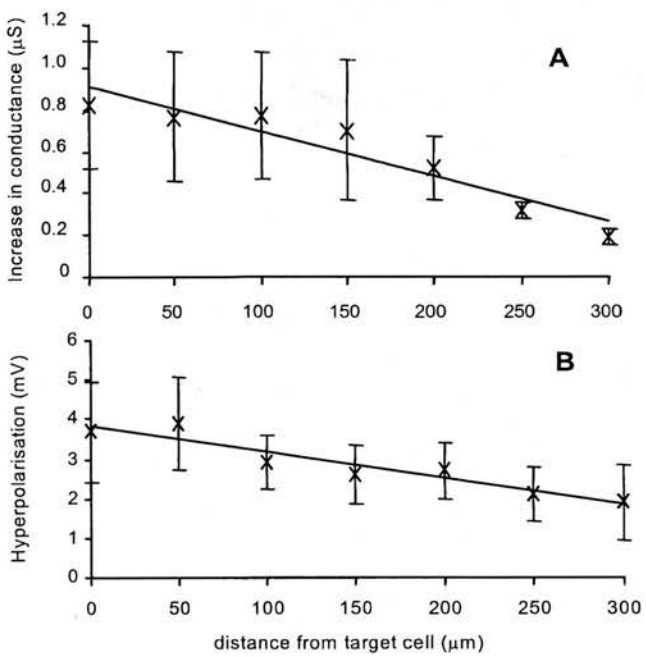

The response of the target cell is plotted against the horizontal distance between the PF4 delivery tube and the cell. Mean responses are shown (X) and the error bars indicate the standard error of the mean. The lines were fitted by linear regression and both have an R squared value of 0.9. n=5. ***A*** *shows the increase in membrane conductance,* ***B*** *shows the hyperpolarisation response. The cells were ~150 to 200 μm in diameter. All responses were measured 18 seconds after the start of a 20 second long PF4 application.*

distance from the target cell. This observation indicates that the PF4 was acting within ~50μm of the muscle bag, i.e. on receptors on the bag region of the muscle, rather than remotely via the nerve cord or hypodermis. Response to a local stimulus implies that there are receptors capable of responding to PF4 on the muscle cell surface.

3.02 Current-clamp results: dose-dependent effects of PF4

The response to PF4 application was dose-dependent, whether measured in terms of hyperpolarisation or increase in conductance. The pressure ejection delivery system allowed the amount of PF4 to be accurately quantified (see Section 2.04.5). The dose of PF4 was calculated from the volume ejected; a method that was employed by other workers using similar equipment (McCaman *et al.*, 1977; Smith & Cunningham, 1983). The dose-response relationship is shown in Figure 3.03; plot A shows the response in terms of conductance, B shows response as hyperpolarisation. The graph shows a linear relationship between the log of the amount of PF4 ejected onto the cell and the subsequent response.

Figure 3.03 The relationship between the quantity of PF4 ejected onto the cell and the response.

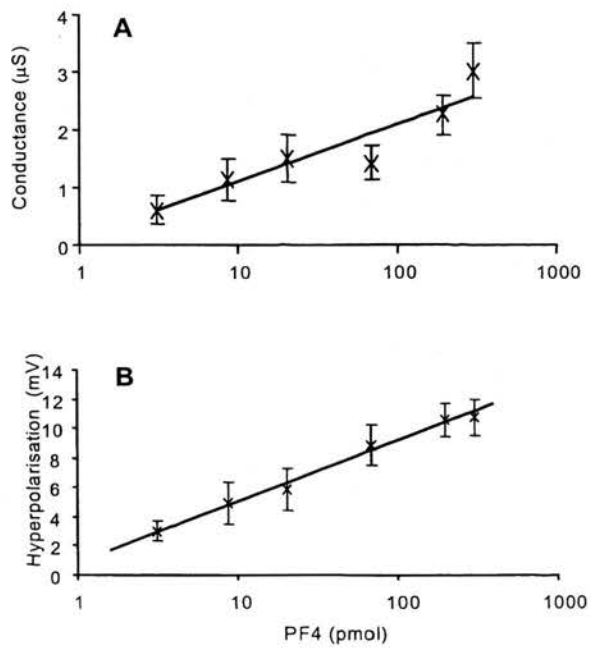

*The cellular response is plotted against the log of the quantity of PF4 ejected onto the target cell (pmol). The mean response values are shown by X and the error bars indicate the s.e.m.. The lines are fitted by linear regression and have R squared values of 0.87 (**A**) and 0.99 (**B**). Each point represents the mean of 7 or 17 experiments. **A** shows response as change in membrane conductance (μS), **B** shows response in terms of hyperpolarisation.*

3.03 Voltage-clamp results

The reversal potential of the PF4 current was determined in the voltage clamp experiments. The PF4 reversal potential was found to be the same as that of GABA.

In order to identify the ions involved in the GABA and PF4 responses, the sharp electrode equipment, (previously used for current clamping) was employed for voltage clamp experiments. By clamping the cell membrane at a predetermined voltage and applying PF4 or GABA to open ion channels, the resulting flow of ions, or electric current, was measured. The direction of current flow was dependent upon the ion concentration gradient and the membrane potential of the cell. Figure 3.04 shows three stages in a voltage clamp experiment: the current response to PF4 reverses at approximately -45 mV in this typical experiment.

Figure 3.04 An example of a voltage clamp trace

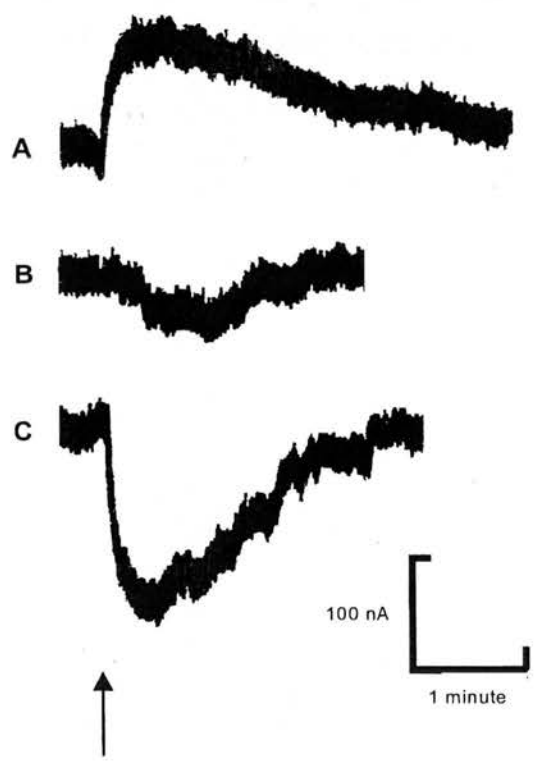

*Three consecutive traces are shown from a voltage clamped cell. In each trace, current flow is zero until the application of PF4, shown by the arrow. In **A**, the cell was clamped at -39 mV. When the PF4 was applied to the cell (arrow), there was an outward current (upward deflected) indicating that anions were moving into the cell. In **B** the cell was clamped at -49 mV. The response to PF4 was an inward current (downward deflected) showing that anions were moving out of the cell. In **C**, the cell was clamped at -59 mV and the PF4-induced current was a larger inward current (downward deflected). In this experiment, the ion flow reversed at approximately -45 mV.*

From the data obtained in voltage clamp experiments, current-voltage (I-V) plots can be drawn (see Figure 3.05 for an example) allowing more accurate calculation of the reversal potential. The I-V plots were produced by plotting the potential at which the cell membrane was clamped (V) against the current response to an application of PF4 or GABA (I). Linear regression was used to fit a line to the data points. The value of V corresponding to I=0, i.e. when no current is flowing, was the reversal potential.

Figure 3.05 A current-voltage plot from a typical experiment

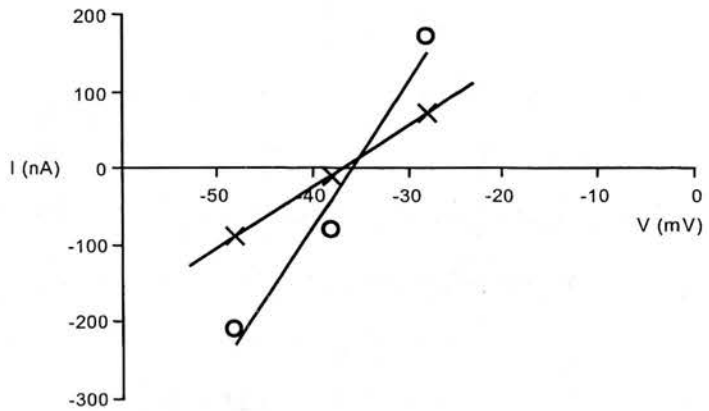

*The current response (I) is plotted against the voltage (V) at which the cell was clamped. PF4 responses are shown as open circles O and GABA responses as **X**. The lines are fitted by linear regression, in both cases R squared >0.9. The reversal potential is the value of the voltage when current is zero, i.e. the x-axis intercept. The reversal potential for PF4 is -36 mV, for GABA it is -37 mV. The different gradients of the lines reflect the different conductance following application of each compound.*

The PF4 reversal potential was -40.6 ± 2.8 mV, GABA's reversal potential was -39.2 ± 5.1 mV (mean ± standard error of the mean). There was no significant difference between the two reversal potentials (paired *t* test, $P>0.3$, n=5), consistent with the interpretation that the same ions are moving across the membrane in response to both GABA and PF4. GABA is known to act on chloride ion channels (Martin, 1982), therefore it is argued that PF4 must also open chloride ion channels. The reversal potential of any ion under given conditions can be calculated using the Nernst equation (Hille, 1992). The Nernst Equation for chloride ions under the experimental conditions described here is Equation 3.01.

Equation 3.01 The Nernst equation for chloride ions

$$E_{rev} = \frac{RT}{zF} \cdot \ln \frac{[Cl^-]_{in}}{[Cl^-]_{out}}$$

where:

E_{rev} is the reversal potential for chloride ions
R is the gas constant, 8.314 J/mol/K
T is the absolute temperature, 305 K
z is the chloride ion valency, 1
F is the Faraday number, 96487 C/mol
$[Cl]_{in}$ is the chloride ion concentration inside the cell, 17 mM (Parri et al., 1990)
$[Cl]_{out}$ is the chloride ion concentration outside the cell, 175.8 mM

E_{rev} is -61.4 mV for the conditions defined above.

The theoretical value for the chloride reversal potential was more negative than the value obtained in the experiments. The most likely explanation for the discrepancy was that it was due to the leakage of chloride ions across the cell membrane. *Ascaris* muscle cell membranes are slightly permeable to chloride ions even in the absence of ligands (Brading & Caldwell, 1971; Martin, 1980). During the course of each experiment, chloride slowly leaked into the cell (diffusing down its concentration gradient) resulting in an increase in the intracellular chloride ion concentration. The increased $[Cl^-]_{in}$ shifted the experimental reversal potential in the positive direction. Another explanation is that the value of 17 mM for intracellular chloride ion concentration was measured using fresh *Ascaris* from a recently slaughtered pig (Parri *et al.*, 1990). During *in vitro* maintenance, worms continue to metabolise glycogen (Harpur, 1963; Blair *et al.*, 1998). The size and contents of the muscle cells changes with time, therefore it is probable that the intracellular chloride ion content changes as well. Thus, it is possible that the older worms used in some of the present experiments had a higher $[Cl^-]_{in}$ than that measured by Parri *et al.* and hence a more positive chloride reversal potential than the theoretical value calculated with Equation 3.01.

3.04 Current clamp results: delay times

The time course of the response to PF4 application was investigated. The delay between application of the peptide and the appearance of a response was compared

with the delay following application of other compounds to the same target cells. This method provided an intrinsic experimental control because the response of each target cell to PF4 was compared directly with its response to the second compound. By making a comparative measurement, the method also took into account any delays intrinsic to the experimental set-up (e.g. mechanical delays in the pressure ejection system, physical delays due to the diffusion from the delivery tube to the target cell surface), see Section 2.04.9. Before measuring the delay between stimulus and response of the cell membrane receptors, the time constant of the membrane was investigated.

3.04.1 The intrinsic time constant of the membrane

Cell membranes act as electrical capacitors. That is, they can store electrical charge on both sides of the membrane separated by the phospholipid bilayer, which is an effective electrical insulator. When the electrical field around the cell membrane changes, the capacitor must discharge and recharge, a process that requires some time. When the capacitance of a cell membrane is slow to change, the electrical response of the cell to stimulus is delayed. The time constant of the cell membrane was measured at the resting membrane potential while depolarising current pulses were injected into the cell. Measurement was carried out by fitting a first order exponential curve to the trace at the point where the membrane was charging to the hyperpolarised potential. The intrinsic time constant of the cell membrane, which describes the rate of change of the membrane potential, was ~10 ms (n=5). This was two orders of magnitude less than the delay in the response to PF4, GABA or PF1. Therefore, the hyperpolarisation response to applied ligands was not significantly delayed by the intrinsic time constant of the membrane.

3.04.2 The delay times

The delays following application of each compound are shown in Table 3.01. The PF4 delay was not significantly different to the GABA delay (two sample *t* test, $P>0.1$; n=50 for PF4, 57 for GABA). PF4 and GABA act on the cell in the same time frame; this is consistent with them having similar modes of action (i.e. direct ligand gating of an ion channel). The delay following PF1 application was significantly longer than the PF4 delay (two sample *t* test, $P<0.01$; n=12 for PF4; 14 for PF1). PF4

and PF1 are different in their delay of action; their modes of action are likely to be different, as well.

Table 3.01 Table to show the delay times and time constants of the hyperpolarisation responses.

	GABA	PF4	PF1
Delay of action (s)	1.22 ± 0.10	1.51 ± 0.11	3.75 ± 0.51
τ (s)	3.20 ± 0.23	4.31 ± 0.28	12.03 ± 1.83
Offset (mV/s)	0.32 ± 0.12	0.05 ± 0.01	0.01 ±0.00

The mean time ± the standard error of the mean is shown for each compound. The values were derived from single exponential curves fitted to the hyperpolarisation responses to each compound. The delay time was obtained by measuring the time between application of the compound and the start of the response. The time constant (τ) was obtained mathematically from the fitted exponential curves. The offset, or rate of recovery, was measured from the chart recordings. n=57 for GABA; 62 for PF4; 14 for PF1.

The delay of 1.2 seconds after application of GABA and 1.5 seconds after PF4 was longer than would have been expected if the compounds had been applied directly to the cell surface. However, the compounds were delivered to the cell surface via a pressure ejection system in which there were three delaying factors; see Section 2.04.5. The first of these was the mechanical delay intrinsic to the pressure ejection apparatus, which was not quantifiable with this experimental set up. The second was the delay due to diffusion from the end of the delivery tube to the muscle bag surface. The third delaying factor (of interest in deciphering the mechanism of action behind the PF4 response) was the time for the cell to process information from stimulated receptors and respond. Equation 3.02 was utilised to investigate the delay period attributable to diffusion.

3.04.3 Measuring the delay of action

The delay times were measured from the hyperpolarisation traces that had been recorded and digitised (see Section 2.04.9). This involved first fitting an exponential curve to the hyperpolarisation and calculating the start of the response from the intersection of the exponential curve with the resting membrane potential. Secondly,

the start of the pressure ejection was subtracted from the calculated start of the response to determine the delay time (see Figures 3.06 and 3.07).

As well as allowing the hyperpolarisation response to be quantified, the fitted exponential decay curves overcame the difficulty of interpreting results visually. In some experiments, pressure ejection caused a small artefact in the trace that obscured the beginning of the hyperpolarisation (see Section 2.04.5). These artefacts made it difficult to resolve the start of the response by eye. An example of a pressure ejection artefact can be seen in the inset box in Figure 3.06A. By superimposing the fitted exponential curve on to the experimental trace (see insets, Figures 3.06 and 3.07), the beginning of the response could be accurately determined mathematically. The start of the response was calculated by fitting the Equation 3.02 (same as Equation 2.02):

Equation 3.02 Exponential decay, arranged in terms of the start of the hyperpolarisation response.

$$x = x_0 - t_1 . \ln\left[\frac{y - y_0}{A_1}\right]$$

where:

x is the x intercept (start of the response),
x_0 is the x offset (close to the minimum value for x),
t_1 is the decay constant of the curve (sec),
y is the y intercept (resting membrane potential),
y_0 is the y offset (the most negative value of y),
A_1 is the amplitude of the response (mV).

Equation 3.02 was used to calculate the start of hyperpolarisation in each experiment; the required values were obtained from the curve that had been fitted to the experimental trace.

The delay time was the time between the beginning of the ejection pulse and the start of the hyperpolarisation. To calculate the delay of action, the distance between the beginning of ligand ejection (shown as a rectangular box on the experimental traces) and the start of the response (x in the above equation) was measured. Figures 3.06 and 3.07 show typical examples of experimental traces fitted with single exponential curves.

Figure 3.06 Experimental trace from a cell to show the delay after PF4 and GABA application.

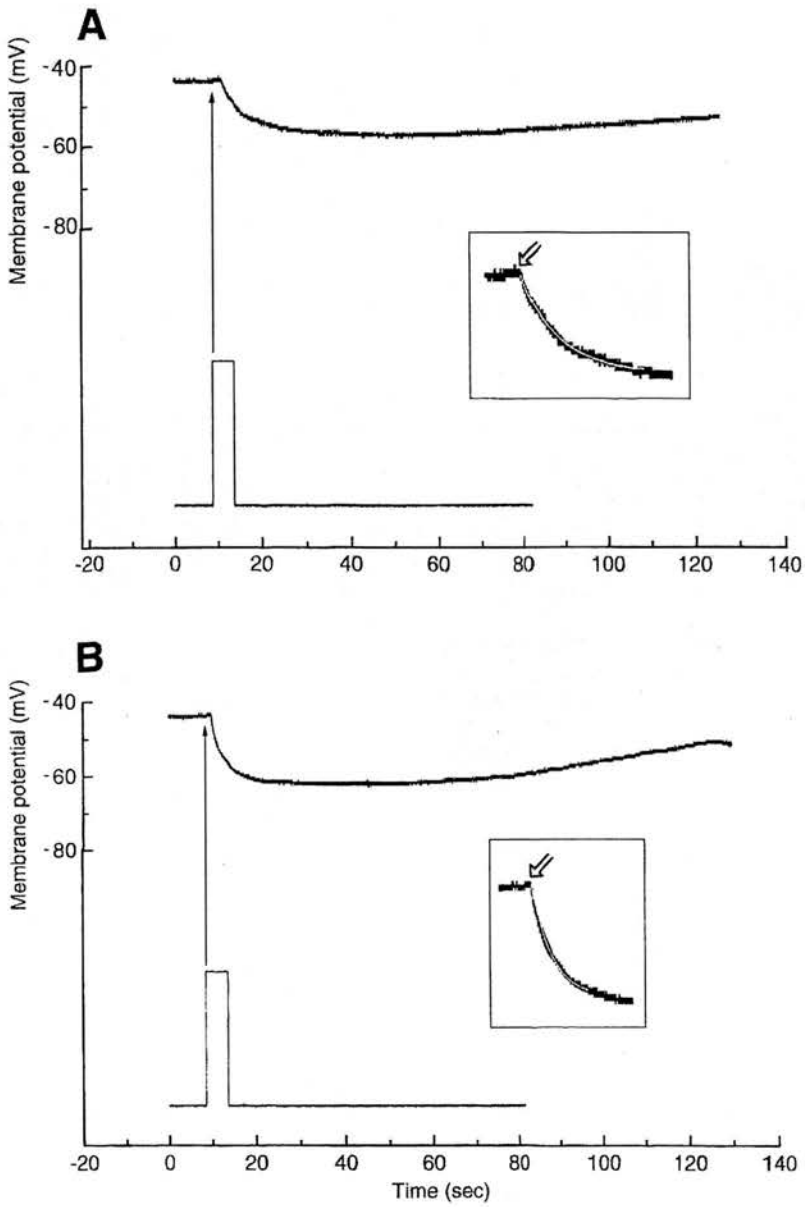

Cell membrane potential is plotted against time. The rectangular pulse indicates the time course of the pressure pulse for PF4 or GABA application; the arrow shows the start of application. PF4 and GABA were applied sequentially to the same target cell. ***A*** *shows the application of, and response to, PF4;* ***B*** *shows GABA. The single exponential curves fitted to the hyperpolarisation are shown as a white line superimposed on the black trace in the inset box. Curves were fitted using the Origin 4.0 program. The open arrow indicates the pressure ejection artefact that occurred intermittently during experiments (see Section 2.04.5); in these examples, pressure ejection caused an apparent depolarisation of the membrane potential prior to the hyperpolarisation responses to PF4 and GABA.*

Figure 3.07 Experimental trace from a cell to show the delay after PF4 and PF1 application.

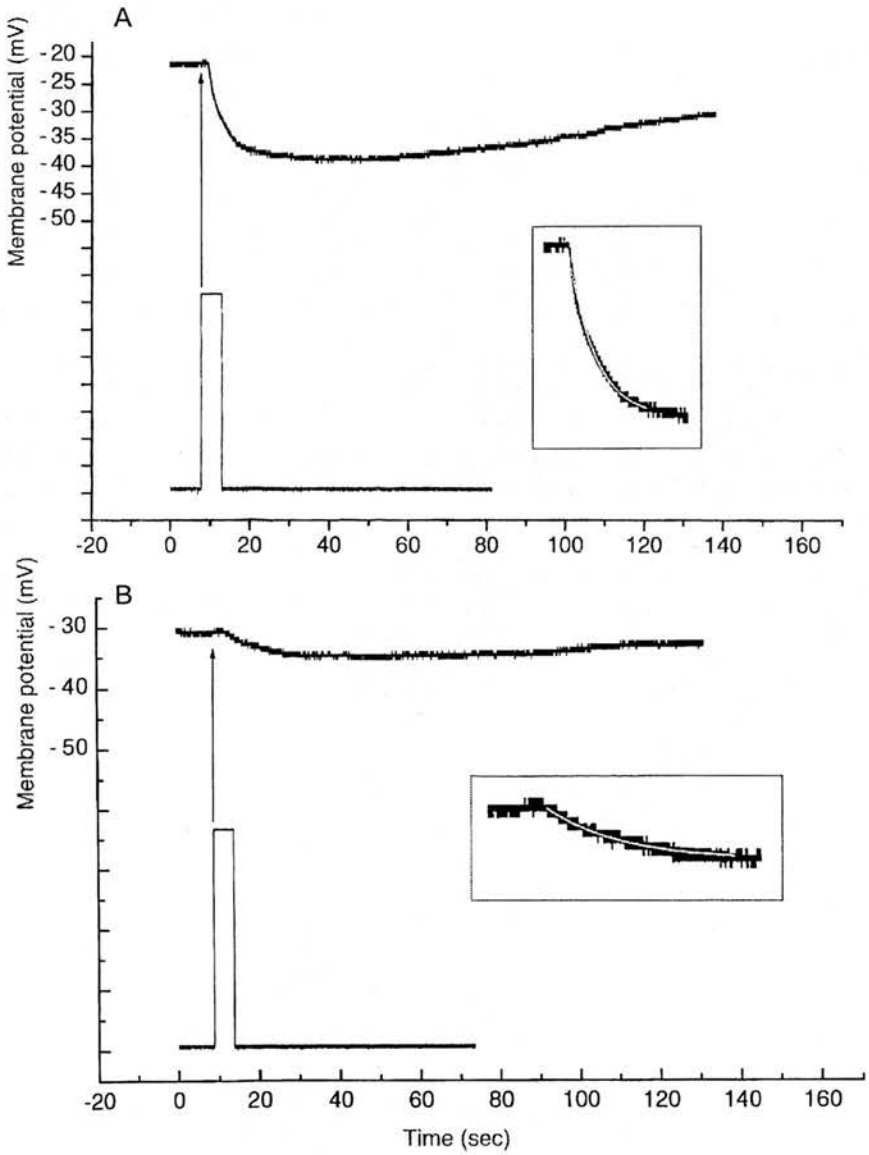

Cell membrane potential is plotted against time. The rectangular pulse indicates the time course of the pressure pulse for PF4 or PF1 application; the arrow shows the start of application. PF4 and PF1 were applied sequentially to the same target cell. ***A*** *shows the application of, and response to, PF4;* ***B*** *shows PF1. The single exponential curves fitted to the hyperpolarisation are shown as a white line superimposed on the black trace in the inset box. Curves were fitted using the Origin 4.0 program.*

3.04.4 Delay due to diffusion

At 1.2 and 1.5 seconds, the delay of action of GABA and PF4 (respectively) was longer than expected for fast acting ligands. The longer duration was caused by the contribution of the mechanical delay and the delay due to diffusion. To investigate the delay of action further, the delay due to diffusion was explored more thoroughly. The diffusion investigation focused on PF4 since the patch clamp study (see Chapter Four) provided information regarding distribution of PF4 receptors.

For the somatic muscle cells to respond to PF4, the ligand had to diffuse from the delivery tube to the cell surface receptors. Since the response to PF4 was dose-dependent (see sections 3.02 and 4.10), the recorded response will be directly proportional to the concentration of PF4 at the receptors. The concentration-time profile for a drug applied to the surface of a cell from a point source may be described by the following diffusion equation (Blackman *et al.*, 1979, based on Purves, 1977):

Equation 3.03 Diffusion equation

$$C = \frac{M}{4\pi\alpha^2(\alpha + x)}\left[\frac{\alpha}{\sqrt{(\pi Dt)}}\exp\left(\frac{-x^2}{4Dt}\right) - \exp\left(\frac{Dt}{\alpha^2} + \frac{x}{\alpha}\right) erfc\left(\frac{\sqrt{(Dt)}}{\alpha} + \frac{x}{2\sqrt{(Dt)}}\right)\right]$$

where:

C is the concentration of ligand at time t
M is the quantity of ligand released from the delivery tube
x is the distance from the cell surface
D is the diffusion coefficient of the compound
t is the time
α is the radius of the cell
exp is exponential function
erfc is error function

From the equation, concentration (C) is directly proportional to M (the amount of ligand released from the delivery tube) and is affected by x, α and D. For clarity, the terms in the equation are illustrated in Figure 3.08.

Figure 3.08 Explanation of the terms of Equation 3.03

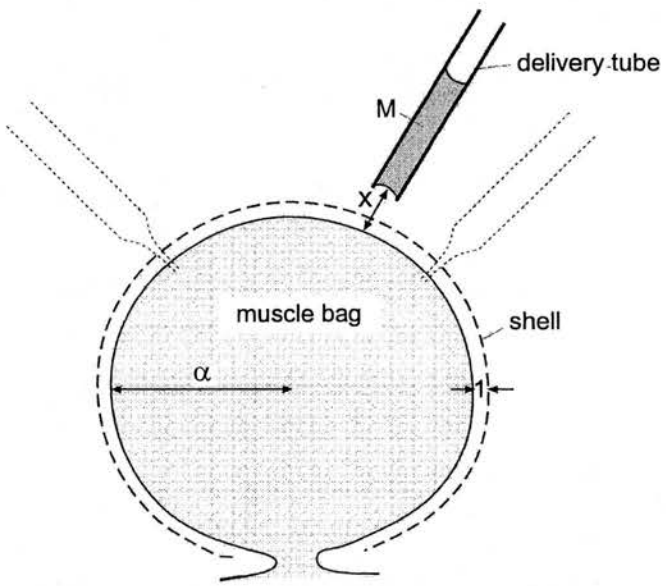

The diagram shows the bag region of the somatic muscle cell (lightly shaded) impaled by two microelectrodes with the delivery tube positioned above the cell; compare with Figure 2.02. The radius of the cell is α and the perpendicular distance between the end of the delivery tube and the bag surface is x. The delivery tube contains M moles of solution (densely shaded). The shell around the muscle bag (dashed line) is 1 nm thick and is the region in which ligand-receptor interactions occur.

The equation does not take into account the force exerted on the ligand molecules during expulsion from the delivery tube, and assumes instantaneous delivery of the ligand, rather than ejection over a few seconds. However, the response to the ligand concentration C is likely to be generated very rapidly compared with the time course of the concentration changes around the cell. Interestingly, the equation does show the profound effect of the diffusion coefficient (D in the equation) on the rate of diffusion. The diffusion coefficient describes the rate of movement of a substance through 1 cm^2. The coefficient depends upon the size and shape of the diffusing molecule, the ambient temperature, and the viscosity of the medium through which the molecules are diffusing. The diffusion coefficient for acetylcholine in aqueous solution is given as $8x10^{-6}$ cm^2/sec (Florence & Attwood, 1998). The diffusion coefficient for GABA is likely to be in the same order since it is a molecule of similar size and also contains a nitrogen group. The diffusion coefficient of the FaRP AF2 is $3.3x10^{-6}$ cm^2/sec (Sheehy *et al.*, 2000); PF4 is likely to have a very similar diffusion coefficient. This assumption is made on the grounds that the FaRPs AF2 and PF4 are alike in molecular weight and shape. Both contain seven amino acids, three of them

identical (proline, arginine and phenylalanine), the other four being similar, which may result in similar tertiary structures:

PF4 structure: **Lys**-Pro-Asn-Phe-Ile-**Arg-Phe**-amide
AF2 structure: **Lys**-His-Glu-Tyr-Leu-**Arg-Phe**-amide

Increasing the molecular weight of the molecule or the viscosity of the medium reduces the diffusion coefficient. Thus, the larger the diffusing molecule or the more viscous the medium, the lower the value of the diffusion coefficient. This is illustrated in Figure 3.09, which was plotted using experimentally-derived values as follows: M = 1 pmole; α = 75 μm; x = 50 μm. The diffusion coefficient, D, was set at $1x10^{-5}$ cm^2/sec to $1x10^{-7}$ cm^2/sec. When the diffusion coefficient is rapid ($1x10^{-5}$ cm^2/sec), the concentration at 1 second is 580 nM. When D is reduced to $1x10^{-6}$ cm^2/sec, the concentration at 1 second becomes 1 nM. When D is even slower ($1x10^{-7}$ cm^2/sec), the concentration at 1 second falls to $2x10^{-24}$ nM.

Figure 3.09 The effect of the diffusion coefficient on ligand concentration at the receptor

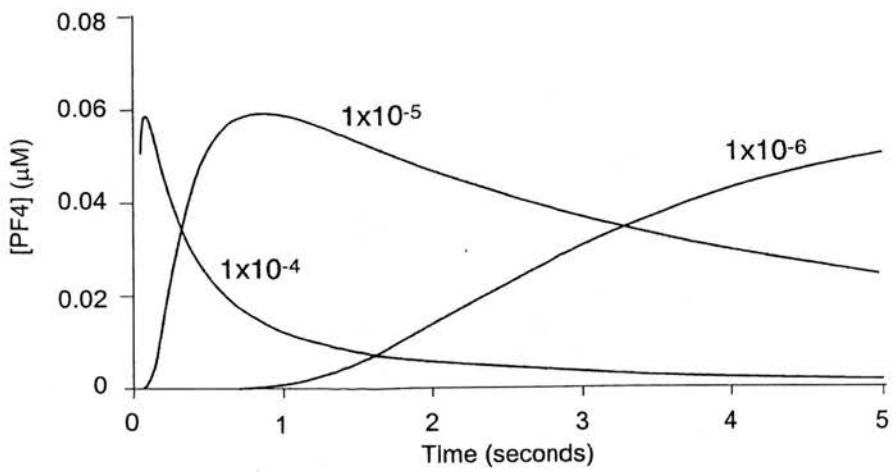

*Concentration is plotted against time according to Equation 3.03 given above. The cell is assumed to be 150 μm in diameter, the tube is positioned 50 μm above the cell, the amount of ligand delivered to the cell surface is 1 pmole. Line **A** is the concentration when $D=1x10^{-4}$; **B** is the concentration when $D=1x10^{-5}$; **C** is the concentration when $D=1x10^{-6}$ cm^2/sec.*

The ligand-receptor interactions take place in a theoretical shell around the cell surface (shown by a dashed line in Figure 3.08). It is 1 nm thick and therefore contains the ligand molecules that are close enough to the cell surface to bind to receptors. The volume of the shell therefore represents the volume of ligand molecules that generate the response. At any chosen time t, the number of molecules in the shell is given by Equation 3.04.

Equation 3.04 Number of potentially active ligand molecules.

$$N_S = C.V_S.N_A$$

where:

N_S is the number of ligand molecules in the shell
C is the concentration of ligand molecules (from equation 3.03)
V_S is the volume of the shell containing active ligand molecules
N_A is Avogadro's constant, 6.02 x 10^{23}/mol

Using the Equations 3.03 and 3.04 with values obtained experimentally, the number of ligand molecules in the theoretical shell around a typical *Ascaris* muscle bag can be predicted. Figure 3.10 shows the change in the number of PF4 molecules in the shell (and therefore available for binding to the receptors) changing with time after pressure ejection.

Figure 3.10 The concentration of PF4 available to bind to receptors on the cell surface

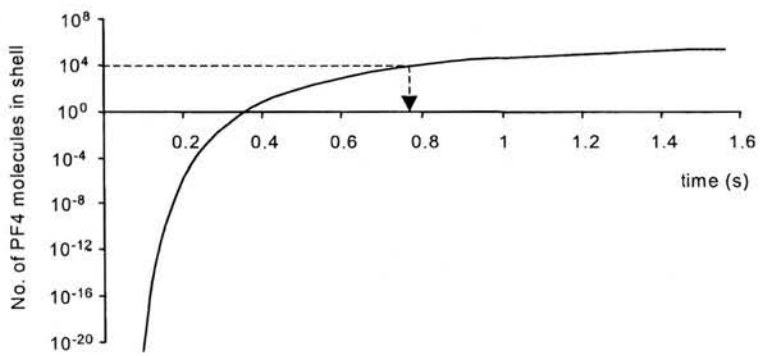

The available concentration of PF4 is plotted against time. The available concentration is the number of molecules in a shell (1 nm wide) surrounding the bag region of the muscle cell, as shown in Figure 3.08. The values used in the equations are from a typical experiment, as in Figure 3.09. The diffusion coefficient is assumed to be 1 x 10^{-6} cm^2/sec. The arrow indicates the time required for 10^4 molecules to diffuse into the shell (see text for full explanation).

From the patch clamp work carried out on *Ascaris* somatic muscle cells (see Chapter Four), the average number of channels per patch was approximately two. The number of channels on the surface of the entire bag region of the muscle cell can be calculated by Equation 3.05.

Equation 3.05 Number of PF4 channels on the bag region of a typical muscle cell

$$N_B = \frac{N_P . A}{a}$$

where:

N_B is the number of PF4 channels on the entire bag region of a typical muscle cell
N_P is the average number of channels per membrane patch, 2
A is the surface area of a typical muscle bag, 71 000μm^2
a is the area of an average membrane patch, 10μm^2 (Sakmann & Neher, 1983)

N_B= 1.4 x 10^4 channels

Hence, the number of PF4 molecules per channel can be calculated from Equation 3.06.

Equation 3.06 Ratio of ligand molecules per PF4 channel

$$r = \frac{N_S}{N_B}$$

where:

r is the ratio of ligand molecules per receptor
N_S is the number of ligand molecules in the shell
N_B is the number of PF channels on the bag region of a typical muscle cell

The structure of the PF4 receptor has not yet been determined so the number of PF4 binding sites per receptor is unknown. Nor have there been studies to determine what level of receptor occupancy is required to precipitate a response to PF4. It is interesting to speculate what level of receptor occupancy is required to produce a response to PF4. For example, if two PF4 molecules were required to bind per

receptor in order for the associated channel to open, a maximal response would be seen only when there were at least twice as many PF4 molecules as channels (i.e. 2 x 1.4 x10^4) in the immediate vicinity of the receptors. Of course, this assumes that full occupancy is required for a response. As shown in Figure 3.10, it would take 0.75 seconds for 10^4 PF4 molecules to diffuse into the immediate vicinity of the receptors. Therefore, approximately 0.75 seconds of the delay can be accounted-for by diffusion. The rest of the delay period is due to an inherent delay in the pressure ejection system and to the response time of the target cell.

From the Equation 3.03 (diffusion equation) and Figure 3.09, it can be seen that the delay of action of both PF4 and GABA is likely to be due, in part, to their diffusion coefficients. The coefficients reflect molecular size and shape, temperature, and the medium through which the molecules are diffusing. The presence of a barrier to diffusion reduces the diffusion coefficient (moving the curve to the right in Figure 3.09). Such a barrier to diffusion exists around the *Ascaris* muscle cells.

3.04.5 The permeability barrier around Ascaris *somatic muscle cells*

The layer around the somatic muscle cells has been described as ground substance that occupies the interstitial space (Rosenbluth, 1965b). However, it can be recognised as collagen by light microscopy (see Figures 3.11 and 3.12) and is removed enzymatically by collagenase (see Section 2.05.1). The histochemical stain used in Figure 3.11 is Mallory's phosphotungstic acid-haematoxylin (PTAH), which stains collagen red. The red colouration is due to the acidic component of the stain binding to acidophillic sites on the collagen molecules, such as arginine residues (Everson Pearse, 1985). Figure 3.12 shows transverse sections through *A. suum* stained with Periodic Acid Schiff (PAS). Since this stain colours complex carbohydrates orange-red (Everson Pearse, 1985), the collagen in the sections has been stained orange-red, as have the glycogen granules in the muscle bags. Figures 3.11A and 3.12A illustrate the distribution of collagen throughout the worm. In particular, collagen can be seen in the cuticle and in the interstitial spaces between the somatic muscle cells. In Figures 3.11B and C, and 3.12B, the collagen is visible as a meshwork of fibres surrounding the muscle bags.

With the electron microscope, the collagen fibres can be seen in the spaces between somatic muscle cells. The collagen has the amorphous structure typical of the lamina densa of basement membranes, which contains collagen type IV (Toner & Carr, 1971; Stevens & Lowe, 1992). The fibres are approximately 75 nm in diameter, which is in the normal range of lamina densa thickness (Stevens & Lowe, 1992). The fibres are corrugated and are cross-linked by fine strands (see Figure 3.13). Presumably, the corrugation allows the collagen to stretch and accommodate the contractile movements of the muscle cells while the cross-linked strands maintain the integrity of the collagen layer; much like the function-dictated structure of elastic fibres (Young & Heath, 2000).

The presence of this layer of collagen around the muscle bags acts as a permeability barrier and thus contributes to the delay between application of compounds to the flap preparation and appearance of a response in the target cell.

Figure 3.11 Light microscope view of* Ascaris suum, *to show the collagen layer surrounding the muscle cells (Mallory's PTAH).

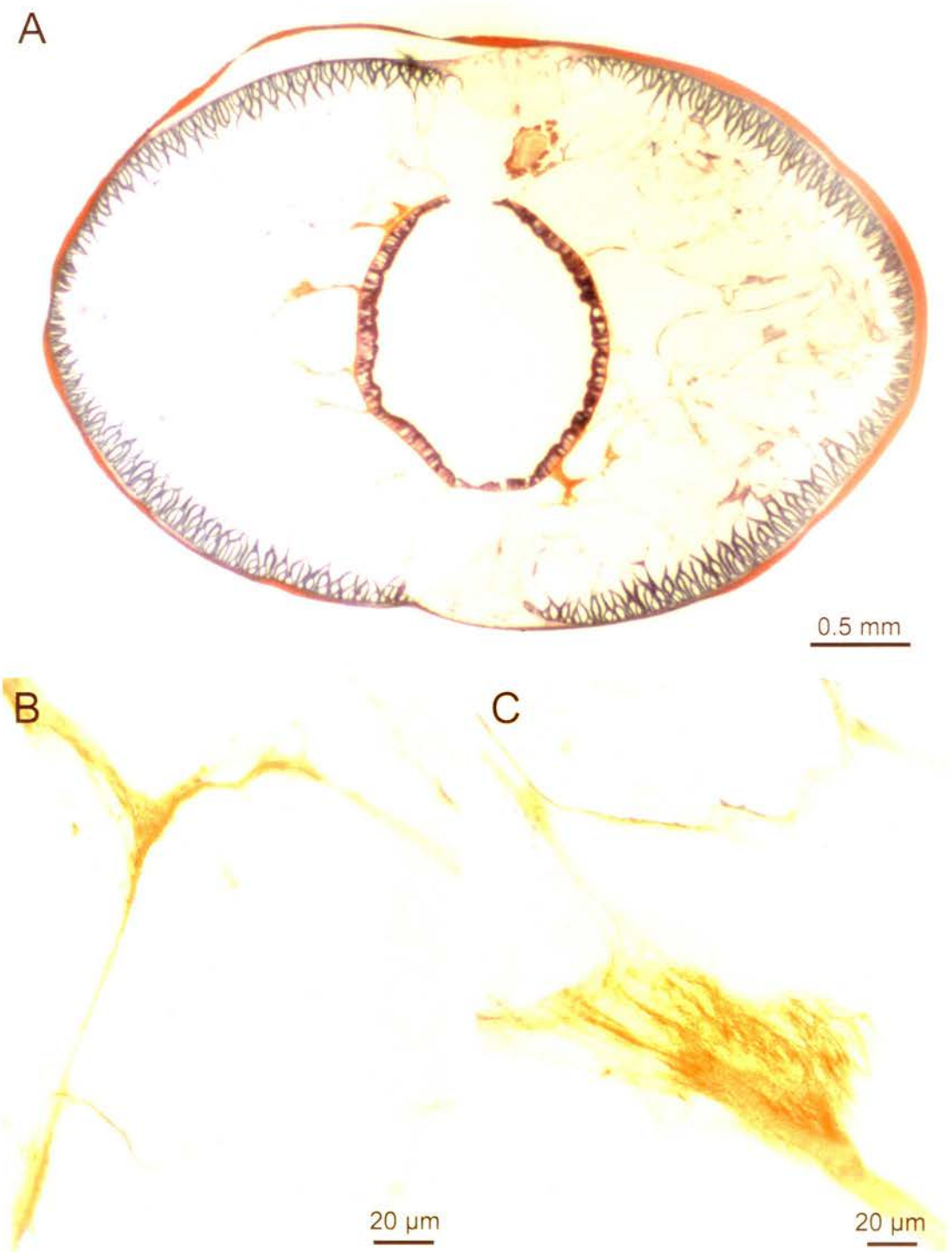

Transverse section of A. suum *stained with Mallory's phosphotungstic acid-haematoxylin (PTAH) to demonstrate collagen. Collagen is stained red, muscle fibres are blue.* ***A*** *is a cross section through the whole worm, showing that the cuticle and the interstitial spaces contain collagen, magnification: 37.5x.* ***B*** *shows two muscle bags (blue) and the surrounding collagen layer (red), magnification: 600x.* ***C*** *illustrates the fibrous structure of the collagen, magnification: 480x.*

Figure 3.12 Light microscope view of* Ascaris suum, *to show the collagen layer surrounding the muscle cells (PAS).

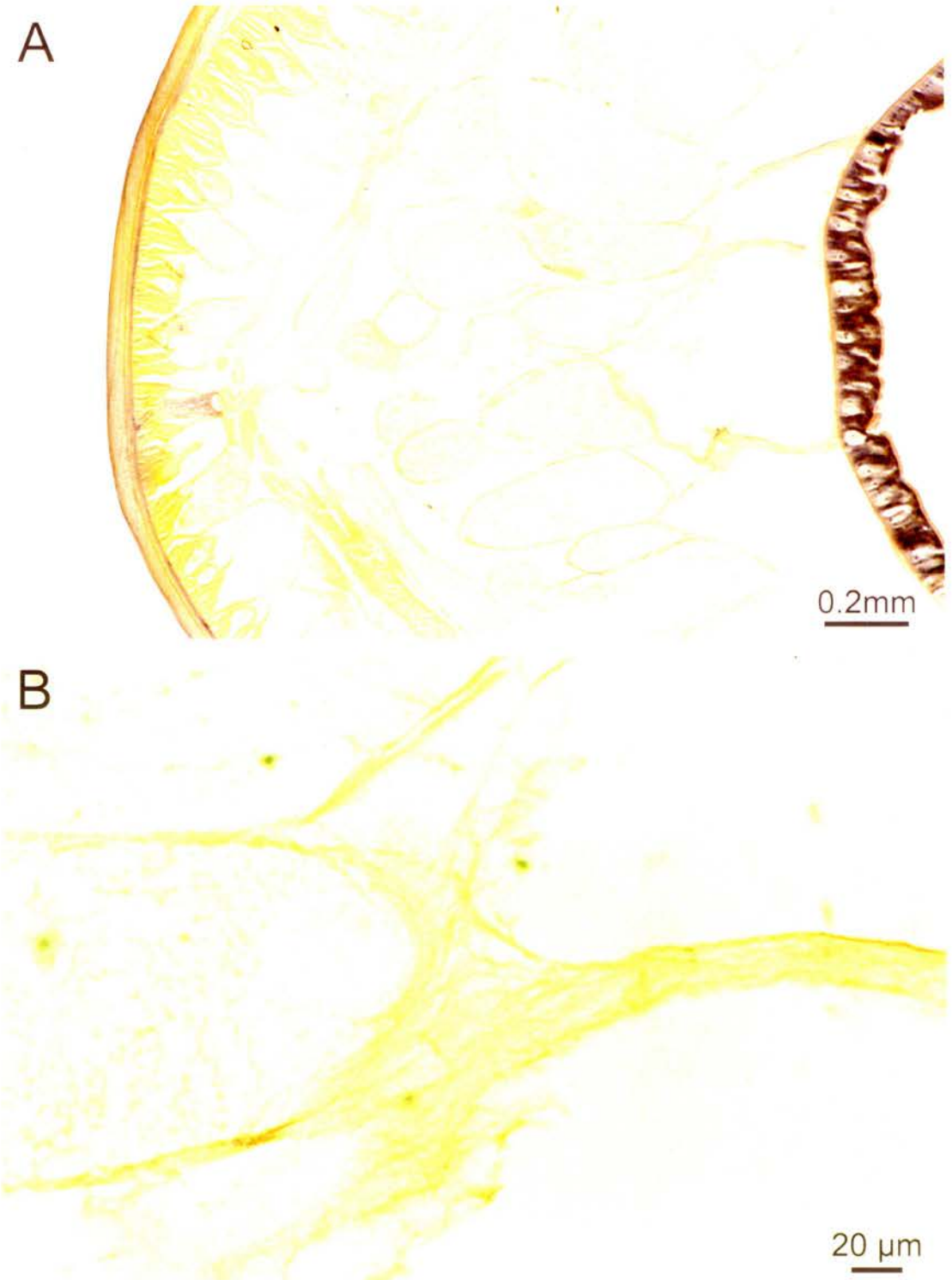

Transverse section of A. suum *stained with Periodic Acid-Schiff (PAS) to demonstrate carbohydrate. Complex carbohydrates such as those in collagen, glycogen or mucus are stained orange.* ***A*** *is a cross section through the whole worm, showing the distribution of complex carbohydrates through the worm, including the cuticle, the mucus-secreting cells in the gut and the interstisital spaces containing collagen, magnification: 64x.* ***B*** *shows muscle bags containing glycogen granules and the surrounding layer of collagen fibres stained orange, magnification: 400x.*

Figure 3.13 Electron micrograph to show the collagen layer surrounding the* Ascaris suum *muscle cells.

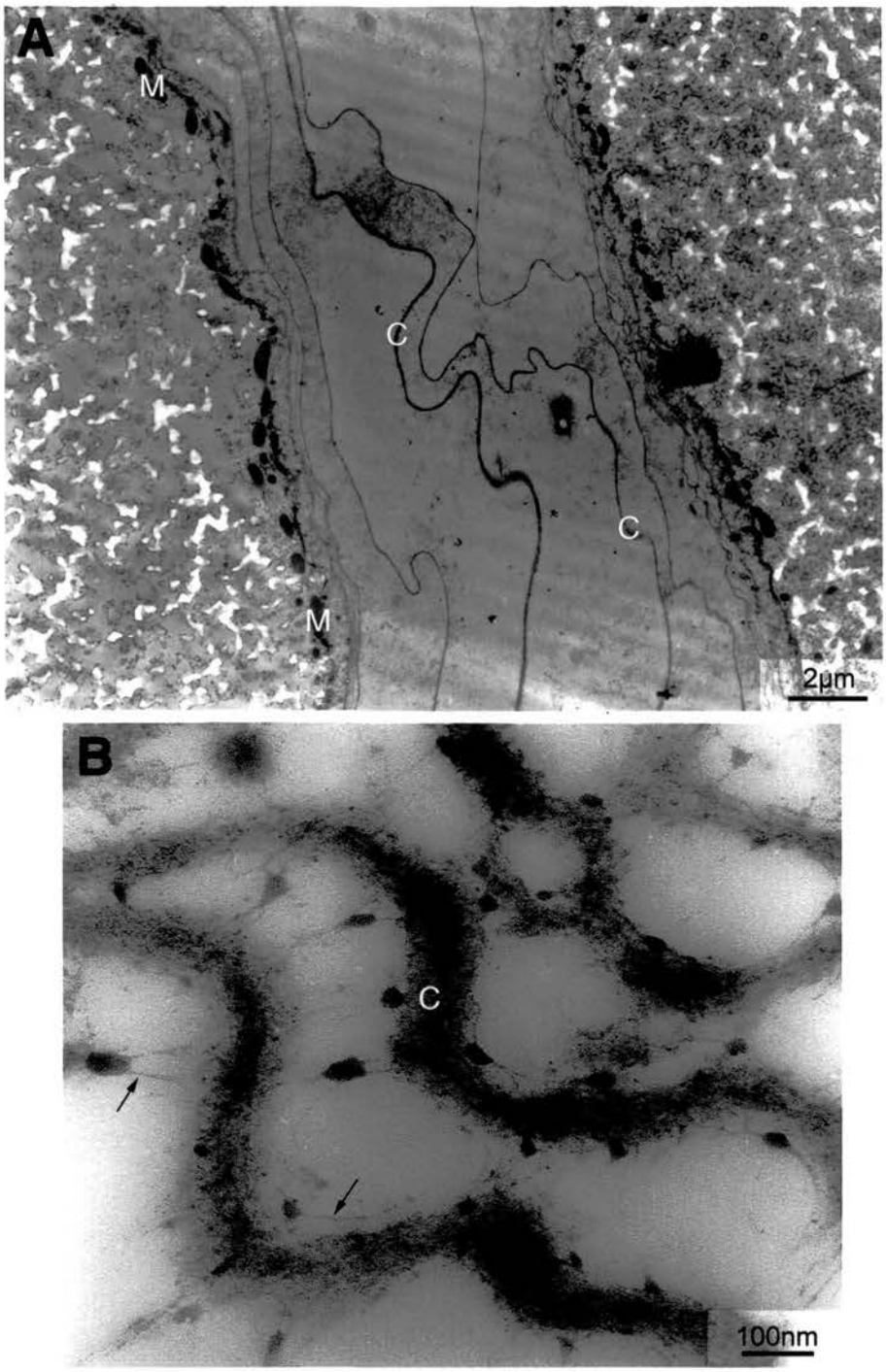

A *shows a transmission electron micrograph (TEM) of the interstitial space between the bag regions of adjacent somatic muscle cells. The edges of the muscle bags are demarcated by the row of mitochondria (**M**) that are found at the periphery of the bag. Intracellular glycogen granules give the bag contents a mottled appearance. The interstitial space contains collagen fibres (**C**).*
B *shows a higher magnification TEM of the interstitial collagen network. The collagen fibres (**C**) have the amorphous appearance of vertebrate basal lamina, a collagenous component of basement membranes. Fine strands appear to connect neighbouring fibres (arrows), consistent with a mesh-like structure.*

3.05 Discussion of current clamp work: an overview

The current clamp experiments showed that PF4 acts on receptors on the *Ascaris suum* muscle cells. The response to PF4 application was an increase in membrane conductance coupled with hyperpolarisation. The combination of a conductance increase and a change in membrane potential indicates that ion channels open in response to PF4. According to the voltage clamp study, the ion channels involved in the PF4 response conduct chloride ions. PF4 was shown to have the same reversal potential as GABA, which is a recognised ligand for chloride ion channels (Martin, 1982). This result concurs with previous work on PF4 (Holden-Dye *et al.*, 1997).

3.06 PF4 Receptors

The receptors activated by PF4 may not be specific for PF4 itself, since this FMRFamide-Related Peptide (FaRP) has not been identified in *Ascaris suum*. PF4 has not been isolated from *Ascaris* tissue nor has an *Ascaris* gene encoding PF4 been discovered. Various FaRPs originally extracted from one nematode species have subsequently been found in others, indicating that free-living and parasitic nematodes contain a complement of similar, and in some cases identical, neuroactive peptides (Maule *et al.*, 1996). An example of a widely-found FaRP is AF2 (the peptide KHEYLRF) which was initially extracted from *A. suum* tissue and later found in *Panagrellus redivivus* (Maule *et al.*, 1994b), *Caenorhabditis elegans* (Marks *et al.*, 1995) and *Haemonchus contortus* (Keating *et al.*, 1995). The observation that PF4 activates receptors in *A. suum* may be because PF4 is intrinsic to *Ascaris* but is yet to be isolated experimentally. Another explanation is that *A. suum* has receptors for an endogenous FaRP that are sufficiently non-specific that PF4 can bind to them and activate their effectors.

3.07 Receptor location

The results indicate that PF4 receptors exist on the bag region of the somatic muscle cell. This is a surprising location for ligand receptors, given that the accepted pattern of neuromuscular stimulation is that neurotransmitter molecules are generally released from the nerve terminals into the synaptic cleft. The neurotransmitter then diffuses across the cleft to the receptors, binds with them, and produces a response (Peper &

Dreyer, 1974; Lester, 1977). Receptors that are outside the neuromuscular junction, e.g. on the muscle bag surface, will not receive neurotransmitter by this route.

There have been no specific studies localising PF4 to the muscle bag surface, but there is a precedent for finding FaRP receptors in this area. Receptors that respond to PF1 have been shown to exist on the muscle cell membranes by a radiolabelled binding assay (Bowman *et al.*, 1995) and in a patch clamp study (Martin & Valkanov, 1996) . The phenomenon is not restricted to FaRP receptors; GABA receptors have also been identified on the muscle bag surface (Martin, 1980), and extra-synaptic receptors have been documented in other invertebrates (Tauc & Gerschenfeld, 1962).

The position of the PF4 receptors on the surface of the muscle bags begs the question as to how they are stimulated *in vivo*. The *Ascaris* nervous system (a source of endogenous FaRPs (Sithigorngul *et al.*, 1990)) is restricted to the hypodermis; the nervous system does not have projections to the somatic muscle cells. Instead, the muscle cells send projections (the muscle arms, see Section 1.03.4) to nerves (Schneider, cited by DeBell *et al.* (1963)). Hence, the receptors on the muscle bag surface can not receive PF4 by direct contact with the nerve terminals. Instead, they must receive PF4 from the pseudocoelomic fluid, possibly originating from the FaRPergic neurons in the hypodermis. This argument assumes that PF4 has a hormone-like action in *Ascaris*, which may be responsible for the resting somatic muscle tone. FaRPs functioning as hormones would need a degree of resistance to enzymatic degradation. The presence of a methionine residue in position three from the C terminal makes FaRPs liable to oxidation and therefore reduces their biological efficacy (Price, 1986). In contrast, FaRPs with a leucine residue in position three (such as PF1) have been shown to be resistant to enzymatic degradation (Price, 1986) and therefore potentially suited to hormonal function (Rosoff *et al.*, 1992). Since isoleucine is similar in structure to leucine, PF4 would also be expected to resist degradation. Also, the proline residue has been shown to be important in making PF4 resistant to endogenous *Ascaris* aminopeptidases (Kubiak *et al.*, 1996).

It follows that PF4 has the potential for hormonal function within *Ascaris* and other nematodes. A hormonal role for PF4 in *Ascaris* does not preclude function as a neurotransmitter as well. In fact, the rapid action of PF4 on somatic muscle is typical

of the response to a neurotransmitter (Brownlee *et al.*, 1996) and several studies have localised FaRPs to secretory vesicles in nematode neurones. It has not yet been possible to identify FaRPs on the muscle bag surfaces. FaRPs have been located by immunofluorescence in *Ascaris* neurones (Sithigorngul *et al.*, 1990), but due to the autofluorescence of the muscle cell membranes, this technique has not been used to examine the muscle cell surfaces.

3.08 Delay of action following PF4 application

3.08.1 Delay of action of PF4

PF4 is a rapidly acting ligand. The speed of action of PF4 was comparable to that of GABA (no significant difference; 2 sample *t* test, $P>0.1$). The delays of action of PF4 and GABA were found to be 1.5 ± 0.1 and 1.2 ± 0.1 seconds long respectively (mean $\pm$ standard error of the mean).

GABA is a directly-gating ligand, as such, there is a very short delay (in the order of ms) between activation of the receptor and appearance of the response. PF4's short delay of action suggests that, like GABA, it is a directly-gating ligand. This is consistent with the observation that the PF4 delay of action was significantly shorter than that of PF1. PF1 is a FaRP that also binds to receptors on the somatic muscle cell surface (Bowman *et al.*, 1995; Martin & Valkanov, 1996) and is independent of the *Ascaris* nerve cords (Maule *et al.*, 1995a). However, PF1 acts via a signal transduction system, rather than directly on ion channels (Bowman *et al.*, 1995). The PF1 response requires intracellular processing before hyperpolarisation is seen, consequently there is a longer delay of action than is seen with the directly-gating ligand, GABA.

There were three components of the delay of action calculated for each experiment (see Section 2.04.9); the mechanical delay, the diffusional delay and the physiological delay of the cell's response mechanism. The first of these was an intrinsic delay in the pressure ejection system. The use of the Neurophore BH-2 pressure ejection system was consistent throughout the experiments, hence the mechanical delay applied to all measurements made. The second cause of the delay was the presence of a collagenous covering on the somatic muscle cell surfaces, see Section 3.08.2. Rates

of diffusion through aqueous solution or through permeability barriers, such as a collagen matrix, vary according to molecular size and charge. The time required for diffusion through the collagen layer was estimated, see Section 3.04.3.

3.08.2 The collagen layer

Three collagen types have been identified in nematodes (Cox, 1992); two types of collagen in the cuticle and basement membrane collagen. While cuticle collagen is unique to nematodes, the basement membrane collagen is type IV, the same as is found in vertebrates. The appearance of the collagen layer identified in the micrographs (Figures 3.11 to 3.13) is consistent with the typical appearance of the collagen in vertebrate basement membranes. The histological staining of the layer shows colouration typical of collagen (Everson Pearse, 1985; Young & Heath, 2000) and the electron micrograph appearance shows a moderately dense, homogenous band, characteristic of basal lamina (the collagenous component of basement membrane) (Toner & Carr, 1971). The width of the strands in the electron micrograph are between 50 and 100 nm wide; within the range of basal lamina thickness (30 to 100 nm) (Stevens & Lowe, 1992).

Basement membrane impedes diffusion because it constitutes a physical barrier and the electric charges on the glycoaminoglycan moieties affect the movement of charged particles (Glanville, 1987; Stevens & Lowe, 1992). As demonstrated in the delay time experiments, the collagen mesh surrounding the somatic muscle cells was functioning as a permeability barrier.

3.08.3 The mechanism of the PF4 response

The hyperpolarisation response of the cell membrane had a significantly different time constant for each of the three compounds, see Table 3.01 (two sample *t* test, $P<0.01$, ANOVA, $P<0.001$). The time constant of an exponential curve is the time for the value to fall by 63 % of the starting value; it is the rate constant for exponential decay. The short time constant for the response to GABA (3.2 ± 0.2 seconds) indicates that the hyperpolarisation developed rapidly. Membrane hyperpolarisation in response to PF4 developed more slowly (τ is 4.3 ± 0.3 seconds), and with PF1 was slower still (τ is 12.0 ± 1.8 seconds). The different time constants indicate that

different cellular mechanisms were involved in the responses to the three compounds. The relatively rapid development of the response to GABA is consistent with its direct mode of action. The PF4 response developed slightly slower; it can be argued that the response is, like the GABA response, the result of activating directly gated ion channels, but because smaller amplitude channels are involved (see Section 4.04), the response takes longer to build up.

There are two factors behind the relatively slow development of the PF1 response. The first is the requirement for signal transduction between the stimulated receptors in the cell membrane and the effector mechanisms (Bowman *et al.*, 1995). The second factor is that the PF1 response does not appear to be the direct result of ion channel opening, since there was only a small change in the membrane conductance on application of PF1 (0 to 0.33 μS). This observation is in agreement with previous workers (Franks *et al.*, 1993; Franks *et al.*, 1994). The small increase in whole cell conductance of 0 to 0.33 μS can not explain the hyperpolarisations recorded from those cells in terms of ion channel activity. It is probable that the PF1 response is due to a mechanism slower than ion channels, perhaps ion pumps in the cell membrane.

3.09 Summary of PF4 effects on the whole cell preparation

In summary, PF4 was shown to have marked effects on *Ascaris suum* somatic muscle cells. These were mediated through chloride ion channels in the bag region of the muscle cells. The response to PF4 was qualitatively similar to the effects of γ-amino butyric acid (GABA) in that the cellular response was a rapid-onset, fast-developing hyperpolarisation. PF4 was not acting on GABA receptors (Holden-Dye *et al.*, 1997). GABA is a directly-gating ligand, hence the speed of the GABA response. PF4 was compared with a second-messenger mediated FaRP, PF1, and with GABA, which led to the conclusion that the response to PF4 is consistent with it acting as a directly-gating ligand of chloride channels. This is investigated further in Chapter 4.

Chapter 4. Response to PF4 at the single channel level: results of the patch clamp study

Patch clamping was carried out on vesicles produced from *Ascaris suum* somatic muscle cells. The main findings are outlined in this paragraph. The channel records produced by the patch clamping procedure showed that the channels activated by PF4 were abundant, small amplitude chloride channels. The channels opened readily for variable periods of time and showed no evidence of desensitisation. Channel characteristics varied with the origin of the worms. Channel opening did not appear to be second messenger mediated; the channel behaviour was consistent with direct activation by PF4.

For clarity of expression in this chapter, the small amplitude chloride ion channels that were activated by PF4 are referred to as "PF4 channels". A typical recording of two PF4 channels responding to PF4 is shown in Figure 4.01.

Figure 4.01 Channel record from a typical patch clamp experiment

Channel record from a typical patch clamp experiment in which two channels were active (i.e. opening and closing). The recording was made at +120 mV with 0.100 μM PF4 in the patch pipette. C indicates the closed level in the trace; O1 is the first level of channel opening; O2 is the second level of opening. The signal was filtered at 1 KHz prior to digitisation, then at 100 Hz before analysis; see Section 2.08.

Table 4.01 illustrates the number of patch clamp experiments undertaken and the quantity that produced results. Criteria for selecting which records were suitable for analysis is discussed in Section 2.08.1.

Table 4.01 The pipettes used during the course of the patch clamp work

652 pipettes were documented during the course of the patch clamp experiments, i.e. 652 pipettes were pulled, fire polished and filled with solution. 181 of the pipettes were used while learning the patch clamp technique.
471 membrane patches were attempted.
212 patches were successfully clamped with a patch pipette.
164 patches gave identifiable results; that is, channels were clearly absent or present. In the other 48 patches, noise obliterated any recognisable pattern.
112 patches showed channel activity on visual inspection.
77 patches yielded results that were clear enough for digitisation and analysis.

4.01 Patch activity

Patch activity, that is, the appearance of any channel openings in a patch, was found to be directly related to the presence of PF4 in the patch pipette. This is shown in the bar chart in Figure 4.02. It illustrates the 164 patches in which channel activity could be clearly discerned or absolutely ruled out. In control patches, where PF4 was absent

Figure 4.02 The occurrence of active patches with dose of PF4 (μM)

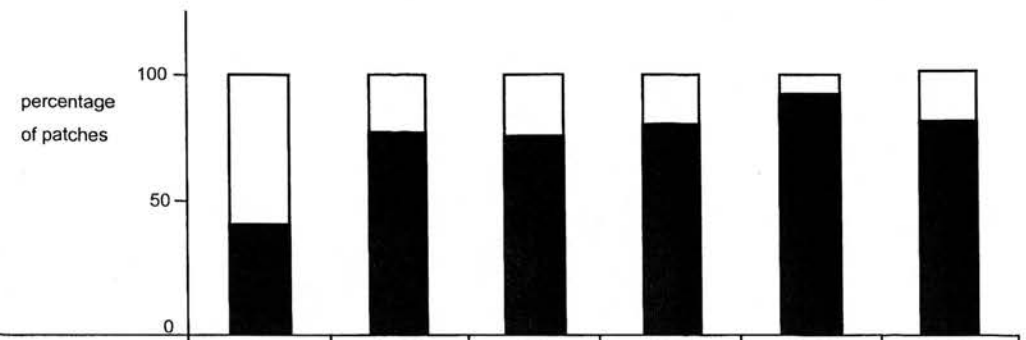

[PF4] (μM)	0	0.003	0.010	0.030	0.100	0.300
% inactive (n)	58 (29)	23.5 (8)	25 (3)	20 (5)	7.4 (2)	18.7 (3)
% active (n)	42 (21)	76.5 (26)	75 (9)	80 (20)	92.6 (25)	81.3 (13)

Bar chart to show the increase in the occurrence of channel activity in membrane patches as the concentration of PF4 in the patch pipette increased. n=164 patches.

from the pipette solution, there was significantly less channel activity (ANOVA, $P<0.001$; two sample t tests, $P<0.05$).

When the patch activity data were investigated further it was clear that there was a relationship between the percentage of patches which showed channel activity and the concentration of PF4 to which they were exposed. The proportion of patches that were active was found to be dose-dependent, as shown in Figure 4.03. The rectangular hyperbola shows that there is a typical Michaelis Menton relationship, and indicates that the EC50 is 1 nM PF4 (see Section 2.10). The low value of EC50 shows that PF4 is a potent ligand for *Ascaris* ion channels.

Figure 4.03. The effect of PF4 concentration on the proportion of active patches.

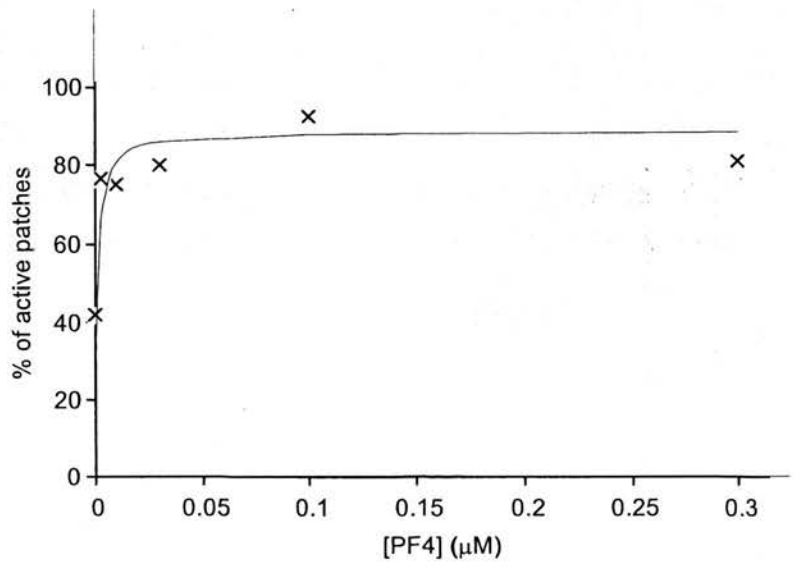

The dose-response relationship between the proportion of patches which were active and the concentration of PF4. A Fortran computer program was used to fit the data with the Michaelis Menton equation. The response was corrected for mean proportion of patches that was active at zero concentration. The program operated a simplex process that minimised the residual sum of squares using NAG subroutine E044CC. The EC50 was 0.001 μM PF4. n=164.

On closer examination of the best resolved recordings of patch activity, the absolute number of open channels per patch was also found to be dose-dependent. It was found to be impossible to count the number of channels in the patch for every record. The channel records in which the base-line drifted or where there was a high probability of channel opening (P_{open}) were excluded, and the number of channels was counted for the remaining 112 patches. The number of channels present was related to

the concentration of PF4 in the patch pipette. The dose-response curve in Figure 4.04 illustrates this. As in Figure 4.03, the data points have been fitted with a Michaelis Menton equation which again gave the EC50 as 1 nM.

Figure 4.04 The effect of PF4 concentration on the number of channels per patch.

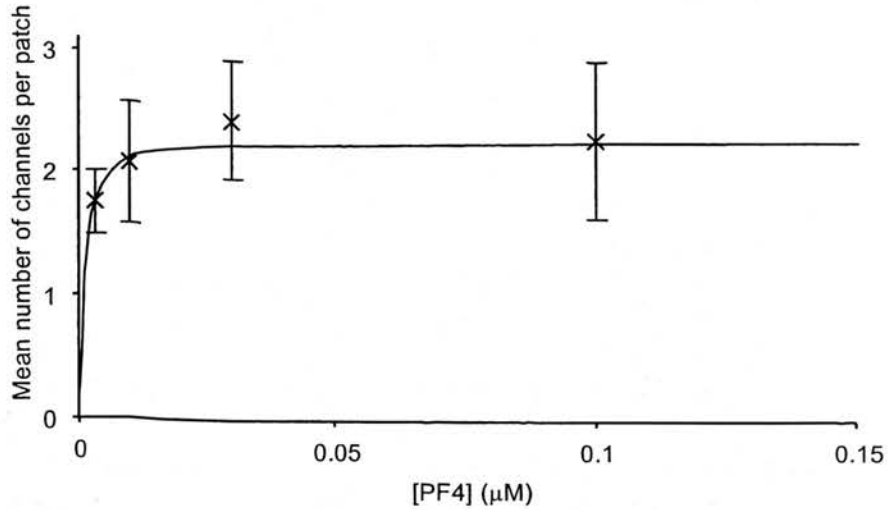

The dose-response relationship between the number of channels per patch and the concentration of PF4 in the patch pipette. The mean number of channels/patch is marked by X and the error bars show the standard error of the mean. The line illustrates the Michaelis Menton equation fit to the data points (EC50=0.001 μM PF4). The response was corrected for the mean number of channels open at zero concentration. n=112.

4.02 Sequential recordings with and without PF4 in the pipette solution

A direct comparison was made of channel activity in sequential patches made from the same vesicles. Each vesicle represented a small area of the cell membrane, over which any ion channels present were assumed to be evenly distributed, see Section 2.05.4. The simplest model of a cell membrane is that its components are spread out uniformly, hence the assumption of even channel distribution over the cell surface. From this premise, it followed that sequential patches clamped from the same vesicle should have similar ion channel populations. Thus, the activity of channels from the same population was directly compared. The first patch of each sequential series was exposed to PF4 in the patch pipette; the second was exposed to control (PF4-free) pipette solution; the third patch was exposed to the same concentration of PF4 as the first. See Figure 4.05. Due to vesicle fragility, a third patch could not always be made. The channel activity in the first and third patches (those exposed to PF4) was

not significantly different (paired *t* test, $P>0.30$, n=5). There was significantly less activity in the control patches than either the first or the third patch (paired *t* test, $P<0.05$, n=12 for comparison with first PF4; 5 for second PF4). Coming from the same vesicle, each patch in the series had a similar population of ion channels, therefore the increase in channel opening seen in the first and third patches was a direct result of the presence of PF4 in the patch pipette.

Channel activity was observed in the absence of PF4. There was no significant difference in the amplitude of the chloride channels seen in the presence and absence of PF4 (ANOVA, $P=0.6$). This was due either to spontaneous channel opening, or to the presence of a low concentration of endogenous FaRP in the vesicle preparation. See Section 4.09 for further discussion.

Figure 4.05 Channel activity in sequential patches from the same vesicle.

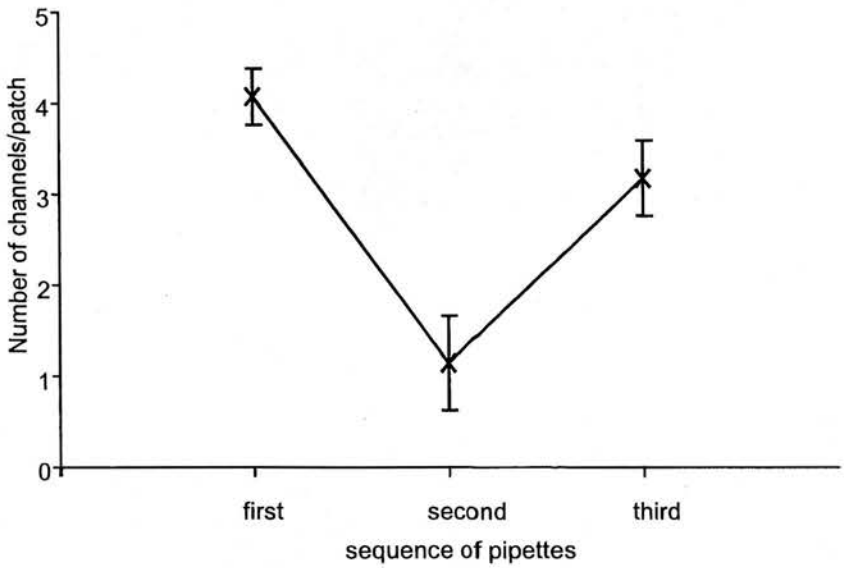

Sequential membrane patches were clamped on the same vesicle. The first was exposed to PF4, the second to the control solution and the third to PF4. The mean number of channels per patch is shown by X and the error bars indicate the standard error of the mean. n=13 for 1st and second patches and 6 for the third patches

4.03 Reversal potential

The reversal potential of the ion channels in each membrane patch was calculated by recording channel current while the patch was held at a series of different voltages.

Channel current was then plotted against the pipette potential. The current was plotted on the ordinate and the voltage on the abscissa. Least squares linear regression analysis was carried out to produce an I-V plot. The I-V plots gave a gradient of I/V, or conductance (pS); and an x-axis intercept, or reversal potential (mV). An I-V plot from a typical experiment is shown in Figure 4.06. Plots composed of less than 3 points or with a poor correlation (R squared less than 0.9) were not considered to be robust enough to interpret, and were rejected.

Figure 4.06 Typical current-voltage plot

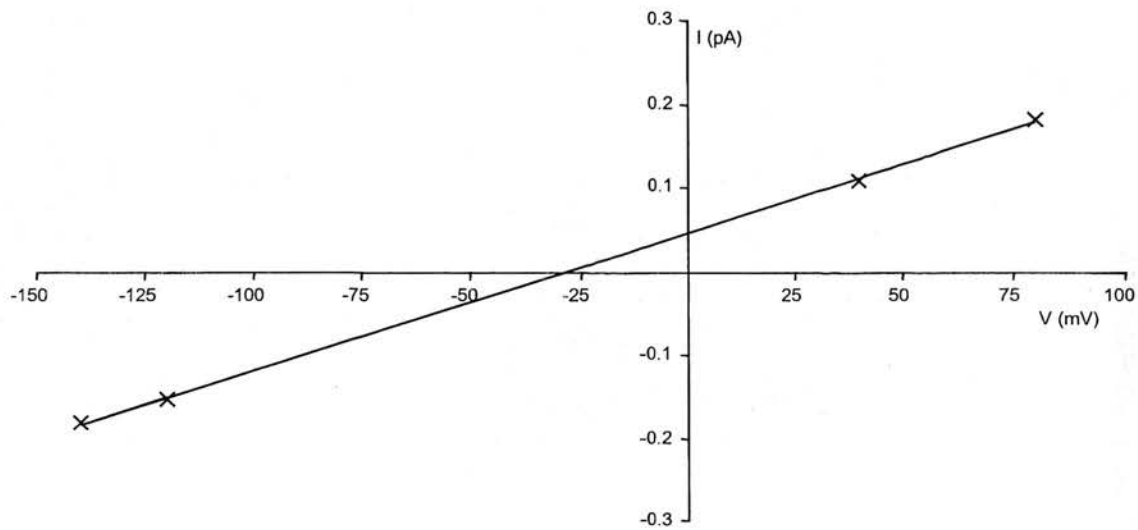

Plot of current against voltage (I-V) from a typical experiment in which the patch pipette contained 0.100 μM PF4 and the current was recorded between membrane potentials of -140 mV and +80 mV. The R squared value for the line (fitted by linear regression) was 0.99, the conductance (gradient of the line) was 1.65 pS and the reversal potential (abscissa intercept) was -28 mV.

The reversal potential data shown in Figure 4.07 are from the most robust I-V plots, as defined above. The reversal potential for all the ion channels under investigation was -24.7 mV ± 3.9 mV (mean ± standard error of the mean). This is slightly more positive than the calculated chloride ion reversal potential for the patch clamp experiments, which was -33.0 mV, according to the Nernst equation (see Equation 3.01). The $[Cl^-]_{in}$ was 41mM (extracellular solution), the $[Cl^-]_{out}$ was 144 mM (pipette solution). The discrepancy between the theoretical and the experimental values of the chloride reversal potential is due to the chloride permeability of the *Ascaris* muscle cell membrane, which allows some chloride ion leakage through the membrane, see

Section 3.03. The resulting increase in chloride ion concentration inside the vesicles shifts the chloride reversal potential. Thus, the value derived experimentally (-24.7 mV) is more positive than the theoretical reversal potential (-33.0 mV), which was calculated using the Nernst equation.

The reversal potentials were distributed as for a normal population (Anderson-Darling Normality Test, P=0.579) and were unaffected by concentration of PF4; potential difference across the membrane patch; or the origin of the worms (no significant difference when tested by ANOVA).

Figure 4.07 Histogram of Reversal Potential.

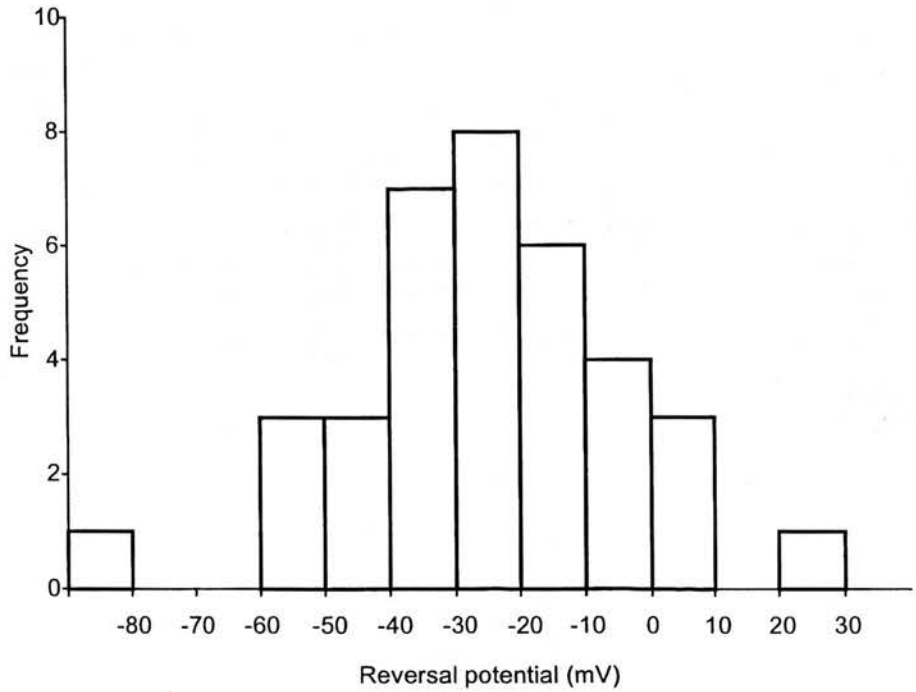

The reversal potential of the ion channels under investigation. Mean value: -24.7 mV; standard error: 3.9 mV; n=36.

4.04 Channel conductance

Like the reversal potentials, the conductance values of the ion channels were calculated from I-V plots (see Section 4.03 for details of I-V plot production). As with the reversal potentials, only the most robust IV plots were used to obtain the conductance values; I-V plots with 3 or more points and an R squared value of at least 0.9 were considered to be robust. Conductance values calculated from the selected I-V plots are illustrated in Figure 4.08. The range of the conductance values was 1.09

to 7.07 pS; these are low values compared with other *Ascaris* chloride channels: 200 pS for the calcium-dependent chloride channel (Thorn & Martin, 1987); 22 pS for the GABA activated chloride channels (Martin, 1985); 21 pS for the glutamate-gated chloride channel (Adelsberger *et al.*, 1997).

Figure 4.08 The channel conductance time-series.

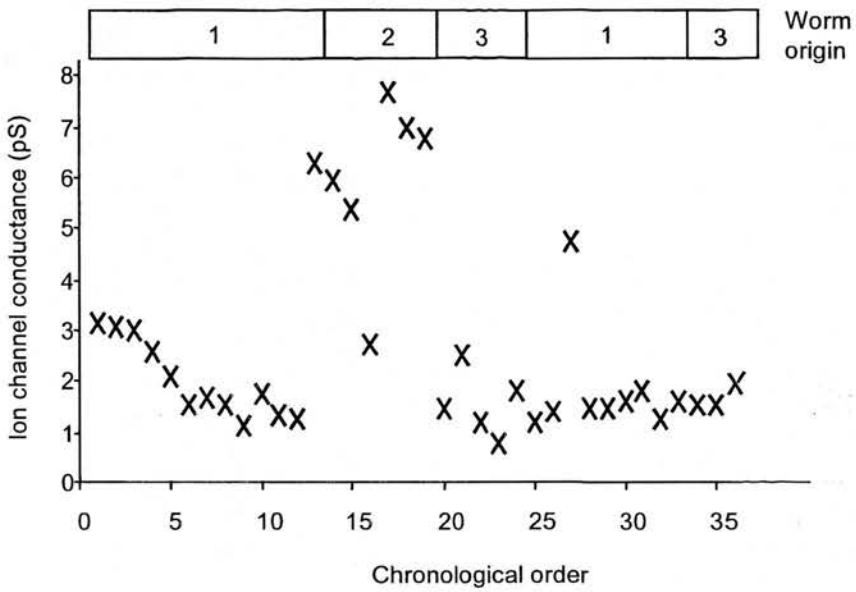

Conductance values (shown by X) are plotted against the chronological order of experiments. The rectangular boxes show the origin of the Ascaris *for each experiment. The origins are as follows: 1=Gloucester; 2=Paisley; 3=Belfast. n=36.*

When the conductance data was collected together it became clear that the range was not normally distributed (Anderson-Darling Normality Test, $P<0.001$). The channel conductances recorded in the year-long series of experiments fell into 3 groups, as shown in the upper graph of Figure 4.09. This is also shown by the conductance time-series shown in Figure 4.08, which illustrates the variation in the channel conductance over the 12 month period of experiments. The origin of the worms used in the experiments is also displayed in the time-series. The conductance values displayed in Figure 4.08 are those from I-V plots deemed to be reliable according to the criteria given above. The graph does not, therefore, show the conductance of every channel examined during the project. As can be seen from the time-series, the channel conductance observed in the *Ascaris* obtained from Paisley abattoir were significantly higher than those seen in the Gloucester or Belfast worms (ANOVA, $P<0.001$; two

sample *t* tests, $P<0.005$). The mean channel conductance in the Paisley worms was 5.91 ± 1.77 pS, in the Gloucester worms it was 2.13 ± 1.28 pS; and in those from Belfast it was 1.59 ± 0.54 pS (mean conductance ± standard deviation). There was no significant difference between the channel conductance seen in worms from Gloucester and in those from Belfast. The Gloucester and Belfast worms form a low-medium conductance subpopulation and the Paisley worms represent a medium-high conductance subpopulation.

The recorded channel conductances formed three groups, with peaks at 1.50, 2.87 and 5.50 pS, as shown in the graph A of Figure 4.09; low, medium and high conductance. Membrane patches made from the Gloucester and Belfast worms showed channel conductances in all three groups, although the majority of observations fell into the low and medium conductance groups (illustrated in Figure 4.09, B). The Paisley abattoir worms had larger channel conductance values, mainly in the 6.20 pS (high conductance) group; see Figure 4.09, C. The Gaussian curves fitted to the groups of individual conductances were determined using a computer program written in Fortran. The program employs a simplex method to minimise the log likelihood (NAG subroutine E04CCF), see Section 2.08.2.

There are three groups of channel conductance distinguishable in the worms used during the study: low, medium and high conductance. The two distinct subpopulations of *Ascaris suum* that occur within the experimental sample are the predominantly low-medium conductance worms from Gloucester and Belfast and the mainly high conductance worms from Paisley. Thus, two statistically different subpopulations of worms exist that have different proportions of high, medium and low channel conductance.

Figure 4.09 Channel conductance histogram fitted with Gaussian curves to illustrate the three conductance groups.

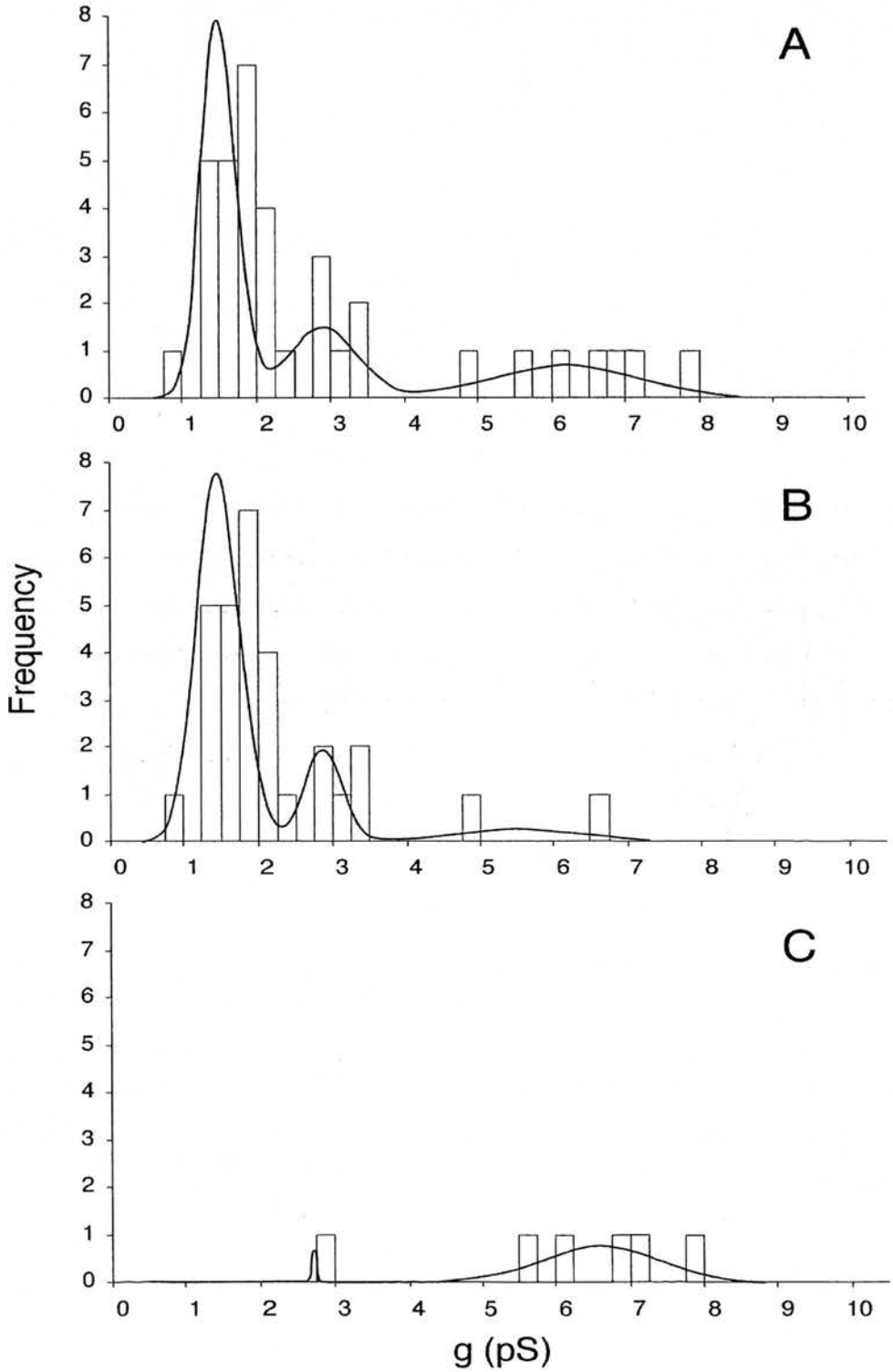

Conductance histograms fitted with Gaussian curves using the NAG subroutine E04CCF to minimise the log likelihood. The Gaussians illustrate the 3 groups of channel conductance which were observed: low conductance (76.6% of total), 1.50 ± 0.29pS (mean ± standard deviation); medium conductance (16.7% of total), 2.87 ± 0.26pS; high conductance (6.7% of total), 6.20 ± 0.80pS. ***A****: worms of all origins;* ***B****: Gloucester and Belfast;* ***C****: Paisley worms. n=36.*

4.05 The probability of channel opening (P_{open})

To calculate the probability of channel opening, events lists, (i.e. lists of channel openings, or "events") were generated in the computer program Fetchan and analysed with Pstat and Excel. The events lists were produced from the first 60 seconds of each channel recording. There was no evidence of desensitisation in the majority of records (see Section 5.05). Any channel records which showed baseline drift in excess of 1 pA; were interrupted by electrical noise or periods of membrane breakdown; or showed evidence of receptor desensitisation (i.e. changed markedly in terms of P_{open} or channel mean open time) were rejected. For the channels under investigation, the probability of channel opening, or P_{open}, occupied a range from 0 to 0.956. The data shown below is from vesicle-attached patches recorded in bath solution only (no other substances added to the bath solution). Outlying values were removed only if they were significantly different from the rest of the experimental population.

The mean P_{open} values varied over time in a similar way to channel conductance, see Section 4.04. This is shown in the time series shown in Figure 4.10, below.

Figure 4.10 Time series of mean P_{open}.

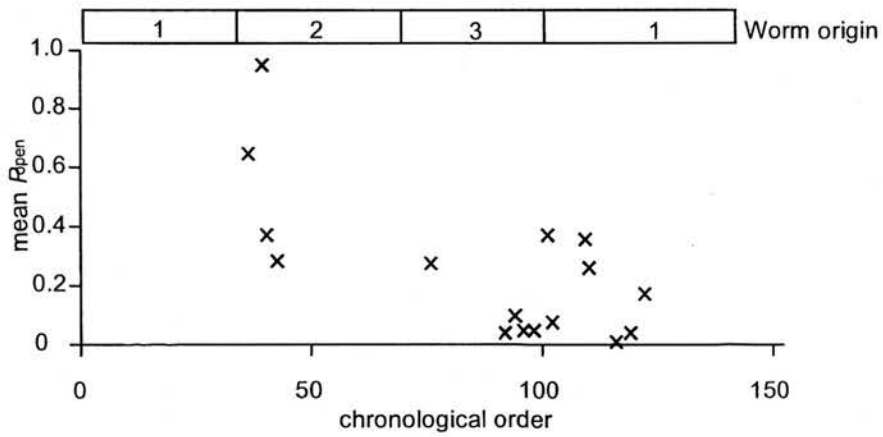

Mean P_{open} values (X) are plotted against the chronological order of the experiments. The values were calculated from patch clamp experiments carried out at [PF4]=0.003 μM. The worm origins are shown by the rectangular boxes at the top of the scatter plot. 1: Gloucester; 2: Paisley; 3: Belfast. The order in which experiments were carried out is shown on the x-axis. n=16.

Each patch was clamped over a range of potentials. The probability of channel opening was measured at each potential and the mean P_{open} was calculated for the patch. P_{open} is inherently variable: averaging the values normalised the data. Taking the mean value over a range of potentials was a legitimate statistical procedure since P_{open} was found to be independent of potential difference across the membrane patch. The correlation between P_{open} and potential difference was very low: R squared was 0.12. When tested for normality, the range of mean P_{open} values within a given PF4 concentration did not conform to a binomial distribution (Anderson-Darling test, $P<0.001$). This is illustrated in Figure 4.11A which shows all the mean P_{open} values recorded at 0.003 μM PF4. Using the same computer program as previously (see Section 2.08.2 and 4.04), which used NAG subroutine E04CCF to minimise the log likelihood, the range of mean P_{open} values was divided into 3 groups of 0.05 ± 0.01; 0.30 ± 0.04; and 0.65 ± 0.21 (mean ± standard error of the mean).

The three groups are shown by Gaussian curves superimposed onto the P_{open} distribution histogram in Figure 4.11. The whole experimental population, that is, worms from all three origins, is represented in the upper graph A. The three Gaussians indicate the three groups of P_{open} values. The middle graph, B, shows the P_{open} values obtained from Gloucester and Belfast worms where the values fall into the low and the medium groups of P_{open}. The Paisley worm P_{open} values are shown in the lower graph, C. They fit in to the medium and high P_{open} groups. The P_{open} values obtained from Paisley worms were significantly higher than those from both the Gloucester and the Belfast worms (two sample t test, $P<0.001$). The Gloucester P_{open} values were not significantly different from those obtained from the Belfast worms (two sample t test, $P>0.3$).

Therefore, the PF4 channel examined in this study showed three different groups of P_{open} values. The *A. suum* used in the experiments were divided into two statistically distinct subpopulations in terms of the probability of channel opening: one subpopulation was the Gloucester and Belfast worms with low-medium P_{open}, the Paisley worms, with medium-high P_{open}, formed the other subpopulation.

Figure 4.11 P_{open} histogram fitted with Gaussian curves to illustrate the three P_{open} groups.

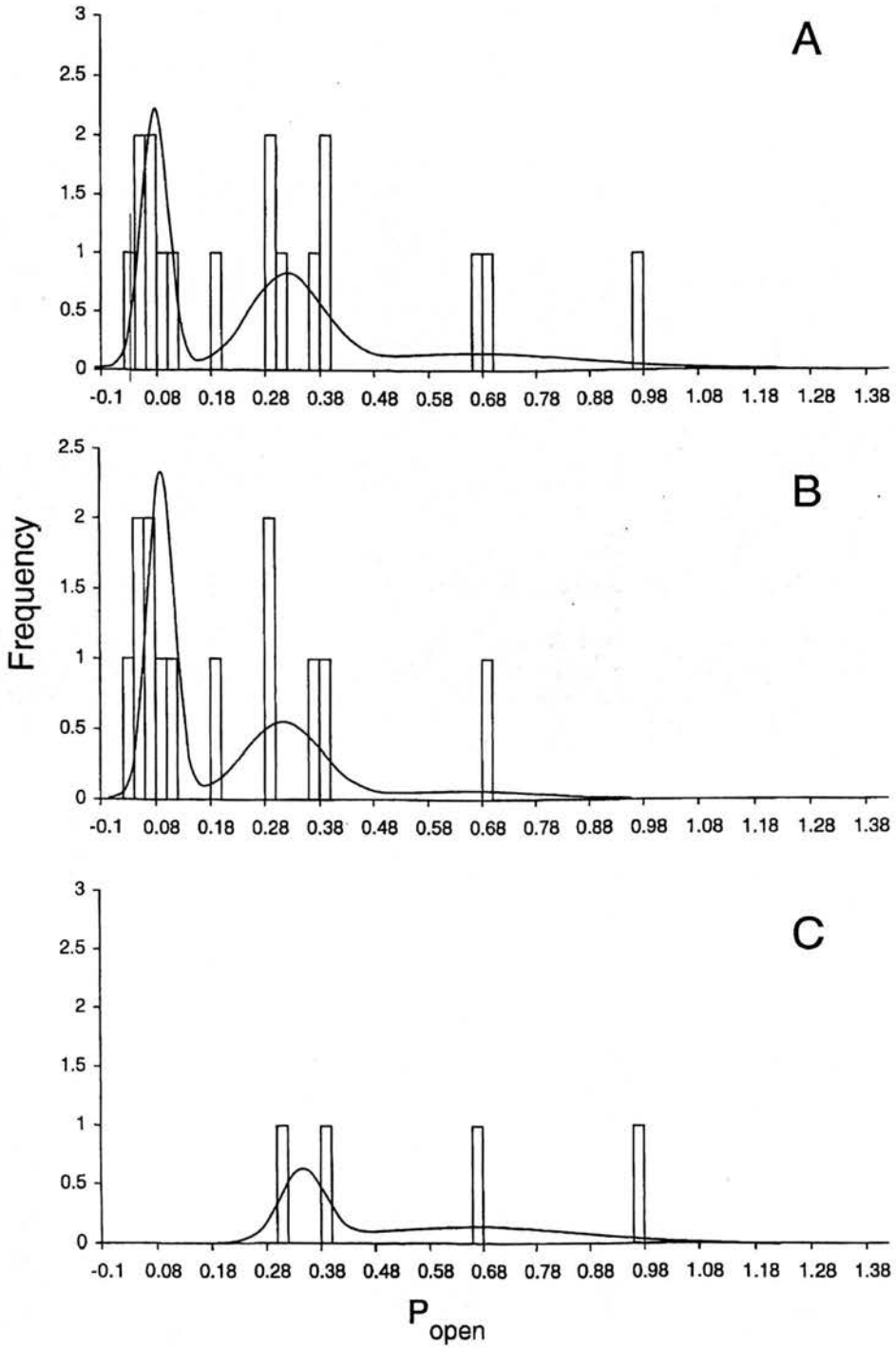

Probability of channel opening measured in patches exposed to 0.003μM PF4. ***A*** *shows the P_{open} histogram for worms of all origins, comprising:* ***B****, the P_{open} values calculated for Gloucester and Belfast worms; and* ***C****, the worms from Paisley. The Gaussian curves superimposed on the histogram indicate the mean and standard deviation of the three groups of P_{open}: 0.049 ± 0.013; 0.296 ± 0.035 and 0.649 ± 0.205 (mean ± standard error of the mean). n=17.*

In the membrane patches produced from Gloucester and Belfast *Ascaris*, the probability of channel opening was dose-dependent, as shown in Figure 4.12. P_{open} was apparently not dose-dependent in Paisley worms. The Gloucester and Belfast worms showed a typical dose-response curve. Using a simplex process employing a NAG E044CC subroutine, the mean P_{open} data were fitted by a rectangular hyperbola to produce Figure 4.12. According to the Michaelis Menton equation, the EC50 was calculated to be 1 nM PF4; the same value as for dose-dependent patch activity, see Section 4.01.

Figure 4.12 P_{open} dose-response curve

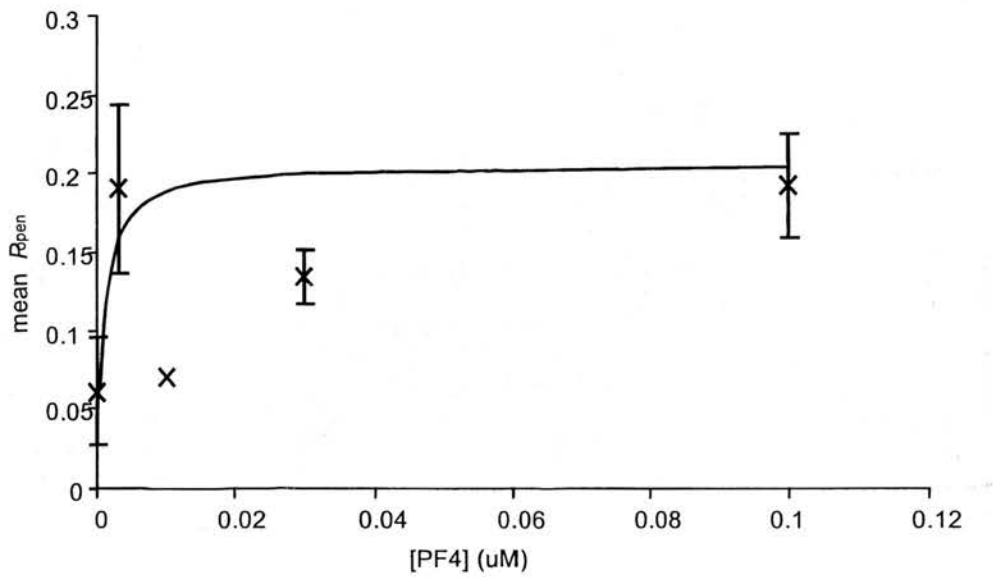

The graph shows the mean P_{open} plotted against the concentration of PF4 in the patch pipette. The mean P_{open} values shown were calculated from experiments carried out on Gloucester and Belfast worms only. Mean P_{open} values are shown by X and the vertical error bars show the standard error of the mean. The data have been fitted with a Michaelis Menton curve by a simplex process using an NAG E044CC subroutine; the EC50 was 0.001μM PF4. The responses were corrected for the value at zero concentration. n=40.

The P_{open} measured in the Paisley worms showed no dose-dependency, it remained at a high level (>0.3) from 0 to 0.030 μM PF4, with a marked decrease at 0.100 μM. This unexpected result is the opposite of the ion channel responses seen in the Gloucester and Belfast worms. It is possible that the Paisley worms are more sensitive to PF4 than the other group, and that the lowest concentration of PF4 used in the present study prompted a maximal response. The decrease in response at higher PF4 concentrations could then be explained by receptor desensitisation (Katz &

Thesleff, 1957). Further dose-response experiments, using lower concentrations of PF4, are required to test this hypothesis.

Regardless of the explanation of the P_{open} dose-dependency in the Paisley worms, the PF4 channels in the *A. suum* from Paisley had a higher probability of opening than that seen in the Gloucester and Belfast worms. Therefore, PF4 channel P_{open} constitutes a significant difference between the two sub populations of worms.

4.06 Mean open time

Mean open time is best calculated from records of single channel activity; it is difficult to ascertain from records in which there is more than one level of channel opening. Due to the high level of patch activity, there were too few single channel recordings available for the mean open times to be fully investigated in terms of dose-dependency or effects of patch isolation. The mean open time of the PF4 channel was obtained from records that showed single channel openings only. The channel records were from vesicle-attached patches where nothing had been added to the bath solution.

The mean open time was calculated in Pstat by fitting exponential curves to the dwell-time histograms, which were plotted from events lists which had been generated in Fetchan. Records in which the channel openings were binomially distributed were fitted by a single exponential curve; this is the simplest model of ion channel opening. Ion channels with only one duration of opening can be described by fitting a single exponential curve to the dwell time histogram. Those records in which there were two distinct types of opening, long and short, were best fitted by a double exponential. Records that showed more complex patterns of opening, with three or more different open times, were fitted with the appropriate number of exponential curves.

To determine how many exponential curves to fit to the experimental data, the "compare" option in Pstat was utilised. This software test assesses the accuracy of the curve fitting. "Compare" works by measuring the sum of the squared errors of each fitting method, whether one, two or more exponentials have been fitted. The sum of the squared errors is displayed as an "F-value", which allows a statistical comparison

of the curve fits to be made by using F tables. As each curve is fitted, the goodness of fit is assessed using the "compare" function. A significant difference according to the F-value indicates a significantly better fit than before. Where there is no statistically significant difference between successive fits, the lower number of exponentials is deemed to be the most appropriate fit to the data. Using this statistical method, the complexity of the channel opening pattern can be judged objectively.

To ensure accurate curve-fitting, the following criteria were applied: the histograms were made up of at least 40 points for a single exponential fit; at least 100 points to fit two exponentials; and at least 200 points to fit three exponential curves. There were 37 channel records that conformed to these criteria, which were fitted with one or more exponential curves using a Simplex maximum likelihood fitting protocol. Of these, 76% (28 records) were fitted best by a single exponential. Since single exponential fits represent the majority of the data, the mean open times reported below are the results of single exponential fits only.

At 0.03 μM PF4, there was a range of channel mean open times. At -80 mV, the range was at its widest; from 11 to 1956ms. The average values for mean open time are shown in Figure 4.13, when the patches were clamped at negative potentials the mean open time was longer and more variable than at positive potentials. This resulted in a variation in mean open time from 522 ± 333ms at -80mV to 25 ± 7 ms at +120mV (mean value ± standard error of the mean).

Figure 4.13 The variation of mean open time with potential difference

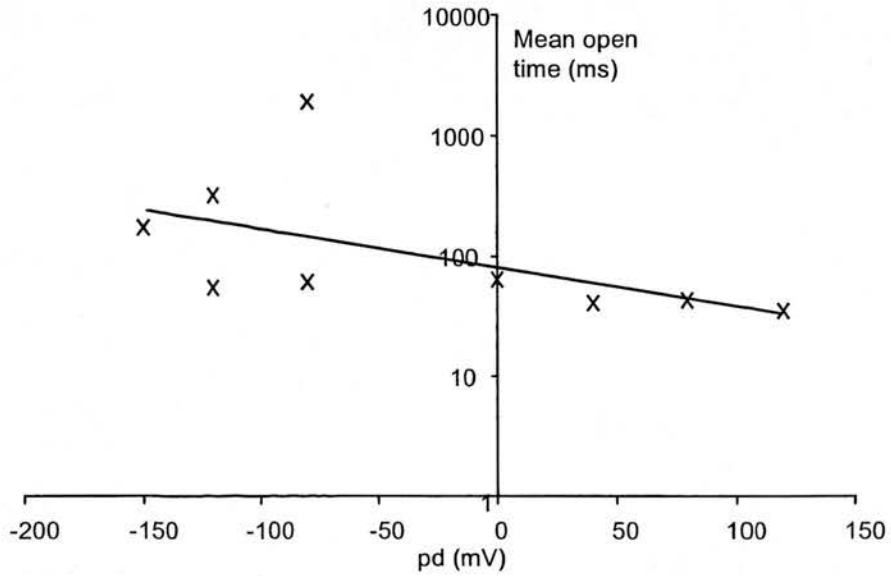

The mean open time of the ion channel varied with potential difference, being longer at negative potentials and shorter at positive potentials. Average values of the mean open times shown in the figure (X) were measured from patches exposed to 0.030μM PF4. The regression line has an R squared value of 0.30 which shows a low correlation but indicates the trend of the data.

There was no statistically significant difference in the mean open time recorded from worms of different origins (ANOVA, $P>0.3$) and there was no clear evidence that channel mean open time was dose-dependent (poor correlation between PF4 concentration and mean open time; R squared=0.16).

4.07 Mechanism of channel action

Broadly speaking, there are two mechanisms of channel opening seen in ligand-gated ion channels; see also Section 1.07.3. Channels can open as a direct result of the ligand binding to the receptor, thought to be due to conformation changes in the integrated receptor-channel molecule. Alternatively, channels can respond to a remote receptor via second messengers (Hille, 1992). These intracellular cascade mechanisms transmit the signal from the cell surface receptor to one or more ion channels. Intracellular signal transmission requires energy and is mediated by G-proteins or other mechanisms. Most of the peptide-gated ion channels which have been investigated operate via intracellular second messenger cascades, often involving G-proteins inside the cell or in the cell membrane itself; the so-called membrane delimited G-proteins (Wickman & Clapham, 1995) . However, two directly-gated peptide channels have been reported (Green *et al.*, 1994), see Section 1.08.1.

In order to investigate the mode of action of the PF4 channels, three experiments were carried out. The aim was to determine whether the channels open as a direct result of PF4 binding to a receptor or whether they open via a signal transduction mechanism.

4.07.1 Mechanism of channel action, experiment 1

In the first of the "mode of action" experiments (see Section 2.05.5), recordings were made from a membrane patch before and after it was isolated from the vesicle. Patches were isolated for at least 15 minutes. After isolation the patch no longer had contact with the vesicle contents, which might include signal transduction mechanisms of various types. Lack of contact with intracellular contents would be expected to cause channel run-down in channels which required second messengers in order to open (Becq, 1996). Patch isolation had no effect on the patch activity (the number of channels per patch), conductance, reversal potential or P_{open} of the channels (paired *t* test, $P>0.25$; ANOVA, $P>0.3$), see Table 4.02. From these observations, it is evident that ion channel activity does not rely on vesicular contents. The ion channels do not, therefore, rely on intracellular second messenger cascades.

The origin of the worms had no influence on the channel activity before and after patch isolation.

Table 4.02

Variable	Before isolation	After isolation	*P* value
Channels/patch	2.14 ± 0.31 (14)	2.57 ± 0.33 (14)	0.27
Conductance (pS)	2.39 ± 0.81 (5)	3.58 ± 1.21 (5)	0.23
Rev potential (mV)	-7.33 ± 9.91 (6)	-10.00 ± 9.66 (6)	0.69
P_{open}	0.223 ± 0.065 (10)	0.137 ± 0.066 (10)	0.14

Mean ± standard error of the mean followed by (n). The P value given was obtained from a paired t test for each comparison.

4.07.2 Mechanism of channel action, experiment 2

The second experiment to determine the mode of channel action was to record from a vesicle-attached patch before and after the addition of PF4 to the bath solution (see Section 2.05.6).

The patch pipette contained a low concentration (0.003 μM) of PF4. The response to the low [PF4] prior to altering the bath solution confirmed that channels were present in the patch. PF4 was then added to the bath solution to give a final concentration of 0.1 μM, and allowed to diffuse for 15 to 20 minutes in order to ensure thorough mixing. The rationale was that if the channels responded to remote receptors in the membrane, the receptors outside the tip of the patch pipette, now exposed to a high concentration of PF4, would be expected to cause increased channel activity. Any channel activity after the 15 to 20 minute period of patch isolation was recorded via the patch pipette. There was no significant difference in the number of channels per patch, channel conductance or P_{open} measured before and after the addition of PF4 to the bath solution, see Table 4.03. This set of results shows that there is no transduction mechanism in place to relay the signal from a remote receptor to the ion channels under observation.

The reversal potential became significantly more positive after the addition of PF4 to the bath solution, moving from -17.3 mV to -9.3 mV. Even the initial value of -17.3 mV is more positive than the theoretical value for the chloride reversal potential (see Section 4.03). This can be explained by chloride ion leakage across vesicle membranes. As discussed in Section 3.03, the *Ascaris* somatic muscle cell is permeable to chloride, allowing equilibration of chloride ions across the membrane with time. Since the addition of PF4 to the bath solution was always carried out at the end of a series of patch clamp experiments, the chloride ions would have had ample time for redistribution between the vesicle contents and the bath solution. Futhermore, the membrane patch was clamped for at least 25 minutes during experiments when PF4 was added to the bath; sufficient time for chloride ion redistribution between the vesicle contents and the patch pipette. The chloride concentration of the pipette solution was 144 mM. An increase in chloride ion

concentration inside the vesicle to 100 mM would cause the chloride reversal potential to shift to -9.5 mV.

Table 4.03

Variable	PF4-free bath solution	PF4 in bath solution	*P* value
Channels/patch	2.60 ± 0.51 (5)	2.60 ± 0.51 (5)	1.00
Conductance (pS)	2.39 ± 0.79 (4)	2.27 ± 0.65 (4)	0.55
Rev potential (mV)	-17.25 ± 5.02 (4)	-9.25 ± 5.45 (4)	0.02
P_{open}	0.169 ± 0.088 (4)	0.246 ± 0.067 (4)	0.24

Mean ± standard error of the mean followed by (n). The P value given was obtained from a paired t test for each comparison. The experiments were carried out on worms from Gloucester and Belfast only with 0.003 μM PF4 in the pipette solution.

4.07.3 Mechanism of channel action, experiment 3

The third experiment investigating the mode of channel action investigated the involvement of G-proteins, see Section 2.05.7. The procedure was to record from the membrane patch before and after G-protein inhibition. This was achieved by using guanosine 5'-O-(2-thiodiphosphate), the non-hydolyzable GDP analogue, which inhibits all G-proteins (Eckstein *et al.*, 1979). Guanosine 5'-O-(2-thiodiphosphate), abbreviated to GDP-β-S, is unlikely to cross cell membranes therefore, when added to the bath solution, it did not enter vesicles in appreciable quantities. To test the effect of GDP-β-S on membrane patches, recordings were made in the vesicle-attached configuration to provide a measure of channel activity prior to GDP-β-S exposure. The patches were then isolated and consequently exposed to GDP-β-S. The channel activity was recorded again in the presence of the G-protein inhibitor. See Section 2.05.7 for a fuller description.

There was no significant difference in the number of channels per patch or the reversal potential before and after exposure to GDP-β-S, therefore G-proteins are not implicated in ion selectivity and are not essential to the opening of the PF4 channel. However, the channel conductance and P_{open} were both significantly altered by

exposure to GDP-β-S. Conductance decreased when G-proteins were inhibited, while P_{open} increased slightly, see Table 4.04.

The results indicate that the P_{open} and conductance of the PF4 channel are both affected by G-proteins, which suggests that the "fine tuning" of channel opening is modulated by G-proteins (Gilman, 1987; Hille, 1994). Modulation of channel characteristics has been recognised in other ligand-gated channels; for example, dopamine-gated ion channels in the snail *Helix aspersa* are modulated via protein kinase C (Green & Cottrell, 1997). Ion channel modulation is complex and numerous intracellular second messengers can be involved. G-proteins contribute to channel modulation both directly (see Brown & Birnbaumer, 1990 and Simon *et al.*, 1991 for reviews) and indirectly, e.g. via protein kinase C (Gilman, 1987).

The mean values for reversal potential both before and after G-protein inhibition were markedly negative, due to two unusually negative values. A possible explanation for these values is a change in micropipette capacitance. This is a recognised phenomenon of patch clamping and can lead to the recording of unexpected values for the membrane potential (Sakmann & Neher, 1983).

Table 4.04

Variable	Before GDP-β-S exposure	After GDP-β-S exposure	*P* value
Channels/patch	2.75 ± 0.85 (4)	3.00 ± 0.71 (4)	0.39
Conductance (pS)	1.22 ± 0.18 (4)	0.87 ± 0.16 (4)	0.01
Rev potential (mV)	-52.5 ± 15.7 (4)	-77.5 ± 37.2 (4)	0.40
P_{open}	0.109 ± 0.038 (4)	0.125 ± 0.039 (4)	0.04

Mean ± standard error of the mean followed by (n). The P value given was obtained from a paired t test for each comparison. The experiments were carried-out on Gloucester and Belfast worms only and the same concentration of PF4 was used throughout (0.030 μM).

The presence of GDP-β-S in the bath had no effects on the parameters being measured prior to patch isolation (no significant difference when compared with vesicle-attached patches in a GDP-β-S free bath solution; two sample *t* test, $P>0.1$).

4.08 Discussion of patch clamp results: an overview

The patch clamp experiments showed that PF4 opens chloride ion channels in *Ascaris suum* somatic muscle cell membranes. The ion channels are numerous and have a low conductance (1 to 7 pS). They respond to PF4 in a dose-dependent manner; both the number of channels recorded per patch and the probability of channel opening increase with increasing PF4 concentration. The ion channels open as though directly gated by PF4, although there is some evidence for modulation. The observed range of channel characteristics is consistent with the existence of subpopulations of *Ascaris suum* in the UK.

4.09 Channel characteristics

The channels examined in this study were small amplitude chloride ion channels located in the somatic muscle cell membrane of *Ascaris suum*. Of the 164 membrane patches that were successfully patch clamped *and* produced clear records, 70% (114 patches) showed channel activity. Even without PF4 in the patch pipette, 21 patches out of 50 (42%) had active ion channels, although significantly fewer channels per patch were seen than when PF4 was present. The PF4 channels were, therefore, ubiquitous on *Ascaris* muscle cell membranes and had a high probability of being open. Similar "spontaneously opening" $GABA_A$ channels have been observed in cultured preparations of mouse neurones (Hamill *et al.*, 1983; MacDonald *et al.*, 1989). Like the PF4 channels in the present study, $GABA_A$ channels were noted to open randomly in the absence of ligand, and to show increased probability of opening in the presence of ligand. A possible explanation for the channel activity when no PF4 was present in the pipette solution is that the "spontaneous opening" could have been due to the presence of some endogenous ligand in the vesicle preparation. The intensive processing involved in vesicle preparation reduces the likelihood of endogenous ligands being present, but it is a possibility that can not be ruled out (Hamill *et al.*, 1983).

The PF4 channels showed a high probability of opening and a long mean open time. These characteristics, in addition to the high expression levels of the functional receptor, compensate for the small amplitude of the channels. Despite their low conductance (the range of conductance values was 1.09 to 7.07 pS), these ion

channels are capable of making a sizeable contribution to the current across the cell membrane, as can be seen from the unequivocal whole cell responses to PF4 (see Chapter Three).

The single PF4 channel conductance can be compared with the whole cell conductance with a simple calculation. The average number of channels per bag region is $1.4x10^4$ (from Equation 3.04), and since mean single channel conductance is ~4 pS, the predicted conductance of the whole bag region is $5.6x10^4$ pS, or 0.056 μS, if all the PF4 channels were to open. This is less than the observed value for whole cell conductance (see Section 3.02) by a factor of 10. One of the possible reasons for this discrepancy is that the arm and the spindle of the cell possess PF4 channels but were not included in the calculation, thus the predicted value of the whole cell conductance was underestimated. Another explanation might be that the concentration of PF4 used in the current clamp experiments was higher than that used in the majority of the patch clamp work. The high concentration of PF4 increased the probability of channel opening and the patch activity so that more channels were open for more of the time than in the patch clamp experiments, making the observed whole cell conductance significantly larger than the value predicted by the single channel conductance.

The mean open time of the PF4 channel was voltage sensitive, varying from 522 ± 333 ms at -80 mV to 25 ± 7 ms at +120 mV. The two notable features of the mean open time are firstly that it varied greatly, and secondly that it was longer, at hyperpolarised potentials. Similar channel characteristics were observed in the calcium-dependent chloride channel found in *Ascaris* (Thorn & Martin, 1987). Thorn and Martin carried out extensive analysis on the kinetics of this calcium-dependent channel. They showed that the gating kinetics were more complex at hyperpolarised potentials, with two open times and three closed times, than when the membrane was depolarised. It is possible that similar complexity lies behind the long and variable mean open time of the hyperpolarised PF4 channel. The mean open time of 522 ms is a relatively prolonged period of channel opening. For comparison, the mean open times of some other *Ascaris* ion channels are 32 ms for the GABA channel (Martin,

1985); 1 ms for the nicotinic acetylcholine channel (Robertson *et al.*, 1999); 0.3 and 10 ms for the glutamate-gated channel (Adelsberger *et al.*, 1997).

4.10 Dose-dependency

There was a dose-response relationship between the concentration of PF4 in the patch pipette and the number of channels open per patch. There was also a clear relationship between PF4 concentration and the response in terms of the probability of channel opening. In both cases, the dose-response relationship conformed to the Michaelis Menton equation (see Section 2.10) and the EC50 for PF4 was calculated to be 1 nM. The high potency of PF4 is consistent with PF4, or a very similar FaRP, being an endogenous *Ascaris* neurotransmitter. Other parameters (conductance, reversal potential and mean open time) were not found to be dose-dependent in this study. Previous work on PF4 by Holden-Dye *et al.* (1997) determined the EC50 as 98 nM for muscle cell hyperpolarisation recorded in current clamp experiments. The discrepancy between these two values for the EC50 of PF4 can be explained by differences in experimental technique (current clamp versus patch clamp experiments) and in the parameters being measured (hyperpolarisation compared with patch activity and P_{open}).

4.11 Voltage sensitivity

Channel characteristics can alter as the membrane potential changes. An obvious example of voltage sensitivity in ion channels is the existence of voltage-gated channels (Hodgkin *et al.*, 1952). Voltage-gated channels open over a limited range of membrane potential. Less extreme examples of voltage sensitivity are changes in individual channel characteristics with membrane potential, such as the phenomenon known as rectification (Hille, 1992), when ion channel conductance alters over a range of membrane potentials; generally, conductance falls at depolarised potentials.

The channels examined in this study showed voltage sensitivity in terms of mean open time. From the suitable records (criteria for suitability are discussed in Section 4.06) it was clear that the mean open time of the channels was longer and more variable at hyperpolarised potentials (see Figure 4.13). This contributed to the noisy and complex appearance of experimental records made at negative potentials. In

general, the records obtained at positive potentials were clearer and easier to interpret than their hyperpolarised counterparts because the channels opened for significantly shorter periods when the patches were clamped at depolarised potentials. Other than mean open time, the ion channels did not show voltage sensitivity; patch activity (i.e. the number of channels per patch), conductance, reversal potential and the probability of channel opening did not alter with the membrane potential. This was true even at potentials 120 mV above and below the resting membrane potential.

4.12 Nematode genetics

Some of the channel properties recorded in this study were distributed over a range regardless of PF4 concentration, namely the probability of channel opening (P_{open}) and channel conductance. Each of these characteristics fell into three statistically discrete groups, which can be categorised as high, medium or low P_{open} and conductance. Each channel could have any combination of conductance and P_{open} value, although the high value of P_{open} was usually associated with high channel conductance.

The worms used during the course of experiments came from three sources in distinct geographical areas; Gloucester in central England, Paisley in central Scotland and Cullybackey (near Belfast) in Northern Ireland. Vesicles were produced from all the worms and PF4 elicited a channel response in the majority of cases. However, while the *Ascaris* from England and Northern Ireland showed similar channel characteristics to each other, the worms from Scotland had significantly different channel properties. The Scottish worms had ion channels with higher mean conductance and higher P_{open} than the Northern Irish or English worms. The existence of these two statistically different worm subpopulations in the UK population of *Ascaris suum* illustrates the marked genetic diversity among these parasitic nematodes, see Section 1.06.2.

4.13 Ion channel mode of action

There are two main methods by which ligand-gated ion channels open. One is the directly-gated method, the other is by signal transduction (Hille, 1992). Directly-gated ion channels open due to a change in molecular conformation, which occurs when the ligand binds to a site on the extracellular face of the ion channel. Signal transduction involves the relay of information from a receptor to one or more separate

ion channels. There are several intracellular and membrane delimited routes that can be used in signal transduction, including various intracellular second messenger cascades and G-proteins. The experiments that were carried out to investigate the mode of action of the ion channels showed that the channels were directly-gated by PF4 and that channel characteristics could be modulated by a G-protein.

In the first set of experiments, isolating the patch from its parent vesicle was shown to have no effect on any of the parameters measured. After being separated from the vesicle for at least 15 minutes, the patches showed no channel run-down (that is, a significant reduction in channel activity following isolation of the membrane from the intracellular contents; for review see Becq, 1996). The ion channels were evidently robust enough to function without whatever intracellular constituents the vesicle contained. This observation rules out ion channel dependence on intracellular second messenger cascades.

The second set of experiments showed that stimulation of remote PF4 receptors (outside the rim of the patch pipette) had no effect on the ion channels in the membrane patch. This finding shows that there was no connection between the ion channels and non-adjacent receptors (Green *et al.*, 1994).

The third set of experiments demonstrated the presence of G-proteins in the membrane vesicles, since the addition of a non-selective G-protein inhibitor (GDP-β-S) significantly affected two of the ion channel characteristics. The probability of channel opening increased when G-protein activity was inhibited, and channel conductance decreased. The involvement of G-proteins in the control of the PF4 channels shows that the channel activity can be modulated.

4.14 Summary of the PF4 channel characteristics

In summary, PF4 channels were shown to be small amplitude chloride channels with a high probability of opening. They were numerous in the somatic muscle cell membrane. The high P_{open} led to spontaneous channel activity in the absence of ligand, which increased with increasing PF4 concentration. Both the number of channels per patch and the P_{open} were dose-dependent characteristics. The channel

mean open time was relatively long, and varied with the membrane potential of the patch.

Three subtypes of channel conductance were recorded, and there were also three subtypes of PF4 channel P_{open}. These subtypes were not distributed evenly throughout the worms studied during this project. Rather, there were two subpopulations of worms, one with significantly lower conductance and lower P_{open} PF4 channels than the other.

The PF4 channel characteristics were independent of patch isolation and there was no response to remotely-applied PF4. The patch activity was undiminished in the presence of a G-protein inhibitor. These observations are consistent with the argument that PF4 channels are directly-gated. There was evidence that some PF4 channel characteristics (P_{open} and conductance) are modulated by G-proteins.

Chapter 5. PF4 channels, a general discussion.

5.01 PF4 channels conduct chloride ions

The ion channels that were observed to respond to PF4 in the present study will be referred to as "PF4 channels" to avoid confusion with the other ion channels present in *Ascaris suum* somatic muscle cell membranes.

This study has shown that PF4 opens chloride ion channels in *Ascaris suum* somatic muscle cells, which confirms earlier work (Maule et al., 1995a; Holden-Dye *et al.*, 1997). Opening of the chloride channels caused muscle cell hyperpolarisation, again shown by other workers using the current clamp method (Holden-Dye *et al.*, 1997). In muscle tension studies carried out in other laboratories, PF4 was associated with hyperpolarisation and marked muscle relaxation (Maule *et al.*, 1995b). In another series of experiments, muscle strips were treated with excitatory FaRPs to cause rhythmical contractions that were abolished by PF4 (Maule *et al.*, 1995a). The observations on *Ascaris suum* muscle strips are consistent with the argument that PF4-induced hyperpolarisation causes muscle relaxation. It follows that activation of the chloride ion channels studied during the course of this project has a role in controlling muscle cell contractility. As noted in section 3.01, during the present study, muscle relaxation was frequently noted after PF4 was applied to flap preparations. In some preparations, the relaxation was sufficient to dislodge the microelectrodes from the target cell, which ended those experiments.

Chloride channels have been shown to conduct volatile fatty acids, the waste products of anaerobic metabolism (Valkanov *et al.*, 1994; Dixon *et al.*, 1993; Valkanov & Martin, 1995; Robertson & Martin, 1996). In the light of this evidence, it is possible that the chloride channels studied here contribute to waste product excretion as well as controlling membrane potential.

5.02 Location of PF4 receptors

PF4 was shown to act on muscle cell receptors, which is concordant with findings from other workers. Experiments carried out on denervated muscle preparations

(Maule *et al.*, 1995a; Maule *et al.*, 1995b) showed that the removal of the *Ascaris* nerve cords did not affect the muscle strip response to PF4. Therefore, PF4 receptors must exist outside the neuromuscular junctions, which, by elimination, means that receptors must be on the hypodermis or alternatively, the bag region or spindle of the muscle cells. There is a precedent for the existence of FaRP receptors on the somatic muscle cells; a binding study has shown the presence of PF1 receptors on the muscle cell membrane (Bowman *et al.*, 1995). PF1 has also been shown to act on the bag region of somatic muscle cells in a patch clamp study (Martin & Valkanov, 1996).

Attempts to localise FaRPs in nematodes have been frustrated by the autofluorescence of nematode muscle cell membranes. Due to autofluorescence, worm tissue is treated to remove muscle cells prior to carrying out immunofluorescence studies (Brownlee *et al.*, 1993), hence, immunocytochemistry has not been used to investigate the FaRP content of somatic muscle cells in *Ascaris*. Several studies have identified FaRPs in the *Ascaris* neuronal and reproductive tissue by immunocytochemistry (Sithigorngul *et al.*, 1990; Cowden *et al.*, 1993; Fellowes *et al.*, 1999). Over 60% of *Ascaris* neurones show immunoreactivity to FMRFamide antisera (Cowden *et al.*, 1993). It is possible that a higher proportion of neurones contain FaRPs since FMRFamide antisera may not cross react with all endogenous *Ascaris* FaRPs (Brownlee *et al.*, 1996). Neurones are evidently a major source of FaRPs in *Ascaris*. To date, a specific antibody to PF4 is not available so there is no direct immunocytological evidence for the presence of PF4 in *Ascaris*.

5.03 Conservation of FaRP receptors in nematodes

Given the marked response seen in *Ascaris* tissue to PF4, workers agree that PF4 or a close analogue must be endogenous to *Ascaris suum* (Maule *et al.*, 1995b; Brownlee *et al.*, 1996). It is plausible that PF4 is reacting with *Ascaris* receptors for the endogenous FaRPs AF1, AF5 or AF6, since all share some amino acid sequence with PF4:

PF4 structure: **Lys-Pro**-Asn-**Phe-Ile-Arg-Phe**-amide

AF1 structure: **Lys**-Asn-Glu-**Phe-Ile-Arg-Phe**-amide

AF5 structure: Ser-Gly-**Lys-Pro**-Thr-**Phe-Ile-Arg-Phe**-amide

AF6 structure: **Phe-Ile-Arg-Phe**-amide

5.04 Survey of PF4 responses: comparing several studies

5.04.1 Hyperpolarisation response to PF4.

In the current clamp studies carried out during this project, PF4 was used at a concentration of 0.1 μM. There was a marked similarity in the initial response to PF4 seen in the current clamp results and the hyperpolarisation responses reported by other workers. The hyperpolarisation recorded by Maule *et al.* (1995a) at 0.001 to 1 μM PF4 was very similar to the response recorded in the present current clamp experiments. Likewise, the hyperpolarisation response published by Holden-Dye *et al.* (1997) to 0.01 to 10 μM PF4 was also very similar to the current clamp results reported here. In all three cases, PF4 induced a rapid hyperpolarisation accompanied by a marked increase in input conductance.

5.04.2 Effects of a high PF4 concentration.

Following exposure of *Ascaris* tissue to PF4, an immediate hyperpolarisation response was seen in this project and was reported by previous workers (Maule *et al.*, 1995a; Holden-Dye *et al.*, 1997). However, after the initial hyperpolarisation response, different responses were reported. In the present current clamp study, PF4 was applied to the target cell for between 2 and 20 seconds. The cell membrane hyperpolarised then recovered, returning to the original resting potential at a rate of 0.05 mV/second. Holden-Dye *et al.* (1997) describe two phases to the muscle cell response to PF4; the "PF4-early" and "PF4-late" phases. PF4-early described the hyperpolarisation that was mirrored in the present current clamp study. PF4-late was the plateauing of the membrane potential during the recovery of the cell from the PF4 application. PF4-late was seen by Holden-Dye *et al.* at concentrations of PF4 greater than 1 μM, after a period of PF4 perfusion lasting at least one minute. There was no evidence of a PF4-late phase in the results of the study reported here, which, since PF4 was not applied at this concentration or for a similar length of time, is unsurprising. 1 μM of PF4 applied for one minute is a large quantity in physiological terms, given that the EC50 determined for PF4 in the present study was 1 nM. Therefore, the PF4-late phase may not be representative of *Ascaris* responses *in vivo*.

An interesting hypothesis for the concentration-dependent effects of FaRPs was put forward by Edison *et al.*, (1999). After observing that FaRP structure markedly affected receptor-binding, they suggested that separate populations of FaRP receptors are bound by molecules with specific conformation. A FaRP molecule that exists in several distinct conformations will bind several specific receptors. If the molecule predominantly occurs in one conformation, one receptor population will be stimulated at low FaRP concentrations. However, at higher concentrations, the alternative molecular conformations become more numerous and reach a high enough concentration to stimulate their own specific receptors. When each receptor population is coupled to a different effector, the effect of a FaRP at low concentration will be unlike the effects at high concentration. This structure-dependency may explain the unexpected effects of FaRPs applied at high concentration.

There were also two qualitative differences in the response reported by Maule *et al.* (1995a) to high concentrations of PF4 ($\geq$ 1 μM). The first of these observations was that tissue preparations desensitised on exposure to $\geq$ 1 μM PF4, a phenomenon also noted following application of $\geq$ 10 μM GABA. Desensitisation to PF4 was not recorded in either the sharp electrode work or the patch clamp study reported here, presumably because the concentrations used did not exceed 0.3 μM PF4.

The second finding reported by Maule *et al.* and not seen in the course of this project was that, following exposure of tissue preparations to low concentrations of PF4 (0.001-0.3 μM), a subsequent high concentration of PF4 ($\geq$ 1 μM) produced the opposite effect. The low dose of PF4 caused muscle relaxation and the ensuing high dose initiated a further transient relaxation followed by a profound contraction. This unexpected effect also occurred after a GABA-mediated relaxation. PF4-induced muscle contraction did not occur in denervated preparations. This observation indicated that the relaxation response is evoked by receptors in the muscle cell membrane while contraction is mediated by the nervous system. It was hypothesised that the contractile response to high-dose PF4 was due to non-specific binding to excitatory FaRP receptors in the nervous system (Maule *et al.*, 1995b). In the present study, the concentration of PF4 did not exceed 0.3 μM, thus only hyperpolarisation

(which, in this system, corresponds to relaxation) of the somatic muscle cells was recorded in response to PF4.

The PF4 concentrations used in the present patch clamp study ranged from 0.003 to 0.3 μM. This concentration range represents the lower end of the concentration ranges used by the other workers; from 0.001 to 10 μM (Maule *et al.*, 1995a; Holden-Dye *et al.*, 1997). It is not possible to make a direct comparison between PF4 concentrations used in the patch clamp experiments in the present study and the whole cell or muscle strip experiments carried out in other laboratories. In the former situation, PF4 was applied directly to cleaned muscle cell membrane, whereas in the latter PF4 was bath applied to the tissue preparation. Any disparity in the results of the two types of experiment can, in part, be explained by the difference in the presentation of PF4 to the receptors in each case. However, the observation of channels opening in response to PF4 in the pipette solution was consistent with the rapid hyperpolarisation response seen in the whole cell sharp electrode experiments.

5.04.3 High potency of PF4 in Ascaris.

In the patch clamp experiments, the PF4 EC50 was 0.001 μM for responses that could be described by the Michaelis Menton equation. This is a low value in comparison with the concentrations used by other workers to obtain the "PF4-late" responses (Holden-Dye *et al.*, 1997) or the contradictory PF4-mediated muscle contraction (Maule *et al.*, 1995a) described above. However, 0.001 μM may be a more realistic value physiologically because it is a low concentration. It is interesting to compare the nanomolar concentration of PF4, when acting extrasynaptically on muscle cells, with the concentration of hormones in vertebrates. In vertebrates, compounds acting as hormones are present in the blood at concentrations ranging from 10^{-6} to 10^{-12} M (Lehninger *et al.*, 1993), which indicates the potency of endogenous peptides *in vivo*. Since 0.001 μM falls in the middle of the concentration range 10^{-6} to 10^{-12} M, it can be argued that the responses recorded in the patch clamp experiments of the present study are the normal responses of the *Ascaris* somatic muscle cells to a physiological concentration of PF4.

5.04.4 PF4 and GABA act on different chloride channels.

The somatic muscle cell response to PF4 was observed to be qualitatively similar to the response to GABA, although PF4 was approximately 10 times more potent than GABA. This comparison has been made by other workers in the field (Maule *et al.*, 1995a; Holden-Dye *et al.*, 1997), who have all shown that PF4 and GABA do not act on the same receptors. In the former study, PF4 and GABA were found to be "functionally cross-desensitising"; that is, following application of a high concentration of either compound (≥ 1 μM PF4, ≥ 10 μM GABA) a subsequent application of PF4 or GABA had no effect. This lack of response could be due to extreme responses to both compounds when applied at non-physiological concentrations (1000 fold greater than the EC50 for PF4 determined in the present study). Receptor desensitisation (Katz & Thesleff, 1957) is a possible explanation for the lack of response following high levels of receptor stimulation. Another reason for the absence of response might be the change in intracellular milieu due to high concentrations of PF4 or GABA. That is, the lengthy period of chloride channel opening caused by application of high concentration of PF4 or GABA would result in a marked increase in intracellular chloride concentration. This would prevent further entry of chloride to the cell until enough time had passed for the chloride concentration to fall to more normal levels. During the period of high intracellular chloride concentration, the cell would be refractory to chloride channel ligands, hence the lack of response.

GABA channels differ from PF4 channels in their larger conductance, 22 pS and shorter mean open time, 32 ms (Martin, 1985).

5.05 PF4 channels did not show desensitisation or run-down

Desensitisation (Katz & Thesleff, 1957) was not a feature of the PF4 channels seen during the experiments reported here. Neither repeated applications of PF4 to target cells nor prolonged exposure of membrane patches to PF4 in the pipette solution caused any reduction in the PF4 response. Similarly, there was no evidence of channel run-down (Becq, 1996). Even after the patches had been isolated from the vesicles, ion channels continued to open in response to PF4. The robust behaviour of the membrane patches argues against the requirement for intracellular regulators in channel opening (Becq, 1996).

5.06 PF4 channel mode of action

The behaviour of PF4 during this project is consistent with it acting directly on ion channels. As well as the absence of channel run-down following membrane patch isolation, there was no evidence of signalling between receptors in one area of the vesicle and ion channels elsewhere. There is a precedent for a channel directly gated by a peptide: Green *et al.* (1994) demonstrated that FMRFamide directly gates two types of sodium ion channels in the snail *Helix aspersa*.

Non-specific inhibition of G-proteins by guanosine 5'-O-(2-thiodiphosphate) (GDP-β-S) changed some of the channel characteristics, reducing the channel conductance and slightly (but significantly) increasing the P_{open}. This discovery suggests a G-protein involvement in ion channel modulation. In view of the observation that the ion channels continue to function normally after patch isolation, any G-protein associated with channel function would have to be closely applied to the membrane and act via second messengers in the immediate vicinity. Alternatively, a membrane delimited G-protein, situated adjacent to the ion channels, could be involved in channel regulation (Wickman & Clapham, 1995). Further investigation is required to demonstrate unequivocally the presence of a membrane delimited G-protein linked to these ion channels.

5.07 PF4 channels are different from other nematode chloride channels

The chloride ion channels studied during the course of this project were distinctly different from others investigated in nematodes (Martin, 1985; Thorn & Martin, 1987; Martin, 1995; Adelsberger *et al.*, 1997). The PF4 channels are low conductance and appear to be numerous in the muscle cell membrane.

5.08 PF4 channels as potential drug targets

The high incidence of nematode parasites (of both humans and the domestic species) demands safe and efficient antiparasitic drugs, see Section 1.01.

There are several criteria for an ideal anthelmintic (Geary *et al.*, 1992a). Firstly, it would be broad-spectrum; that is, it would act on all parasitic nematodes, regardless of species or stage in the life cycle. Secondly, it would be highly effective, rapidly

killing or paralysing the nematodes. Thirdly, it would be safe for use in vertebrate host species.

The FaRPergic nervous system in nematodes has been recognised as a potential target for anthelmintics, see Geary *et al.*, 1999 for a review. There are several advantages of FaRPergic neurones or FaRP receptors as anthelmintic targets. The first is that FaRPs are wide spread among nematodes, including the parasitic nematodes so far examined (see Day & Maule, 1999 for a review), thus FaRP receptors fulfil the requirement for being a broad-spectrum target. Secondly, FaRPs are an intrinsic part of the nematode neuromuscular system (Maule *et al.*, 1996); interference with FaRP function would severely compromise the nematode. Thirdly, the FaRPs identified in nematodes are distinct from those that exist in their potential hosts.

FaRPs have been identified in vertebrates (Yang & Majane, 1990), but have different structures from the nematode FaRPs (see Section 1.05.7). Evidence in support of the structural differences between FaRPs was given by Lingueglia *et al.* (1995). They used the *Xenopus* oocyte expression system to express FMRFamide-gated sodium channels derived from *Helix aspersa*. While FMRFamide opened the channels, other molluscan FaRPs and the mammalian FaRP, NPFF, had no effect on the ion channels when they were applied to the oocytes. Any difference in structure can be exploited in drug design, making compounds targeted at FaRP receptors more specific, and therefore safer for the host species. The effect of subtle structural changes in FaRP molecules on receptor-binding affinity has been shown (Edison *et al.*, 1999); careful design of molecules should result in highly specific binding.

PF4 channels show some promise as potential drug targets. First: although derived from *Panagrellus redivivus*, a free-living nematode, PF4 is active in *Ascaris suum*, a parasitic nematode. Since there is a short phylogenetic distance between the two species, see Section 1.06.1 and Figure 1.03, this suggests conservation of PF4 receptors across three clades of nematodes. Conserved nematode proteins make attractive anthelmintic targets because ideally, these drugs should affect as broad a spectrum of parasitic worms as possible. Second: the profound neuromuscular effects of PF4, already demonstrated by other workers (Maule *et al.*, 1995b; Holden-Dye *et al.*, 1997), were confirmed during this project. PF4 is active at low concentrations in

Ascaris suum (EC50 of 1 nm in the patch clamp experiments), which suggests that PF4 is an important neurotransmitter in nematodes. Drugs affecting PF4 signalling would be expected to severely compromise nematode parasites.

As yet, the effect of PF4 on vertebrate gut has not been established. PF4 receptors can only be considered as safe anthelmintic targets if they are not present in the host's own tissues. PF4-sensitive receptors in the host species' gut would be of particular interest since any anthelmintic ingested by the host will come into contact with the gut wall, regardless of drug absorption. The mammalian FaRP NPFF has modulatory effects on the guinea pig ileum in experiments where muscle strips made from the gut wall were bathed in NPFF solution (Demichel *et al.*, 1993). Although the NPFF was not applied exclusively to the gut mucosa, this experiment demonstrates the presence of receptors sensitive to FaRPs in the small intestine. The structural differences between FaRPs may render PF4 completely ineffectual on vertebrate FaRP receptors, making PF4 channels a suitable choice of anthelmintic target with respect to safety. Careful investigation of the effects of PF4 in vertebrate tissue is essential to verify this assertion.

The properties of PF4 channels have been explored during this project. As yet, there are no reports of other chloride ion channels that are directly gated by PF4 or any other peptide, making the PF4 channels unique. In itself, this observation is a strong argument for selecting PF4 channels as an anthelmintic target.

Project summary

From the aims stated at the outset of the project, the following results were obtained:

- PF4 receptors were localised to the bag region of the *Ascaris suum* somatic muscle cells.

- The response of the whole cell to the application of PF4 was a rapid-onset hyperpolarisation accompanied by an increase in input conductance.

- The ions involved in the PF4 response were shown to be chloride ions.

- The delay of action following PF4 application to the cell was short; i.e. it was not significantly different from that of γ-amino butyric acid, a directly-gating ligand.

- The ion channels activated by PF4 were distinguishable by their small amplitude, high probability of opening and their long mean open time.

- The PF4 response was dose-dependent; both channel activity and probability of channel opening increased with increasing dose of PF4.

- The channels mediated by PF4 were independent of cell contents, therefore were not mediated by intracellular second messengers. There was evidence for channel modulation by membrane-delimited G-proteins.

Whilst exploring the hypotheses for PF4 action, variation emerged in the response of the population of UK *Ascaris suum* to PF4. This project showed evidence of several PF4 receptor subtypes that are not distributed randomly throughout the whole population. Instead, specific receptor subtypes predominate in each subpopulation of worms.

Bibliography

Adelsberger, H., Scheuer, T., & Dudel, J. (1997). A patch clamp study of a glutamatergic chloride channel on pharyngeal muscle of the nematode *Ascaris suum*. *Neuroscience Letters* **230**, 183-186.

Adrian, R. H. (1956). The effect of internal and external potassium concentration on the membrane potential of frog muscle. *Journal Of Physiology* **133**, 631-658.

Aidley, D. J. & Stanfield, P. R. (1996). *Ion Channels Molecules in Action*, 1 ed. Cambridge University Press, Cambridge, UK.

Anderson, R. C. (1984). *CIH keys to the nematode parasites of vertebrates. Numbers 1-10* CAB International, Wallingford.

Anderson, R. C. (1992). *Nematode parasites of vertebrates. Their development and transmission*, 1 ed., pp. 1-14. CAB International, Wallingford, UK.

Atkinson, H. J., Isaac, R. E., Harris, P. D., & Sharpe, C. M. (1988). FMRFamide-like immunoreactivity within the nervous system of the nematodes *Panagrellus redivivus, Caenorhabditis elegans* and *Heterodera glycines*. *Journal of Zoology, London* **216**, 663-671.

Bader, C. R., Bertrand, D., & Schwartz, E. A. (1982). Voltage-activated and calcium-activated currents studied in solitary rod inner segments from the salamander retina. *Journal Of Physiology* **331**, 253-284.

Baldwin, E. & Moyle, V. (1949). A contribution to the physiology and pharmacology of *Ascaris lumbricoides* from the pig. *British Journal Of Pharmacology* **4**, 145-152.

Barish, M. E. (1983). A transient calcium-dependent chloride current in the immature *Xenopus* oocyte. *Journal Of Physiology* **342**, 309-325.

Becq, F. (1996). Ionic channel run down in excised membrane patches. *Biochimica Et Biophysica Acta-Biomembranes* **1286**, 53-63.

Bishop, Y. M. (ed.) (1998). Endoparasiticides. In *The veterinary formulary*, pp. 185-217. Pharmaceutical Press, London, UK.

Blackman, J. G., Ginsborg, B. L., & House, C. R. (1979). On the time course of the electrical response of salivary gland cells of *Nauphoeta Cinerea* to ionophoretically applied dopamine. *Journal Of Physiology* **287**, 81-92.

Blair, K. L., Barsuhn, C. L., Day, J. S., Ho, N. F. H., Geary, T. G., & Thompson, D. P. (1998). Biophysical model for organic acid excretion in *Ascaris suum*. *Molecular And Biochemical Parasitology* **93**, 179-190.

Blaxter, M. L., DeLey, P., Garey, J. R., Liu, L. X., Scheldeman, P., Vierstraete, A., Vanfleteren, J. R., Mackey, L. Y., Dorris, M., Frisse, L. M., Vida, J. T., & Thomas, W. K. (1998). A molecular evolutionary framework for the phylum Nematoda. *Nature* **392**, 71-75.

Blouin, M. S., Yowell, C. A., Courtney, C. H., & Dame, J. B. (1995). Host movement and the genetic structure of populations of parasitic nematodes. *Genetics* **141**, 1007-1014.

Bourne, H. R. (1998). Drug Receptors and Pharmacodynamics. In *Basic and Clinical Pharmacology*, ed. Katzung, B. G., Appleton and Lange, Stamford, USA.

Bowery, N. G., Hill, D. R., & Hudson, A. L. (1983). Characteristics of GABA-B receptor binding sites on rat whole brain synaptic membranes. *British Journal Of Pharmacology* **78**, 191-206.

Bowman, J. W., Friedman, A. R., Thompson, D. P., Ichhpurani, A. K., Kellman, M. F., Marks, N., Maule, A. G., & Geary, T. G. (1996). Structure-activity-relationships of KNEFIRFamide (AF1), a nematode FMRFamide-related peptide, on *Ascaris suum* muscle. *Peptides* **17**, 381-387.

Bowman, J. W., Winterrowd, C. A., Friedman, A. R., Thompson, D. P., Klein, R. D., Davis, J. P., Maule, A. G., Blair, K. L., & Geary, T. G. (1995). Nitric-oxide mediates

the inhibitory effects of SDPNFLRFamide, a nematode FMRFamide-related neuropeptide, in *Ascaris suum*. *Journal Of Neurophysiology* **74**, 1880-1888.

Brading, A. F. & Caldwell, P. C. (1964). The effect of ions on the resting potentials of muscle cells in *Ascaris lumbricoides*. *Journal Of Physiology* **173**, 36P.

Brading, A. F. & Caldwell, P. C. (1971). The resting membrane potential of the somatic muscle cells of *Ascaris lumbricoides*. *Journal Of Physiology* **217**, 605-624.

Brezina, V. (1988). Guanosine 5'-triphosphate analogue activates potassium current modulated by neurotransmitters in *Aplysia* neurones. *Journal Of Physiology* **407**, 15-40.

Brown, A. M. & Birnbaumer, L. (1990). Ionic channels and their regulation by G-protein subunits. *Annual Review of Physiology* **52**, 197-213.

Brownlee, D. J. A., Fairweather, I., Holden-Dye, L., & Walker, R. J. (1996). Nematode neuropeptides: localization, isolation and functions. *Parasitology Today* **12**, 343-351.

Brownlee, D. J. A., Fairweather, I., Johnston, C. F., & Shaw, C. (1994). Immunocytochemical demonstration of peptidergic and serotoninergic components in the enteric nervous system of the roundworm, *Ascaris suum* (Nematoda, Ascaroidea). *Parasitology* **108**, 89-103.

Brownlee, D. J. A., Fairweather, I., Johnston, C. F., Smart, D., Shaw, C., & Halton, D. W. (1993). Immunocytochemical demonstration of neuropeptides in the central nervous system of the roundworm, *Ascaris suum* (Nematoda, Ascaroidea). *Parasitology* **106**, 305-316.

Brownlee, D. J. A., Holden-Dye, L., Fairweather, I., & Walker, R. J. (1995). The action of serotonin and the nematode neuropeptide KSAYMRFamide on the pharyngeal muscle of the parasitic nematode, *Ascaris suum*. *Parasitology* **111**, 379-384.

Colquhoun, D. & Hawkes, A. G. (1983). The Principles of the Stochastic Interpretation of Ion-Channel Mechanisms. In *Single-Channel Recording*, eds. Sakmann, B. & Neher, E., pp. 135-175. Plenum Press, New York.

Coscoy, S., Lingueglia, E., Lazdunski, M., & Barbry, P. (1998). The phe-met-arg-phe-amide-activated sodium channel is a tetramer. *Journal Of Biological Chemistry* **273**, 8317-8322.

Cottrell, G. A., Davies, N. W., & Green, K. A. (1984). Multiple actions of a molluscan cardioexcitatory neuropeptide and related peptides on identified *Helix* neurones. *Journal Of Physiology* **356**, 315-333.

Cowden, C., Sithigorngul, P., Brackley, P., Guastella, J., & Stretton, A. O. W. (1993). Localisation and Differential Expression of FMRFamide-Like Immunoreactivity in the Nematode *Ascaris suum*. *Journal Of Comparative Neurology* **333**, 455-468.

Cowden, C. & Stretton, A. O. W. (1993). AF2, an *Ascaris* Neuropeptide: Isolation, Sequence and Bioactivity. *Peptides* **14**, 423-430.

Cowden, C. & Stretton, A. O. W. (1995). 8 novel FMRFamide-like neuropeptides isolated from the nematode *Ascaris suum*. *Peptides* **16**, 491-500.

Cowden, C., Stretton, A. O. W., & Davis, A. E. (1989). AF1, a sequenced bioactive neuropeptide isolated from the nematode *Ascaris suum*. *Neuron* **2**, 1465-1473.

Cox, G. N. (1992). Molecular and biochemical aspects of nematode collagens. *Journal Of Parasitology* **78**, 1-15.

Crompton, D. W. T. (1999). How much human helminthiasis is there in the World? *Journal Of Parasitology* **85**, 397-403.

Culling, C. F. A., Allison, R. T., & Barr, W. T. (1985). *Cellular Pathology Technique*, 4 ed. Butterworth and Co. (Publishers) Ltd., London, UK.

Cully, D. F., Wilkinson, H., Vassilatis, D. K., Etter, A., & Arena, J. P. (1996). Molecular biology and electrophysiology of glutamate-gated chloride channels of invertebrates. *Parasitology* **113**, S191-S200.

Curtis, H. J. & Cole, K. S. (1942). Membrane resting and action potentials from the squid giant axon. *Journal of Cellular and Comparative Physiology* **19**, 135-144.

Day, T. A. & Maule, A. G. (1999). Parasitic peptides! The structure and function of neuropeptides in parasitic worms. *Peptides* **20**, 999-1019.

DeBell, J. T., Del Castillo, J., & Sanchez, V. (1963). Electrophysiology of the Somatic Muscle Cells of *Ascaris lumbricoides* . *Journal of Cellular and Comparative Physiology* **62**, 159-177.

Del Castillo, J., De Mello, W. C., & Morales, T. (1964a). Influence of Some Ions on the Membrane Potential of *Ascaris* Muscle. *Journal Of General Physiology* **48**, 129-140.

Del Castillo, J., De Mello, W. C., & Morales, T. (1964b). Mechanism of the paralysing action of piperazine on *Ascaris* muscle. *British Journal Of Pharmacology* **22**, 463-477.

Del Castillo, J., Riviera, J., Soloranzo, A., & Serrato, J. (1989). Some aspects of the neuromuscular system of *Ascaris*. *Quarterly Journal of Experimental Physiology* **74**, 1071-1088.

Demichel, P., Rodriguez, J. C., Roquebert, J., & Simonnet, G. (1993). NPFF, a FMRF-NH2-like peptide, blocks opiate effects on ileum contractions. *Peptides* **14**, 1005-1009.

Dionne, V. E., Steinbach, J. H., & Stevens, C. F. (1978). An analysis of the dose-response relationship at voltage-clamped frog neuromuscular junctions. *Journal Of Physiology* **281** , 421-444.

Dixon, D. M., Valkanov, M. A., & Martin, R. J. (1993). A patch-clamp study of the ionic selectivity of the large conductance, Ca-activated chloride channel in muscle vesicles prepared from *Ascaris suum*. *Journal Of Membrane Biology* **131**, 143-149.

Dockray, G. J., Reeve, J. R., Shively, J., Gayton, R. J., & Barnard, C. S. (1983). A novel active pentapeptide from chicken brain identified by antibodies to FMRFamide. *Nature* **305**, 328-330.

Donahue, M. J., Yacoub, N. J., Michnoff, C. A., Masaracchia, R. A., & Harris, B. G. (1981). Serotonin (5-Hydroxytryptamine): a possible regulator of glycogenolysis in perfused muscle segments of *Ascaris suum*. *Biochemical & Biophysical Research Communications* **101**, 112-117.

Dorris, M., DeLey, P., & Blaxter, M. L. (1999). Molecular Analysis of Nematode Diversity and the Evolution of Parasitism. *Parasitology Today* **15**, 188-193.

Eckstein, F., Cassel, D., Levkovitz, H., Lowe, M., Selinger, Z. (1979). Guanosine 5'-O-(2-Thiodiphosphate): an inhibitor of adenylate cyclase stimulation by guanine nucleotides and fluoride ions. *Journal of Biological Chemistry* **254**, 9829-9834.

Edison, A. S., Espinoza, E., & Zachariah, C. (1999). Conformational ensembles: The role of neuropeptide structures in receptor binding. *Journal Of Neuroscience* **19**, 6318-6326.

Edison, A. S., Messinger, L. A., & Stretton, A. O. W. (1997). *Afp-1*: a gene encoding multiple transcripts of a new class of FRMFamide-like neuropeptides in the nematode *Ascaris suum*. *Peptides* **18**, 929-935.

Everson Pearse, A. G. (1985). *Histochemistry, theoretical and applied*, 4 ed. Churchill Livingstone, Edinburgh, UK.

Fellowes, R. A., Dougan, P. M., Maule, A. G., Marks, N. J., & Halton, D. W. (1999). Neuromusculature of the Ovijector of *Ascaris suum* (Ascaroidea, Nematoda): An Ultrastructural and Immunocytochemical Study. *Journal Of Comparative Neurology* **415**, 518-528.

Fellowes, R. A., Maule, A. G., Marks, N. J., Geary, T. G., Thompson, D. P., Shaw, C., & Halton, D. W. (1998). Modulation of the motility of the vagina vera of *Ascaris suum in vitro* by FMRFamide-related peptides. *Parasitology* **116**, 277-287.

Florence, A. T. & Attwood, D. (1998). *The Physicochemical Principles of Pharmacy*, 3 ed. Macmillan Press Ltd, Basingstoke, UK.

Foskett, J. K. (1998). ClC and CFTR chloride channel gating. *Annual Review of Physiology* **60**, 689-717.

Franciolini, F. & Petris, A. (1990). Chloride channels of biological membranes. *Biochimica Et Biophysica Acta* **1031**, 247-259.

Franks, C. J., Holden-Dye, L., & Walker, R. J. (1993). The nematode peptide, Ser-Asp-Pro-Asn-Phe-Leu-Arg-Phe-NH2 (PF1), inhibits synaptic transmission in the parasitic nematode *Ascaris suum*. *Journal Of Physiology-London* **473**, P 239-P 239.

Franks, C. J., Holden-Dye, L., Williams, R. G., Pang, F. Y., & Walker, R. J. (1994). A nematode FMRFamide-like peptide, SDPNFLRFamide (PF1), relaxes the dorsal muscle strip preparation of *Ascaris suum*. *Parasitology* **108**, 229-236.

Gadsby, D. C. (1996). Two-bit anion channel really shapes up. *Nature* **383**, 295-296.

Geary, T. G., Bowman, J. W., Friedman, A. R., Maule, A. G., Davis, J. P., Winterrowd, C. A., Klein, R. D., & Thompson, D. P. (1995). The pharmacology of FMRFamide-related neuropeptides in nematodes - new opportunities for rational anthelmintic discovery. *International Journal For Parasitology* **25**, 1273-1280.

Geary, T. G., Klein, R. D., Vanover, L., Bowman, J. W., & Thompson, D. P. (1992a). The nervous systems of helminths as targets for drugs. *Journal Of Parasitology* **78**, 215-230.

Geary, T. G., Marks, N. J., Maule, A. G., Bowman, J. W., Alexander-Bowman, S. J., Day, T. A., Larsen, M. J., Kubiak, T. M., Davis, J. P., & Thompson, D. P. (1999).

Pharmacology of FMRFamide-related peptides in helminths. *Annals Of The New York Academy Of Sciences* **897**, 212-227.

Geary, T. G., Price, D. A., Bowman, J. W., Winterrowd, C. A., Mackenzie, C. D., Garrison, R. D., Williams, J. F., & Friedman, A. R. (1992b). 2 FMRFamide-like peptides from the free-living nematode *Panagrellus redivivus*. *Peptides* **13**, 209-214.

Gicquel, S., Mazarguil, H., Desprat, C., Allard, M., Devillers, J. P., Simonnet, G., & Zajec, J. M. (1994). Structure-activity study of neuropeptide FF: contribution of N-terminal regions to affinity and activity. *Journal Of Medicinal Chemistry* **37**, 3477-3481.

Gilman, A. G. (1987). G-proteins: transducers of receptor-generated signals. *Annual Review Of Biochemistry* **56**, 615-649.

Glanville, R. W. (1987). Type IV Collagen. In *Structure and Function of Collagen Types*, eds. Mayne, R. & Burgeson, R. E., pp. 43-79. Academic Press, Inc. (London) Ltd., London, UK.

Glauert, A. M. & Glauert, R. H. (1958). Araldite as an embedding medium for electron microscopy. *Journal of Biophysical and Biochemical Cytology* **4**, 409.

Graham, M. K., Fairweather, I., & McGeown, J. G. (1997). The effects of FaRPs on the motility of isolated muscle strips from the liver fluke, *Fasciola hepatica*. *Parasitology* **114**, 455-465.

Grahame-Smith, D. G. & Aronson, J. K. (1992). *Oxford Textbook of Clinical Pharmacology and Drug Therapy*, 2 ed. Oxford University Press, Oxford, UK.

Gray, P. T. A., Bevan, S., & Ritchie, J. M. (1984). High conductance anion-selective channels in rat cultured Schwann cells. *Proceedings Of The Royal Society Of London Series B-Biological Sciences* **221**, 395-409.

Green, K. A. & Cottrell, G. A. (1997). Modulation of ligand-gated dopamine channels in *Helix* neurones. *Pflugers Archiv-European Journal Of Physiology* **434**, 313-322.

Green, K. A., Falconer, S. W. P., & Cottrell, G. A. (1994). The neuropeptide Phe-Met-Arg-Phe-NH2 (FMRFamide) directly gates 2 ion channels in an identified *Helix* neuron. *Pflugers Archiv-European Journal Of Physiology* **428**, 232-240.

Grenningloh, G., Rienitz, A., Schmitt, B., Methfessel, C., Zensen, M., Beyreuther, K., Gundelfinger, E. D., & Betz, H. (1987). The strychnine-binding subunit of the glycine receptor shows homology with nicotinic acetylcholine receptors. *Nature* **328**, 215-220.

Halliwell, J. V. & Whitaker, M. J. (1987). Using Microelectrodes. In *Microelectrode Techniques: The Plymouth Workshop Handbook*, eds. Standen, N. B., Gray, P. T. A., & Whitaker, M. J., pp. 1-12. The Company of Biologists, Ltd., Cambridge, UK.

Hamill, O. P., Bormann, J., & Sakmann, B. (1983). Activation of multiple-conductance state chloride channels in spinal neurones by glycine and GABA. *Nature* **305**, 805-808.

Hamill, O. P., Marty, A., Neher, E., Sakmann, B., & Sigworth, F. J. (1981). Improved patch clamp techniques for high-resolution current recording from cells and cell-free membrane patches. *Pflugers Archiv-European Journal Of Physiology* **391**, 85-100.

Harpur, R. P. (1963). Maintenance of *Ascaris lumbricoides in vitro*-II. Changes in muscle and ovary carbohydrates. *Canadian Journal of Biochemistry and Physiology* **41**, 1673-1689.

Harris, J. E. & Crofton, H. D. (1957). Structure and function in the nematodes: internal pressure and cuticular structure in *Ascaris*. *Journal Of Experimental Biology* **34**, 116-130.

Harrow, I. D. & Gration, K. A. F. (1985). Mode of Action of the Anthelmintics Morantel, Pyrantel and Levamisole on Muscle Cell Membrane of the Nematode *Ascaris suum*. *Pesticide Science* **16**, 662-672.

Hayat, H. A. (1970). *Principles and techniques of electron microscopy*, pp. 166. Van Nostrand Reinhold Company, New York, USA.

Hille, B. (1992). *Ionic Channels of Excitable Membranes*, Second ed. Sinauer Associates Inc, Sunderland, Massachusetts.

Hille, B. (1994). Modulation of ion-channel function by G--protein-coupled receptors. *Trends In Neurosciences* **17**, 531-536.

Hodgkin, A. L. (1951). The ionic basis of electrical activity in nerve and muscle. *Biological Review* **26**, 339-409.

Hodgkin, A. L. & Huxley, A. F. (1939). Action potentials recorded from inside a nerve fibre. *Nature* **144**, 710-711.

Hodgkin, A. L., Huxley, A. F., & Katz, B. (1952). Measurement of current-voltage relations in the membrane of the giant axon of *Loglio*. *Journal Of Physiology-London* **116**, 424-448.

Holden-Dye, L., Brownlee, D. J. A., & Walker, R. J. (1997). The effects of the peptide KPNFIRFamide (PF4) on the somatic muscle cells of the parasitic nematode *Ascaris suum*. *British Journal Of Pharmacology* **120**, 379-386.

Holden-Dye, L., Krogsgaard-Larsen, P., Neilsen, L., & Walker, R. J. (1989). GABA receptors on the somatic muscle cells of the parasitic nematode, *Ascaris suum*: stereoselectivity indicates similarity to a GABA-type agonist recognition site. *British Journal Of Pharmacology* **98**, 841-850.

Jarman, M. (1959). Electric activity in muscle cells of *Ascaris* muscle. *Nature* **184**, 1244-1244.

Jentsch, T. J., Steinmeyer, K., & Schwarz, G. (1990). Primary structure of *Torpedo marmorata* chloride channel isolated by expression cloning in *Xenopus* Oocytes. *Nature* **348**, 510-514.

Johnson, C. D., Reinitz, C. A., Sithigorngul, P., & Stretton, A. O. W. (1996). Neuronal localization of serotonin in the nematode *Ascaris suum*. *Journal Of Comparative Neurology* **367**, 352-360.

Johnson, C. D. & Stretton, A. O. W. (1985). Localization of choline-acetyltransferase within identified motoneurons of the nematode *Ascaris*. *Journal Of Neuroscience* **5**, 1984-1992.

Katz, B. & Thesleff, S. (1957). A study of the 'desensitization' produced by acetylcholine at the motor end-plate. *Journal Of Physiology* **138**, 63-80.

Keating, C., Thorndyke, M. C., Holden-Dye, L., Williams, R. G., & Walker, R. J. (1995). The isolation of a FMRFamide-like peptide from the nematode *Haemonchus contortus*. *Parasitology* **111**, 515-521.

Khan, F. A., Jain, M. R., Saha, S. G., & Subhedar, N. (1998). FMFRamide-like immunoreactivity in the olfactory system responds to morphine treatment in the Teleost *Clarias batrachus*: involvement of opiate receptors. *General And Comparative Endocrinology* **110**, 79-87.

Kubiak, T. M., Maule, A. G., Marks, N. J., Martin, R. A., & Wiest, J. R. (1996). Importance of the proline residue to the functional activity and metabolic stability of the nematode FMRFamide-related peptide, KPNFIRFamide (PF4). *Peptides* **17**, 1267-1277.

Lehninger, A. L., Nelson, D. L., & Cox, M. M. (1993). *Principles of Biochemistry*, 2 ed., pp. 747.

Lester, H. A. (1977). The Response to Acetylcholine. *Scientific American* **236**, 106-118.

Li, C., Nelson, L. S., Kim, K., Nathoo, A., & Hart, A. C. (1999). Neuropeptide gene families in the nematode *Caenorhabditis elegans*. *Annals Of The New York Academy Of Sciences* **897**, 239-252.

Ling, G. & Gerald, R. W. (1949). The normal membrane potential of frog sartorius fibers. *Journal of Cellular and Comparative Physiology* **34**, 383-396.

Lingueglia, E., Champigny, G., Lazdunski, M., & Barbry, P. (1995). Cloning of the amiloride-sensitive FMRFamide peptide-gated sodium channel. *Nature* **378**, 730-733.

Ludewig, U., Pusch, M., & Jentsch, T. J. (1996). Two physically distinct pores in the dimeric ClC-0 chloride channel. *Nature* **383**, 340-343.

MacDonald, R. L., Rogers, C. J., & Twyman, R. E. (1989). Kinetic properties of the $GABA_A$ receptor main conductance state of mouse spinal cord neurones in culture. *Journal Of Physiology* **410**, 479-499.

Malin, D. H., Lake, J. R., McDermitt, L. S., Smith, D. A., Witherspoon, W. E., Jones, J. A., Schumann, M. D., Payza, K., Ho, K. K., & Burgess, K. (1996). Enhanced antiopiate activity and enzyme resistance in a peptidomimetic of FMRFamide containing E-2,3-methanomethionine and E- 2,3-methanophenylalanine. *Peptides* **17**, 83-86.

Mano, I. & Driscoll, M. (1999). DEG/ENaC channels: a touchy superfamily that watches its salt. *Bioessays* **21**, 568-578.

Manson-Bahr, P. E. C. & Bell, D. R. (1987). Soil-transmitted helminths. In *Manson's Tropical Diseases*, eds. Manson-Bahr, P. E. C. & Bell, D. R., pp. 407-447. Balliere-Tindall, London, UK.

Marks, N. J., Maule, A. G., Geary, T. G., Thompson, D. P., Li, C., Halton, D. W., & Shaw, C. (1998). KSAYMRFamide (PF3/AF8) is present in the free-living nematode, *Caenorhabditis elegans*. *Biochemical And Biophysical Research Communications* **248**, 422-425.

Marks, N. J., Sangster, N. C., Maule, A. G., Halton, D. W., Thompson, D. P., Geary, T. G., & Shaw, C. (1999). Structural characterisation and pharmacology of KHEYLRFamide (AF2) and KSAYMRFamide (PF3/AF8) from *Haemonchus contortus*. *Molecular & Biochemical Parasitology* **100**, 185-194.

Marks, N. J., Shaw, C., Maule, A. G., Davis, J. P., Halton, D. W., Verhaert, P., Geary, T. G., & Thompson, D. P. (1995). Isolation of AF2 (KHEYLRFamide) from

Caenorhabditis-elegans: evidence for the presence of more than one FMRFamide related peptide-encoding gene. *Biochemical And Biophysical Research Communications* **217**, 845-851.

Martin, R. J. (1980). The effect of gamma-aminobutyric acid on the input conductance and membrane potential of *Ascaris* muscle. *British Journal Of Pharmacology* **71**, 99-106.

Martin, R. J. (1982). Electro-physiological effects of piperazine and diethylcarbamazine on *Ascaris suum* somatic muscle. *British Journal Of Pharmacology* **77**, 255-265.

Martin, R. J. (1985). Gamma-aminobutyric acid-activated and piperazine-activated single- channel currents from *Ascaris suum* body muscle. *British Journal Of Pharmacology* **84**, 445-461.

Martin, R. J. (1996). An electrophysiological preparation of *Ascaris suum* pharyngeal muscle reveals a glutamate-gated chloride channel sensitive to the avermectin analogue, milbemycin D. *Parasitology* **112**, 247-252.

Martin, R. J., Kusel, J. R., & Pennington, A. J. (1990). Surface properties of membrane vesicles prepared from muscle cells of *Ascaris suum*. *Journal Of Parasitology* **76**, 340-348.

Martin, R. J., Pennington, A. J., Duittoz, A. H., Robertson, S., & Kusel, J. R. (1991). The physiology and pharmacology of neuromuscular-transmission in the nematode parasite, *Ascaris suum*. *Parasitology* **102**, S41-S58.

Martin, R. J. & Valkanov, M. A. (1996). Effects of acetylcholine on a slow voltage-activated non-selective cation current mediated by non-nicotinic receptors on isolated *Ascaris* muscle bags. *Experimental Physiology* **81**, 909-925.

Marty, A. & Neher, E. (1983) Tight-Seal Whole-Cell Recording. *In Single-Channel Recording*, eds. Sakmann, B. & Neher, E., pp 107-121. Plenum Press, New York and London.

Marty, A., Tan, Y. P., & Trautmann, A. (1984). Three types of calcium-dependent channel in rat lacrimal glands. *Journal Of Physiology* **357**, 293-325.

Maule, A. G., Bowman, J. W., Thompson, D. P., Marks, N. J., Friedman, A. R., & Geary, T. G. (1996). FMRFamide-related peptides (FaRPs) in nematodes: occurrence and neuromuscular physiology. *Parasitology* **113**, S119-S135.

Maule, A. G., Geary, T. G., Bowman, J. W., Marks, N. J., Blair, K. L., Halton, D. W., Shaw, C., & Thompson, D. P. (1995a). Inhibitory effects of nematode FMRFamide-related peptides (FaRPs) on muscle strips from *Ascaris suum*. *Invertebrate Neuroscience* **1**, 255-265.

Maule, A. G., Shaw, C., Bowman, J. W., Halton, D. W., Thompson, D. P., Geary, T. G., & Thim, L. (1994a). KSAYMRFamide - a novel FMRFamide-related heptapeptide from the free- living nematode, *Panagrellus redivivus*, which is myoactive in the parasitic nematode, *Ascaris suum*. *Biochemical And Biophysical Research Communications* **200**, 973-980.

Maule, A. G., Shaw, C., Bowman, J. W., Halton, D. W., Thompson, D. P., Geary, T. G., & Thim, L. (1994b). The FMRFamide-like neuropeptide AF2 (*Ascaris suum*) is present in the free-living nematode, *panagrellus redivivus* (Nematoda, Rhabditida). *Parasitology* **109**, 351-356.

Maule, A. G., Shaw, C., Bowman, J. W., Halton, D. W., Thompson, D. P., Thim, L., Kubiak, T. M., Martin, R. A., & Geary, T. G. (1995b). Isolation and preliminary biological characterization of KPNFIRFamide, a novel FMRFamide-related peptide from the free living nematode, *Panagrellus redivivus*. *Peptides* **16**, 87-93.

McCaman, R. E., McKenna, D. G., & Ono, J. K. (1977). A pressure system for intracellular and extracellular ejection of picoliter volumes. *Brain Research* **136**, 141-147.

Middleton, R. E., Pheasant, D. J., & Miller, C. (1996). Homodimeric architecture of a ClC-type chloride ion channel. *Nature* **383**, 337-340.

Minault, M., Lecron, J. C., Labrouche, S., Simonnet, G., & Gombert, J. (1995). Characterization of binding-sites for neuropeptide FF on T lymphocytes of the Jurkat cell-line. *Peptides* **16**, 105-111.

Mount, L. E. (1968). *Climatic Physiology of the Pig*, 1 ed. Edward Arnold (Publishers) Ltd., London, UK.

Neher, E. (1981). Unit conductance studies in biological membranes. In *Techniques in cellular physiology*, ed. Baker, P. F., Elsevier, Amsterdam.

Nelson, L. S., Kim, K. Y., Memmott, R. E., & Li, C. (1998). FMRFamide-related gene family in the nematode, *Caenorhabditis elegans*. *Molecular Brain Research* **58**, 103-111.

Painter, S. D. (1982). FMRFamide catch contractures of a molluscan smooth muscle: pharmacology, ionic dependence and cyclic nucleotides. *Journal of Comparative Physiology* **148A**, 491-501.

Panula, P., Aarnisalo, A. A., & Wasowicz, K. (1996). Neuropeptide FF, a mammalian neuropeptide with multiple functions. *Progress In Neurobiology* **48**, 461-461.

Parri, H. R., Djamgoz, M. B. A., Holden-Dye, L., & Walker, R. J. Ion sensitive microelectrode study of chloride balance in the somatic muscle bag cells of *Ascaris suum*. *Society for Neuroscience Abstracts* **16**, 669. 1990.

Payza, K. & Yang, H.-Y. T. (1993). Modulation of Neuropeptide FF Receptors by Guanine Nucleotides and Cations in Membranes of Rat Brain and Spinal Cord. *Journal Of Neurochemistry* **60**, 1894-1899.

Pennington, A. J. & Martin, R. J. (1990). A patch-clamp study of acetylcholine-activated ion channels in *Ascaris suum* muscle. *Journal Of Experimental Biology* **154**, 201-221.

Peper, K. & Dreyer, F. (1974). Structure and Ultrastructure of the Frog Motor Endplate. *Cell And Tissue Research* **149**, 437-455.

Perry, S. J., Huang, E. Y. K., Cronk, D., Bagust, J., Sharma, R., Walker, R. J., Wilson, S., & Burke, J. F. (1997). A human gene encoding morphine modulating peptides related to NPFF and FMRFamide. *Febs Letters* **409**, 426-430.

Price, D. A. (1986). Evolution of a molluscan cardioregulatory neuropeptide. *American Zoologist* **26** , 1007-1015.

Price, D. A. & Greenberg, M. J. (1977). Structure of a molluscan cardioexitatory neuropeptide. *Science* **197**, 670-671.

Purves, R. D. (1977). The time course of cellular responses to iontophoretically applied drugs. *Journal of Theoretical Biology* **65**, 327-344.

Pusch, M. & Jentsch, T. J. (1994). Molecular Physiology of Voltage-Gated Chloride Channels. *Physiological Reviews* **74**, 813-827.

Raffa, R. B. (1988). The action of FMRFamide (Phe-Met-Arg-Phe-NH2) and related peptides on mammals. *Peptides* **9**, 915-922.

Reynolds, E. S. (1963). The use of lead citrate at high pH as an electron opaque stain in electron microscopy. *Journal of Cell Biology* **17**, 208-212.

Riddle, L. R., Blumenthal, T., Meyer, B. J., & Priess, J. R. (1997). *C.elegans II* Cold Spring Harbour Laboratory Press, New York.

Robertson, A. P., Bjorn, H. E., & Martin, R. J. (1999). Resistance to levamisole resolved at the single-channel level. *Faseb Journal* **13**, 749-760.

Robertson, A. P., Bjorn, H. E., & Martin, R. J. (2000). Pyrantel resistance alters nematode nicotinic acetylcholine receptor single-channel properties. *European Journal of Pharmacology* **394**, 1-8.

Robertson, A. P. & Martin, R. J. (1996). Effects of pH on a high conductance Ca-dependent chloride channel: a patch-clamp study in *Ascaris suum*. *Parasitology* **113**, 191-198.

Rosenbluth, J. C. (1965b). Ultrastructural Organization of Obliquely Striated Muscle Fibres in *Ascaris Lumbricoides*. *Journal of Cell Biology* **25**, 495-515.

Rosenbluth, J. C. (1965a). Ultrastructure of somatic muscle cells in *Ascaris lumbricoides*. *Journal of Cell Biology* **26**, 579-591.

Rosoff, M. L., Burglin, T. R., & Li, C. (1992). Alternatively spliced transcripts of the *flp-1* gene encode distinct FMRFamide-like peptides in *Caenorhabditis elegans*. *Journal Of Neuroscience* **12**, 2356-2361.

Sabatini, D. D., Bensch, K., & Barrnett, R. J. (1962). New means of fixation for electron microscopy and histochemistry. *Anatomical Record* **142**, 274.

Sakmann, B. & Neher, E. (1983). Geometric parameters of pipettes and membrane patches. In *Single-Channel Recording*, eds. Sakmann, B. & Neher, E., pp. 37-51. Plenum Press, New York and London.

Saz, H. J. (1981). Energy metabolisms of parasitic helminths: adaptations to parasitism. *Annual Review of Physiology* **43**, 323-341.

Schofield, P. R., Darlison, M. G., Fujita, N., Burt, D. R., Stephenson, F. A., Rodriguez, H., Rhee, L. M., Ramachandran, J., Reale, V., Glencorse, T. A., Seeburg, P. H., & Barnard, E. A. (1987). Sequence and functional expression of the $GABA_A$ receptor shows a ligand-gated receptor super-family. *Nature* **328**, 221-227.

Sheehy, B. A., Ho, N. F. H., Burton, P. S., Day, J. S., Geary, T. G., & Thompson, D. P. (2000). Transport of model peptides across *Ascaris suum* cuticle. *Molecular & Biochemical Parasitology* **105**, 39-49.

Simon, M. I., Strathman, M. P., & Gautam, N. (1991). Diversity of G Proteins in Signal Transduction. *Science* **252**, 802-808.

Sithigorngul, P., Stretton, A. O. W., & Cowden, C. (1990). Neuropeptide Diversity in *Ascaris*: An Immunocytochemical Study. *Journal Of Comparative Neurology* **294**, 362-376.

Smart, D., Shaw, C., Curry, W. J., Johnston, C. F., Thim, L., Halton, D. W., & Buchanan, K. D. (1992). The primary structure of TE-6: a novel neuropeptide from the nematode *Ascaris suum*. *Biochemical & Biophysical Research Communications* **187**, 1323-1329.

Smith, T. G. & Cunningham, M. F. (1983). Pressure ejection system for quantitative focal application of neuroactive substances from micropipettes. *Medical and Biological Engineering and Computing* **21**, 138-144.

Standen, N. B. (1987). Separation and analysis of ionic currents. In *Microelectrode Techniques: The Plymouth Workshop Handbook*, eds. Standen, N. B., Gray, P. T. A., & Whitaker, M. J., pp. 29-40. The Company of Biologists, Ltd., Cambridge, UK.

Standen, N. B., Gray, P. T. A., & Whitaker, M. J. (1987). *Microelectrode Techniques: The Plymouth Workshop Handbook*, 1 ed. The Company of Biologists, Ltd., Cambridge, UK.

Standen, N. B., Stanfield, P. R., Ward, T. A., & Wilson, S. W. (1984). A new preparation for recording single-channel currents from skeletal muscle. *Proceedings Of The Royal Society Of London Series B-Biological Sciences* **221**, 455-464.

Steinmeyer, K., Lorenz, C., Pusch, M., Koch, M. C., & Jentsch, T. J. (1994). Multimeric structure of ClC-1 chloride channel revealed by mutations in dominant myotonia congenita (Thomsen). *Embo Journal* **13**, 737-743.

Stevens, A. & Lowe, J. S. (1992). *Histology*, 1 ed. Gower Medical Publishing, London,UK.

Stretton, A. O., Fishpool, R. M., Southgate, E., Donmoyer, J. E., Walrond, J. P., Moses, J. E., & Kass, I. S. (1978). Structure and physiological activity of the

motoneurons of the nematode *Ascaris*. *Proceedings of the National Academy of Sciences of the United States of America* **75**, 3493-3497.

Stretton, A. O. W., Davis, R. E., Angstadt, J. D., Donmoyer, J. E., & Johnson, C. D. (1985). Neural control of behavior in *Ascaris*. *Trends In Neurosciences* **8**, 294-300.

Stryer, L. (1995). *Biochemistry*, 4 ed. W.H.Freeman and Co., New York, USA.

Sundblom, D. M., Panula, P., & Fyhrquist, F. (1995). Neuropeptide FF-like immunoreactivity in human plasma. *Peptides* **16**, 347-350.

Tauc, L. & Gerschenfeld, H. M. (1962). A cholinergic mechanism of inhibitory synaptic transmission in a molluscan nervous system. *Journal Of Neurophysiology* **25**, 236-262.

Tensen, C. P., Cox, K. J. A., Smit, A. B., vanderSchors, R. C., Meyerhof, W., Richter, D., Planta, R. J., Hermann, P. M., vanMinnen, J., Geraerts, W. P. M., Knol, J. C., Burke, J. F., Vreugdenhil, E., & vanHeerikhuizen, H. (1998). The *Lymnaea* cardioexcitatory peptide (lyCEP) receptor: a G-protein coupled receptor for a novel member of the rfamide neuropeptide family. *Journal Of Neuroscience* **18**, 9812-9821.

Thompson, D. P., Klein, R. D., & Geary, T. G. (1996). Prospects for rational approaches to anthelmintic discovery. *Parasitology* **113**, S217-S238.

Thorn, P. & Martin, R. J. (1987). A high-conductance calcium-dependent chloride channel in *Ascaris suum* muscle. *Quarterly Journal Of Experimental Physiology And Cognate Medical Sciences* **72**, 31-49.

Tielens, A. G. M. & van der Bergh, S. G. (1993).
Aerobic and anaerobic metabolism in the life cycle of parasitic helminths. In *Surviving Hypoxia mechanisms of control and adaptation.*, eds. Hochachka, P. W., Lutz, P. L., Sick, T., Rosenthal, M., & van der Thillart, G., CRC Press, London, UK.

Toner, P. G. & Carr, K. E. (1971). *Cell Structure An Introduction to Biological Electron Microscopy*, 2 ed. Churchill Livingstone, Edinburgh and London,UK.

Twyman, R. M. (1998). *Advanced Molecular Biology*, 1 ed. BIOS Scientific Publishers Ltd., Oxford, UK.

Urquhart, G. M., Armour, J. A., Duncan, J. L., & Dunn, A. M. (1987). *Veterinary Parasitology*, 1 ed. Longman Scientific and Technical, London, UK.

Valkanov, M. A. & Martin, R. J. (1995). A Cl channel in *Ascaris suum* selectivity conducts dicarboxylic anion product of glucose fermentation and suggests a role in removal of waste organic anions. *Journal Of Membrane Biology* **148**, 41-49.

Valkanov, M. A., Martin, R. J., & Dixon, D. M. (1994). The Ca-activated channel of *Ascaris suum* conducts volatile fatty acids produced by anaerobic respiration: a patch-clamp study. *Journal Of Membrane Biology* **138**, 133-141.

Volterra, A. & Siegelbaum, S. A. (1988). Role of two different guanine nucleotide-binding proteins in the antagonistic modulation of the S-type K^+ channel by cAMP and arachidonic acid metabolites in *Aplysia* sensory neurons. *Proceeding of the National Academy of Sciences of the United States of America* **85**, 7810-7814.

Waggoner, L. E., Zhou, G. T., Schafer, R. W., & Schafer, W. R. (1998). Control of alternative behavioural states by serotonin in *Caenorhabditis elegans*. *Neuron* **21**, 203-214.

Walker, P. M. B. (ed.) (1995). *Larousse Dictionary of Science and Technology*, 1 ed. Larousse, Plc., Edinburgh, UK.

Waller, P. J. (1994). The development of anthelmintic resistance in ruminant livestock. *Acta Tropica* **56**, 233-243.

Wickman, K. D. & Clapham, D. E. (1995). G-protein regulation of ion channels. *Current Opinion In Neurobiology* **5**, 278-285.

Williams, J. A., Shahkolahi, A. M., Abbassi, M., & Donahue, M. J. (1992). Identification of a novel 5-HTN (Nematoda) receptor from *Ascaris suum* muscle.

Comparative Biochemistry & Physiology - C: Comparative Pharmacology & Toxicology **101**, 469-474.

Yang, H.-Y. T., Fratta, W., Majane, E. A., & Costa, E. (1985). Isolation, sequencing, synthesis and pharmacological characterization of two brain neuropeptides that modulate the action of morphine. *Proceedings of the National Academy of Sciences, USA* **82**, 7757-7761.

Yang, H. Y. & Majane, E. A. (1990). Mammalian Phe-Met-Arg-Phe-NH2-like peptides: structure, biological activity and distribution. *Progress in Comparative Endocrinology* **342**, 86-91.

Young, B. & Heath, J. W. (2000). *Wheater's Functional Anatomy*, 4 ed. Churchill Livingstone, Edinburgh, UK.

Young, G. P. H., Young, J. D. E., Deshpande, A. K., Goldstein, M., Koide, S. S., & Cohn, Z. A. (1984). A Ca^{2+}-activated channel from *Xenopus laevis* oocyte membranes reconstituted into planar bilayers. *Proceeding of the National Academy of Sciences of the United States of America* **81** , 5155-5159.